Heterochromatin dynamics upon release from stationary phase in budding yeast

Hrvoje Galic

THÈSE POUR OBTENIR LE GRADE DE DOCTEUR DE L'UNIVERSITÉ DE MONTPELLIER

En Biologie-Sante

École doctorale CBS2

Unité de recherche Institute de Génétique Moléculaire de Montpellier

Heterochromatin dynamics upon release from stationary phase in budding yeast

Présentée par Hrvoje GALIC

Le 29 Mai 2019

Sous la direction de Marta RADMAN-LIVAJA

Devant le jury composé de

Armelle LENGRONNE-CAU	Directrice de Recherche	Institut de Génétique Humaine, France	Président du Jury
Angela TADDEI	Directrice de Recherche	Institut Curie, France	Rapporteur
Fred van LEEUWEN	Chercheur principal	The Netherlands Cancer Institute, Pays Bas	Rapporteur
Gaëlle LEGUBE	Directrice de Recherche	Centre de Biologie Intégrative, France	Examinateur

UNIVERSITÉ DE MONTPELLIER

Acknowledgments

I would like to thank my thesis director Marta Radman-Livaja for giving me the opportunity to be part of her project and for supervising this thesis. Marta, thank you for being with me on this path which started with my adaptations to this PhD research and included bacteria on yeast plates, inconclusive (ugly) electrophoresis gels, ChIPped noise and postmodern Western blots (which still sometimes happen) and finished with maturity and results included in this thesis.

Huge thanks to all my lab colleagues for being there (although contractually obliged) during all my different mood swings. Alain, thank you for all your words of wisdom. Rahima, thank you for all the hour-long conversations and Heidelberg walks (after all the lectures of course). Saphia and Pauline for my initial experimental training and all the orders even at inappropriate times. Sorry I ditched the hood more often than not. Arame, our time was short but I enjoyed working with you and eating your delicious dishes. Thank you. Pritha and Ana, thank you for our hilarious office conversations, watching my back and being not only colleagues, but friends together with Uriel, Iva, Marco and Jen. Who will ever forget all of the benches in Montpellier we visited, endless Panama nights with toxic shots, champagne showers, fabulous red carpet-like entrances and payments without credit cards in the machine. Ana, posebno hvala sto si bila tu, pogotovo u trenucima kad engleski jezik nije bio dovoljan za izraziti emocije i humor, drago mi je da smo se upoznali, stvarno ne bi bili isti dani na poslu bez tebe.

To all my jury members, thank you for participating in my thesis defense and providing helpful, thought-provoking commentary which will shape my thinking in all future endeavors. Special thanks to Armelle and Gaëlle for being my thesis committee all these years. Our every encounter was pleasant and informative and you made a usually stressful event for a student enjoyable and helpful.

During my stay in Montpellier, it’s not a secret my friend circle was more a triangle and I kept it very close.

Alejandro, thank you for all your invaluable support, kindness and help in obtaining all of my PS platinum trophies. Of course, all the help while writing the thesis as well. Since we met, I knew I would be writing these acknowledgments to you one day. However, I am still waiting for Colombian souvenirs…Thank you for

always being here for me. I would go through the thesis again to relive all the memories from these years in Montpellier. Eres un ser humano precioso.

Anne-Sophie thank you for being part of my friend triangle, hosting beautiful evenings, birthday parties and gatherings in which you invested so much love and care.

Marina, stvarno postoji nesto neobjasnivo sto nas je spojilo ovdje, makar smo se znali kao kolege u Zagrebu. Hvala ti sto si bila tu i hvala ti na svim prekrasnim razgovorima. Pomogla si mi staviti zivotne zelje u perspektivu i motivirati me pozitivnom energijom i optimizmom.

Ne bih bio ova osoba danas, da nije bilo mojih prijatelja u Hrvatskoj. Kilometri udaljenosti su nebitni jer smo uvijek tu jedni za druge.

Martina, ti ces uvijek biti moja femme fatale ratnica i hvala ti sto si prava prijateljica koju bi pozelio svim ljudima da imaju u zivotu. Ne mogu zamisliti da bi dogurao do ovog trenutka bez da smo mi rasclanili, prokomentirali (citaj: sprdali) i razgovarali o svim dobrim i losim zivotnim situacijama. Uvijek si tu za mene kad mi treba dotociti. S tobom sam otkrio nas magicni omjer 80:20, da su proteini u prahu smece, a kiseline tajna za ne biti basic, sto je sigurno utjecalo i na moj znanstveni rad.

Marta, hodam sam satima, gledam tuzna lica ta, srecu cuvam u sebi, da je netko ne zgrabi, ali u jednoj ulici u Dubravi dobro znam da zivis ti! Sasvim siguran sam ja da si moja sudbina, nemoj nikom pustiti da ovu nasu ljubav unisti nego dolje na koljena ako sam tvoj voljeni jer mozda jutro donosi kraj, pa budi jos malo moja dok svice zora, a atmosfera je do plafona.

Ivana, hvala ti sto si tu uz mene od kad smo se upoznali davne 2005. do dan danas kad smo “jako odgovorni” odrasli ljudi. Ne moze ni vrijeme ni mjesto promjeniti da si mi poput obdarene sestre koju sam uvijek htio imati.

Za kraj mi ostaje moja najstarija partnerica u zlocinu. Sura, hvala ti sto me poznajes od kad smo glumili u predstavama u vrticu (za koje smo mislili da su u rangu nagrade Tony) do osnovne (kad smo hejtali svijet) do svih nasih putovanja i avantura (kad smo i dalje hejtali svijet) koje ce se zauvijek prepricavati i pamtiti. Ti si moj hitni broj za trenutke kratkotrajnog i dugotrajnog ludila i jedina s kojom sam

davnih dana potpisao ugovor na neodredeno prijateljstvo. I mozda bi treabli ponovno razmisliti o Vegasu? S novom placom priustim nam barem hostel.

Dino, mislim da je dovoljno pronaci sve nase arhivirane razgovore i glasovne poruke da se jasno vidi koliko smo obojica se mijenjali ovih godina i koliko smo daleko dogurali od, sad vec davne, prve Mreznice. Ne mogu zamisliti kako bih prosao ovaj doktorski studij bez nasih misa i terapija razgovora u kojima se gubi pojam o vremenu i mjestu. Hvala ti sto si pravi prijatelj i Batman kojeg je samo potrebno signalizirati i uvijek je tu za mene. Amen.

Lipovac, ima l' u gradu p…? Znam da na tebe uvijek mogu racunati bez obzira koliko se cujemo i vidimo, pravi si pokazatelj da prava prijateljstva nadilaze bilo kakve restrikcije vremena i mjesta. Hvala ti sto mi cuvas ledja i brines, sto slusas i sto me svaki put razveselis svojim nekonvencionalnim smislom za humor, da ne kazem pojavom. Greenchevino, ostani ovakav i ne zaboravi da Galic uvijek jedva ceka nase iduce druzenje.

Ostavio sam jednu poooosebnu osobu za kraj. Ivek, nikad necu zaboraviti da smo zajedno sjedili na Jarunu kad sam dobio mail da mi se pruza ova prilika u Francuskoj. Osoba koja je rekla da je tesko uspostaviti prijateljstva, kamoli prava, kad smo "stariji" nije nas vidjela. A bome smo pojava i pol, ne? Hvala ti sto svakom druzenju doprinosis s toliko pozitivne atmosfere, sto je s tobom lako razgovarati, sto slusas i brines i sto si uvijek tu kao pravi prijatelj, najcesce s nekim domacim vinom.

Htio bih zahvaliti svojoj obitelji, posebno dragom Tati, Tatjani, Bruni, Franu i Emanuelu. Hvala vam na svim lijepim druzenjima uz hrpu nedjeljnih ruckova i ugodnih razgovora punih potpore i ponosa na moj rad i trud. Zahvalan sam sto se brinete za mene i sto uvijek mogu racunati na vas bez obzira na udaljenost.

Za kraj, zahvaljujem od srca svojoj Mami, Noni i Nonotu i posvecujem vam ovaj rad. Bez vas i vase potpore ne bih uspio dogurati do ovdje i ne bih bio ista osoba. Hvala vam sto se brinete za mene i sto ste uvijek tu za mene puni razumjevanja i ljubavi. Nono, hvala sto si mi priustio prekrasno i nezaboravno djetinjstvo i cjelozivotno skolovanje. Nona, hvala ti sto uvijek pazis da mi nista u zivotu ne fali i da sam sretan. Bez brige, trudio sam se dobro jesti tijekom citavog boravka u Montpellieru. Mama, hvala od srca sto si uvijek tu za mene i sto si mama kakvu svatko moze pozeljeti, puna ljubavi i razumjevanja. Cestitam rodila si doktora!

Résumé

La complexe protéique Sir (Silent Information Regulator) de la levure bourgeonnante est l'acteur principal dans la formation de l'hétérochromatine, qui provoque l'atténuation de l'expression génique par un mécanisme épigénétique. Le complexe Sir lié à la chromatine maternelle est démonté lors de la réplication génomique et puis réformé sur les deux brins nouvellement répliqué. La dynamique de maintien de Sir sur la chromatine pendant le cycle cellulaire et dans de variables conditions de croissance n'est pas bien comprise. Pour comprendre comment la structure chromatinienne telle que l'hétérochromatine peut être héritée et par conséquent comment les structures épigénétiques sont transmises d'une génération cellulaire à l'autre, nous avons besoin de mesurer la vitesse d'échange des sous-unités du complexe Sir au cours du cycle cellulaire dans différentes conditions de croissance. Nous avons donc utilisé le système RITE qui permet d'échanger deux épitopes attachés à Sir3 (une des sous-unités de Sir) et par la suite mesurer la cinétique de remplacement de Sir3. Nous avons constaté que la Sir3 maternelle est complètement remplacée par la Sir3 nouvellement synthétisées dans les régions télomériques durant le premier cycle cellulaire après la sortie de la phase stationnaire. Nous proposons que cette reprogrammation du complexe hétérochromatique est un mécanisme d'adaptation qui assure l'activation des gènes de réponse au stress par la déstabilisation transitoire de la structure hétérochromatinienne.

Abstract

The budding yeast SIR complex (Silent Information Regulator) is the principal actor in heterochromatin formation, which causes epigenetically regulated gene silencing phenotypes. The maternal chromatin bound SIR complex is disassembled during replication and then, if heterochromatin is to be restored on both daughter strands, the SIR complex has to be reformed on both strands to pre-replication levels. The dynamics of SIR complex maintenance and re-formation during the cell-cycle and in different growth conditions are however not clear. Understanding exchange rates of SIR subunits during the cell cycle and their distribution pattern to daughter chromatids after replication has important implications for how heterochromatic states may be inherited and therefore how epigenetic states are maintained from one cellular generation to the next. We therefore used the tag switch RITE system to measure genome wide turnover rates of the SIR subunit Sir3 before and after exit from stationary phase and show that maternal Sir3 subunits are completely replaced with newly synthesized Sir3 at subtelomeric regions during the first cell cycle after release from stationary phase. We propose that the observed “reset” of the heterochromatic complex is an adaptive mechanism that ensures the activation of subtelomeric stress response genes by transiently destabilizing heterochromatin structure.

TABLE OF CONTENTS

List of Figures

List of Tables

List of Abbreviations

Abf1	ARS binding factor
acetyl-CoA	Acetyl coenzyme A
ADE2	Phosphoribosylaminoimidazole carboxylase 2
ADPr	ADP ribose
ARS	Autonomously replicating sequence
Asf-1	Antisilencing function
BAH domain	Bromo-adjacent domain
CAF-1	Chromatin assembly factor 1
Chip	Chromatin inmmunoprecipitation
CR	Caloric restriction
DNA	Deoxyribonucleic acid
Dot1	Disruptor of telomeric silencing 1
ERC	Extrachromosomal rdna circle
Esc1	Establishes silent chromatin 1
ETC	Extra TFIIIC
H3	Histone 3
H3K4me	Methylation of histone 3 lysine 4
H3K79me	Methylation of histone 3 lysine 79
H4	Histone 4
H4K16ac	Acetylation of histone 4 lysine 16
HO	Homothallic switching endonuclease
HP1	Heterochromatin protein 1
Jhd2	Jmjc domain-containing Histone Demethylase
MAT locus	Mating type locus
Mcm1	Minichromosome maintenance 1
Mps3	Mono polar spindle
NA	Nicotinic acid
NAD^+	Nicotinamide adenine dinucleotide
NAM	Nicotinamide
NaMN	Nicotinic acid mononucleotide
NFR	Nucelosome free region
Npt1	Nicotinate phosphoribosyltransferase
NQ cell	Non-quiescent cell
NTS1	Non-transcribed spacer 1
NTS2	Non-transcribed spacer 2
Nup170	Nuclear pore 170
OAADPr	O-acetyl-ADP-ribose
ORC	Origin recognition complex
PCNA	Proliferating cell nuclear antigen
PKA	Protein kinase A
Pnc1	Pyrazinamidase/nicotinamidase 1

Pol I	RNA polymerase I
Pol II	RNA polymerase II
Pol III	RNA polymerase III
Q cell	Quiescent cell
Rap1	Repressor activator protein
Rir1/2	Rap1- Interacting factor
Rpd3	Reduced potassium dependency
rDNA	Ribosomal DNA
RENT complex	Regulator of nucleolar silencing and telophase
RNA	Ribonucleic acid
Rrm3	Rdna recombination mutation
rRNA	Ribosomal RNA
RSC	Remodel the structure of chromatin
Sas2	Something about silencing 2
Sir complex	Silent information regulator complex
Sir1	Silent information regulator 1
Sir2	Silent information regulator 2
Sir3	Silent information regulator 3
Sir4	Silent information regulator 4
Snf1	Sucrose nonfermenting
TAS	Telomere associated sequences
TFIIIB	Transcription factor III C
TFIIIC	Transcription factor III B
TOR	Target of rapamycin
TPE	Telomere position effect
tRNA	Transport RNA

Brief Thesis Overview

This manuscript begins with introductory chapters (1-4) which provide the necessary theoretical background and synthesize parts of the growing body of knowledge on heterochromatin in budding yeast.

Chapter 5 presents the thesis results, methodology and discussion in the form of a research article, which currently awaits submission. The article is self-contained and includes a list of references. The references cited in the introductory chapters are listed in Chapter 6.

1 HETEROCHROMATIN IN BUDDING YEAST

In eukaryotes, nuclear DNA associates with histone proteins to form a complex called chromatin. In this form, the linear and relatively long DNA double helix is able to fit inside the tiny nucleus, thus restraining the organism's genome to a specialized compartment. However, chromatin provides more than just a packaging arrangement. Both DNA and histones are sites of extensive post-translational modifications that alter the accessibility of the DNA template to a variety of processing enzymes. This system orchestrates gene expression programs in response to environmental and developmental cues and consequently maintains all processes necessary for cell function (Grewal & Moazed, 2003). The study of changes in gene function that are mitotically and/or meiotically heritable and are not caused by a change in DNA sequence is commonly defined as epigenetics (Wu & Morris, 2001). Researchers have been focusing on elucidating the variety of mechanisms by which a cell modifies the chromatin template in both physiological and pathological circumstances in order to define the role of chromatin in epigenetic processes (Grewal & Moazed, 2003).

In the late 1920s, Emil Heitz developed a staining technique to help visualize nuclear components of liverworts during the cell cycle. By comparing differentially stained regions, he discovered chromatin is comprised of two distinct regions he named euchromatin and heterochromatin. Euchromatin regions were stained solely during mitosis, while heterochromatin regions retained the stain throughout the cell cycle. He further noted certain heterochromatin regions were stained in a cell-specific manner and named them facultative heterochromatin. Other heterochromatin regions, however, remained a common feature of all examined cells and he appropriately named them constitutive heterochromatin. Almost a century later, our understanding of differences in chromatin composition and function goes beyond different levels of compaction and stain retention to include a more nuanced molecular understanding of euchromatin and heterochromatin respectively (for review see Allshire & Madhani, 2017).

Genetically, euchromatin is defined as the transcriptionally active, gene rich form of chromatin bearing specific DNA and histone modifications. The most common molecular features of euchromatin include the presence of acetylated histones, specific histone variants and dynamic histone turnover during DNA-transaction processes (i.e. transcription, replication, recombination and repair). On the other hand, heterochromatin is the transcriptionally inactive (silenced) and gene-depleted form of chromatin, often associated with developmentally-regulated genes (facultative heterochromatin) and repetitive, structural regions (constitutive heterochromatin). The compaction level of facultative heterochromatin may vary depending on different environmental cues that drive specific expression patterns during differentiation and development of multicellular organisms. Molecularly, heterochromatin of most eukaryotes is defined by the presence of specific histone methylations (e.g. H3K9me and H3K27me for facultative and constitutive heterochromatin, respectively), heterochromatin-forming proteins (HP1 and Polycomb for constitutive and facultative heterochromatin, respectively) and noncoding RNAs (Martienssen & Moazed, 2015; Wang, Jia, & Jia, 2016). Some eukaryotes, such as *Saccharomyces cerevisiae* (hereafter referred to as yeast), lack certain heterochromatin hallmarks like specialized histone methylations present in other eukaryotes. Despite these differences, yeast chromatin still possesses the same functional and structural distinctions typical of heterochromatin and euchromatin in other eukaryotes and thanks to its small compact genome it is a model organism of choice to study chromatin organization and dynamics on a genomic scale (Bühler & Gasser, 2009).

Yeast are unicellular eukaryotes widely used for a variety of fermentation processes, including baking and winemaking. In addition to their practical utility, yeast have been used for decades as a model organism in molecular biology. They share the complex intracellular organization and most fundamental chromatin features with other eukaryotes. However, as unicellular organisms with a simpler genome, they are more amenable to experimental manipulations and genome-wide studies. Furthermore, they provide a less artificial and more biologically relevant experimental system for probing the influence of environmental changes on chromatin structure and gene expression than cell culture systems from multicellular

organisms (Botstein & Fink, 2011). Yeast has also some singular genomic features, including a global enrichment in transcriptionally-active regions and a relatively low percentage of repetitive regions. Functionally, the yeast genome can still be divided into euchromatin and heterochromatin based on their specific chromatin landscapes (Figure 1).

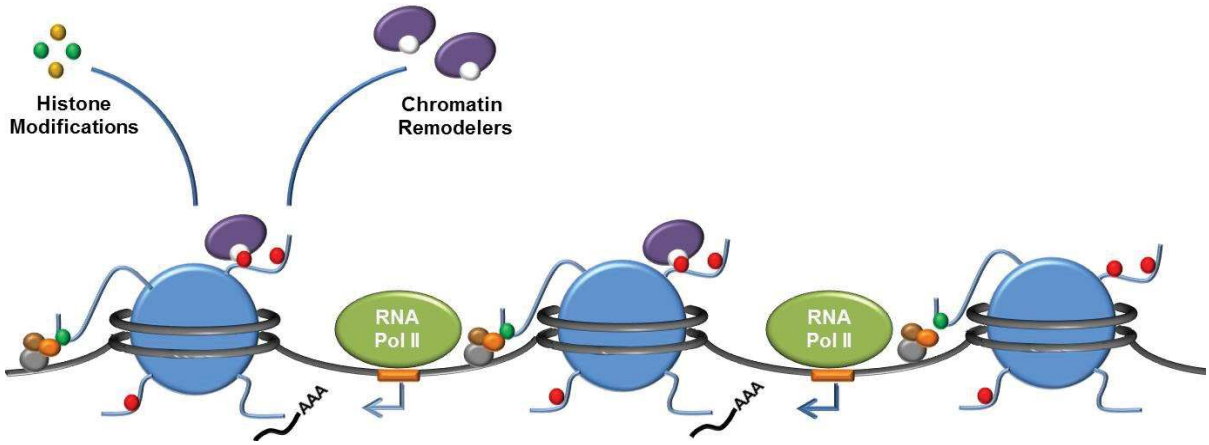

A) Euchromatin

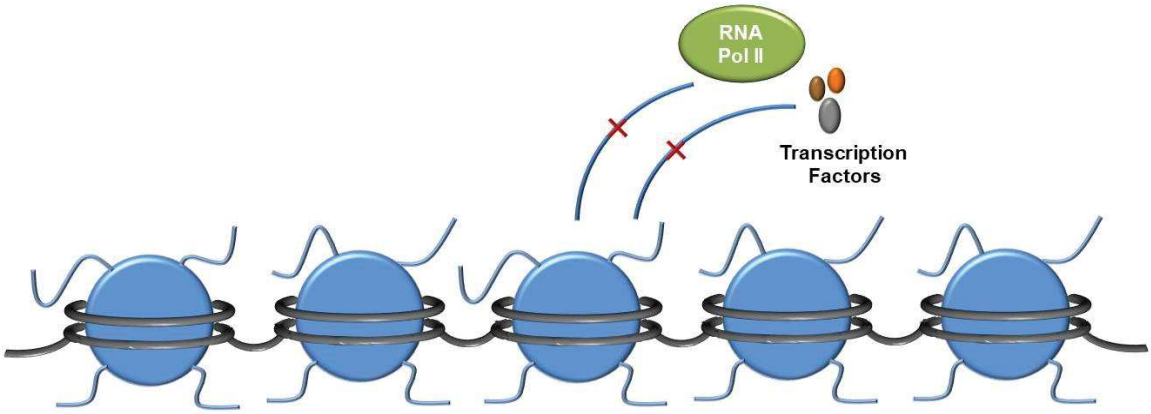

B) Heterochromatin

Figure 1: Euchromatin and heterochromatin in yeast (modified from Croken, Nardelli, & Kim, 2012). (A) Euchromatin is the transcriptionally active and less structurally condensed form of chromatin enriched in nucleosomes which bear active marks (e.g. acetylated and methylated lysines) and associated factors (e.g. active remodelers and template-processing enzymes). (B) Heterochromatin is the transcriptionally inactive and more structurally condensed form of chromatin that lacks the majority of histone marks and other euchromatin hallmarks. A bare-bones structure critical for the overall stability and integrity of chromatin.

Similar to constitutive heterochromatin in other eukaryotes, yeast heterochromatin is formed in a domain-specific manner comprising kilobase-stretches of DNA (Gartenberg & Smith, 2016). There is, however, no RNA interference mechanisms guiding the formation of the repressive structure and most histone modifications are completely depleted, leaving a relatively bare-bones silent region compared to other eukaryotes (Briggs et al., 2001; Wood, Tellier & Murphy, 2018). Despite the abovementioned structural differences, the general locus-inactivating function of heterochromatin remains the same in yeast. Heterochromatin regions are dynamic structures that silence specific genes and thus ensure the stability and integrity of the genome. Gene silencing can however be reversed if heterochromatic complexes are disassembled in response to environmental signals or simply as a consequence of the stochasticity inherent to the cellular processes that maintain chromatin structure (Gartenberg & Smith, 2016).

Based on the prevalent steric hindrance model, heterochromatin domains achieve functionality by blocking access of transcription factors and other template-processing enzymes to the underlying DNA. Heterochromatin domains are anchored at the nuclear periphery. The localization of heterochromatin away from the rest of the genome is thought to minimize promiscuous silencing of critical, transcriptionally-active regions by physically separating silencing factors from euchromatin (for review see Gartenberg & Smith, 2016).

There are three well-defined heterochromatin domains in yeast: the silent mating type loci, subtelomeric regions and rDNA repeats described below (Fourel et al, 1999; Gottschling, 1992).

1.1 Silent mating type loci

In favorable growth conditions with sufficient nutrient availability, yeast are able to propagate by simple cell division (vegetatively), either as haploid or diploid cells, although they are predominantly diploid in their natural environment outside of the laboratory. In fact, the ability of yeast to form diploids proves to be critical for

survival when nutrients become scarce. Endangered by limiting nutrient conditions, diploids enter sporulation (meiosis) and produce four dormant spores, thereby extending survivability until favorable metabolic conditions are restored. Successful conjugation depends largely on the configuration of the mating type (MAT) locus on chromosome III (Haber, 2012).

The MAT locus can contain either the a (*MATa*) or α (*MATα*) cassette. Only haploids of opposing mating types (*MATa* or *MATα*) can successfully conjugate and form a diploid cell. Unlike *MATa* gene products, the function of *MATα* genes is much better understood. *MATα* can produce two functional products: α1 and α2. α1, together with the transcriptional factor Mcm1 (**M**in**iC**hromosome **M**aintenance), induces transcription of several genes, including the α-factor pheromone and a *trans*-membrane receptor for the opposite mating pheromone (a-factor). On the other hand, α2 and Mcm1 repress a-specific genes, including those that encode for a-factor and the α-factor *trans*-membrane receptor. Consequently, *Matα* cells secrete α-factor pheromones which bind to receptors on *MATa* cells in the population and vice-versa. The binding of pheromones to their corresponding surface receptors triggers a signaling cascade, which prepares cells for mating and induces G1 arrest, thus ensuring that the newly-formed diploids contain homologous, but unreplicated chromosomes (Haber, 2012).

The mating type identity is not fixed. Yeast evolved a remarkable mechanism by which they can freely switch their mating type, a process called homothallism. Switching includes a gene conversion event by which additional donor loci containing a or α sequences replace α or a in the *MAT* locus, respectively. Since simultaneous transcription of both a and α sequences destabilizes the mating identity of the cell, both donor sequences (a and α) are packaged into transcriptionally repressed heterochromatin domains called silent mating type loci. These two silent mating type loci are located on chromosome III, upstream (*HMLα*) and downstream (*HMRa*) of the *MAT* locus (Jensen, Sprague, & Herskowitz, 1983; Nasmyth & Tatchell, 1980).

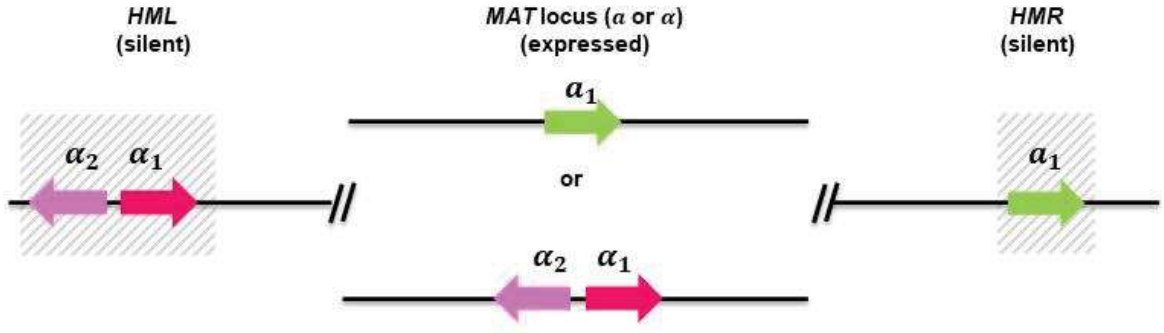

Figure 2: A schematic representation of the mating type locus (MAT) and silent mating type loci (HMLα and HMRa) on chromosome III (modified from Hanson & Wolfe, 2017). The *MAT* locus designates the mating phenotype of the haploid cell by containing either the a or the α sequence. Only haploid cells with opposing mating types can form a diploid, but in natural conditions, haploid cell are able to freely switch their mating type by recombining the *MAT* locus with either *HMLα* or *HMRa*. Both *HMLα* and *HMRa* are transcriptionally repressed to avoid destabilizing the identity of the cell.

Mating type switching is restricted to the G1 phase of the cell cycle and is triggered by the site-specific endonuclease HO (**HO**mothallic switching endonuclease). After a haploid mother cell divides, the daughter cell asymmetrically inherits an HO repressor. The loss of the HO repressor stimulates the activity of HO, leading to the cleavage of the *MAT* locus and transfer of the opposite donor sequence (*HMLα* or *HMRa*) in a unidirectional way. The heterochromatin structure of the silent mating type loci protects the underlying sequences from HO dependent cleavage thus ensuring the directionality of the gene conversion event and preventing the replacement of silent mating type sequences. The reactivation of the HO repressor in diploid cells suppresses mating type switching until spore germination (Haber, 2012; Jensen et al., 1983).

In conclusion, heterochromatin at silent mating type loci is critical for maintaining the cellular identity and genomic stability in yeast. Heterochromatin prevents DNA cleavage of silent mating type loci by HO and represses transcription

of potentially deleterious DNA sequences during critical physiological processes - a recurring theme in the biological function of heterochromatin.

2.2 Subtelomeric regions

One of the defining characteristics of eukaryotic chromosomes is the association of linear DNA molecules with histone proteins. Yeast chromosomes are linear molecules terminating in well-defined ends called telomeres, which can form high-order structures facilitated by specific protein-protein interactions. Telomeric DNA is highly repetitive and heterogeneous, consisting of 300 ± 75 bp repeats, usually abbreviated $C_{1-3}A/TG_{1-3}$. Furthermore, telomeres are not blunt ends, but rather contain G-rich tails. The size of the tails depends on the cell cycle and ranges from around 15 to almost 100 G nucleotides in late S/early G2 phase. The process of generating G tails occurs after genomic replication by degrading the complementary C strand of the newly-synthesized CG repeats, leaving only a series of G nucleotides. G tails are substrates for telomerase, an enzyme with reverse transcription activity necessary for maintaining telomere length after each round of genomic replication, and preserving the structural integrity of yeast chromosomes. Telomeres are not mere chromosome caps, they are also highly dynamic regions where both euchromatin and heterochromatin intersect (Wellinger & Zakian, 2012).

Yeast chromosomes contain repetitive sequences located in close proximity to telomeric DNA. These sequences are often referred to as subtelomeric regions or telomere associated sequences (TAS). TAS are highly-variable in number and size, but usually consist of two repetitive patterns called X and Y' elements (Figure 3). Y' elements are usually present immediately downstream of telomeric repeats in zero to four tandem copies ranging in size from 6.7 (Y' long) to 5.2 kb (Y' short). The location and presence of Y' elements is both strain and chromosome-specific with some TAS completely lacking associated Y' elements. X elements, on the other hand, are indispensable parts of all subtelomeric regions. They consist of a series of repeats whose composition varies from one chromosome end to another (Fourel et al., 1999).

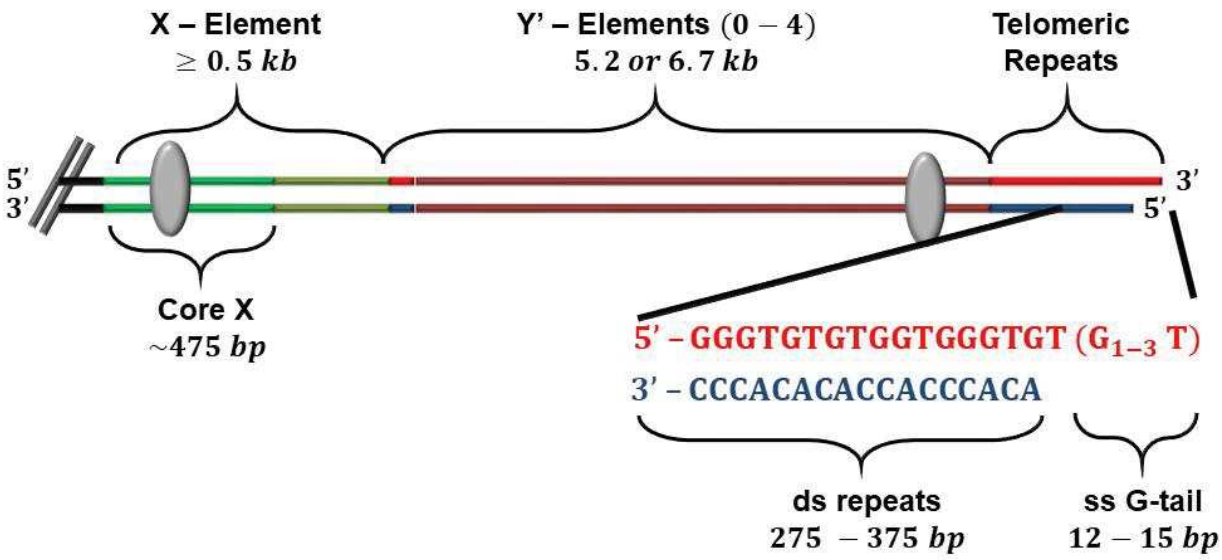

Figure 3: DNA elements of a conventional yeast telomere and the adjacent subtelomeric region (modified from Wellinger & Zakian, 2012). Telomeric DNA is heterogeneous but typically contains 300 ± 75 bp repeats (abbreviated $C_{1\text{-}3}A/TG_{1\text{-}3}$) and a G-rich tail readily processed by telomerase during telomere maintenance. Subtelomeric regions typically contain either XY or X-only elements. The Y elements are areas of active chromatin, whereas X elements and proximal regions have features of heterochromatin silencer regions (i.e. low nucleosome density and lack of histone modifications).

TAS can be characterized as XY' or X-only regions, based on the presence of X and Y' elements. X elements are similarly organized in both XY' and X-only regions and share common features with known silencer regions which serve as heterochromatin nucleation sites. These features include low nucleosome density, the absence of histone modifications and the presence of binding sites for silencing factors. On the other hand, distal Y' elements of XY' regions contain high nucleosome density, histone modifications and factors associated with active chromatin (Wellinger & Zakian, 2012).

A number of studies have shown that telomeres and associated regions are anchored to the inner nuclear membrane where they form small clusters. This particular nuclear organization could potentially have a regulatory role by

sequestrating silencing factors to the nuclear periphery. According to this hypothesis the isolation of heterochromatic repressors from euchromatin would prevent the unwanted silencing of transcriptionally active regions. Subtelomeres contain a variety of conditionally-expressed genes involved in the stress response, rapamycin resistance and the metabolism of nonstandard carbon sources. These genes are repressed under standard growth conditions due to their proximity to heterochromatinized subtelomeric regions (position effect). Changes in the cellular environment, can however trigger the release of silencing factors from subtelomeric heterochromatin domains and activate these genes in order to preserve cell survival (Taddei et al., 2009; Wellinger & Zakian, 2012).

In summary, subtelomeric heterochromatin is thought to protect the structural integrity of chromosome ends and to serve as a regulatory mechanism that ensures the rapid activation of stress-related genes in response to environmental challenges.

1.3 rDNA

Ribosomal RNA (rRNA) is a major component of ribosomes, RNA-protein complexes necessary for protein biosynthesis. In yeast, genes encoding rRNA molecules (rDNA) are contained in a 9.1-kb locus present in 150 to 200 tandem copies on chromosome XII. The rDNA locus forms a distinct nuclear structure called the nucleolus, which is localized at the nuclear periphery. Given the importance of proteins as effectors of biochemical processes, it is not surprising that rDNA transcription accounts for ~ 60% of cellular transcription in yeast. The rDNA array is normally accessible only to Pol I and Pol III transcription, while Pol II transcription is repressed by the RENT complex (**RE**gulator of **N**ucleolar **S**ilencing and **T**elophase). The RENT complex includes the Sir2 protein (Silent Information Regulator 2) a component of yeast heterochromatin complexes. However, unlike the silent mating type loci and subtelomeric regions, rDNA silencing only requires the the Sir2 subunit of the Sir complex discussed below (Gartenberg & Smith, 2016; Smith & Boeke, 1997).

The rDNA array is organized into repeats containing the Pol I-transcribed 35S precursor rRNA that are separated by small intergenic regions, which contain 5S rRNA transcribed with Pol III flanked by two non-transcribed spacers: NTS1 and NTS2 (Figure 4). The spacers contain binding sites for the RENT complex whose main function is to silence Pol II dependent transcription of NTS1/2 which destabilizes rDNA (Gartenberg & Smith, 2016).

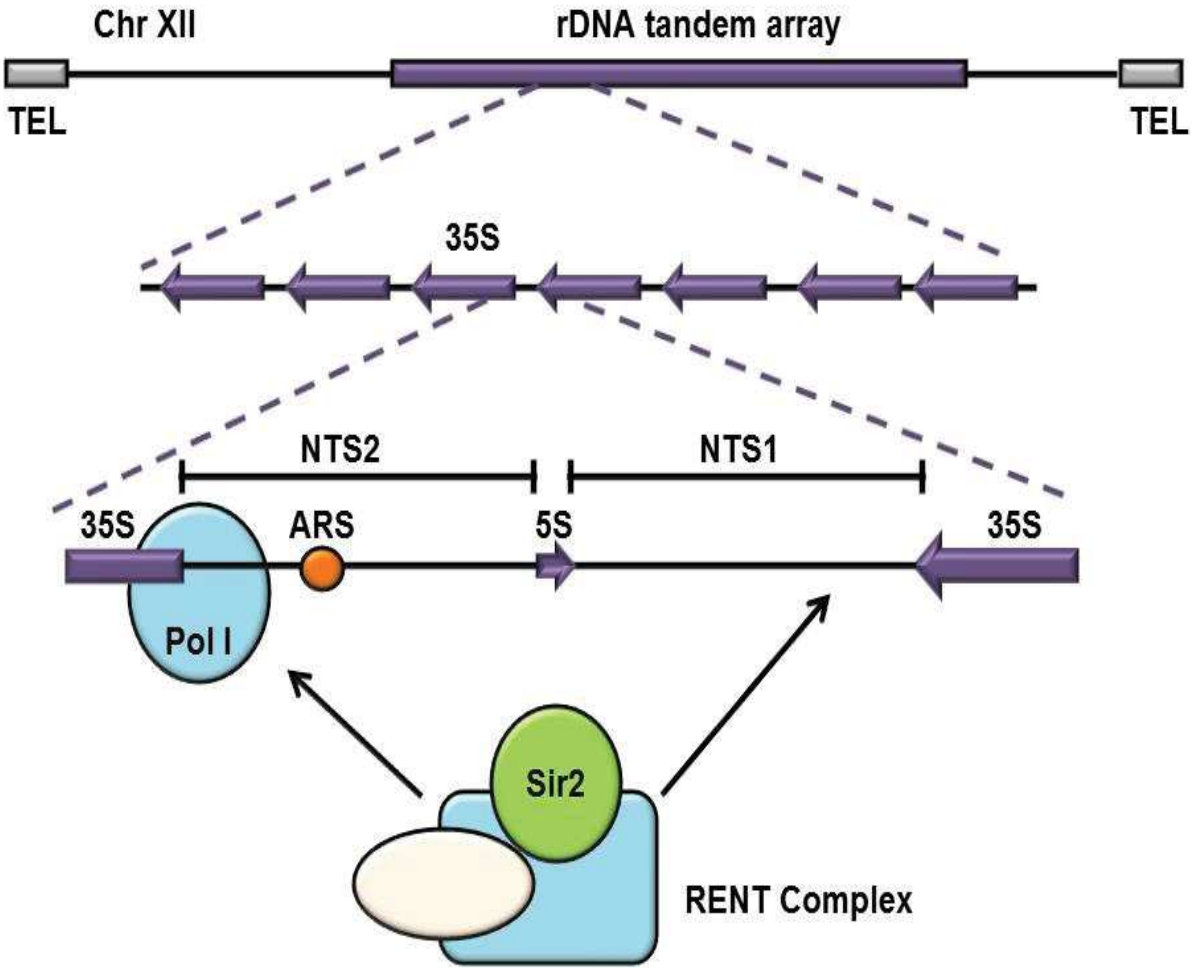

Figure 4: Organization of the rDNA array on chromosome 12 (modified from Gartenberg & Smith, 2016). The array consists of 150-200 repeats of 9.1 kb. Each repeat contains the transcriptional unit of the 35S precursor rRNA transcribed by Pol I. Between repeats lies the intergenic region consisting of the spacer NTS1, the 5S rRNA gene (transcribed by Pol III) and the spacer NTS2. Both spacers contain binding sites for the RENT complex which serves as the mediator of rDNA silencing and stabilization.

Despite the repetitive nature of the rDNA array, unequal chromatid exchange events rarely occur due to Sir2-mediated silencing. Indeed, aberrant Sir2 expression or function can render rDNA repeats highly unstable and promote recombination events which result in the formation of ERCs (**E**xtrachromosomal **r**DNA **C**ircles). ERCs contain their own ARS (**A**utonomously **R**eplicating **S**equence) allowing circle replication during S phase. It has therefore been proposed in one ERC-centric model of aging, that the asymmetrical accumulation of ERCs in mother cells eventually results in the sequestration of essential replication and transcription factors from the rest of the genome, which would then theoretically cause senescence and cell death (Gartenberg & Smith, 2016; Saka, Ide, Ganley, & Kobayashi, 2013).

In conclusion, rDNA silencing recapitulates previously established heterochromatin features. The accumulation of silencing factors, renders rDNA refractory to Pol II transcription and recombination, thus ensuring genomic stability and correct rDNA expression.

2 MOLECULAR FEATURES OF HETEROCHROMATIN

Despite individual differences and domain-specific particularities, three distinctive molecular features of heterochromatin domains can be generalized:

a) The presence of specific DNA sequences (silencers) and silencer-binding factors which recruit silencing proteins to designated domains.
b) The presence of silencing proteins, which form a complex called Sir (**S**ilent **I**nformation **R**egulator).
c) The depletion of all known histone modifications (most importantly, the acetylation of H4K16 and methylation of H3K79 and H3K4) (Gartenberg & Smith, 2016).

The following subchapters will provide more details on one of these molecular features.

2.1 Silencers and their binding factors

Silencers are *cis*-acting regulatory sequences which flank heterochromatin domains. They contain their own ARS (**A**utonomously **R**eplicating **S**equence) and binding sequences for factors that recruit Sir proteins, with the exception of NTS regions in rDNA repeats that seem to recruit the RENT complex without the mediation of silencer-binding factors (Figure 5) (Gartenberg & Smith, 2016). While silencer binding factors, namely, Rap1 (**R**epressor **A**ctivator **P**rotein), Abf1 (**A**RS **B**inding **F**actor) and ORC (**O**rigin **R**ecognition **C**omplex) (Bi, 2014; Cuperus, Shafaatian, & Shore, 2000)- individually perform different functions unrelated to heterochromatin, it is the additive effect of their collective binding to silencers that appears to be critical for the recruitment of the Sir complex (Bi, 2014; Cuperus et al., 2000).

Rap1 is an essential and multifunctional yeast protein implicated in the transcriptional regulation of different genomic loci. In addition to its role in heterochromatin establishment, Rap1 functions as a transcriptional activator of many genes, including glycolytic enzymes and ribosomal proteins. Rap1 is also recruited to the highly repetitive telomeric DNA where it maintains telomere-length homeostasis

by inhibiting telomere fusion and DNA damage response pathways (Feldmann & Galletto, 2014; Negrini, Ribaud, Bianchi, & Shore, 2007). Structural studies identified three functional Rap1 domains in yeast. Two central Myb domains responsible for DNA binding and a C-terminal RCT domain responsible for Sir3/4 interaction (in telomere silencing) and Rif1/2 (**R**AP1-**I**nteracting **F**actor) interaction (in telomere length homeostasis). A conserved binding module of the RCT domain is evolutionary conserved, but seems to play different roles in mammals (telomere regulation and protection) and yeast (silencing) (Chen et al., 2011). Additionally, Rif1 and Rif2 seem to recruit and stabilize Rap1 binding at telomeric DNA (telosome) where they form a heterogeneous assembly (molecular Velcro). According to this binding model, Rif1 and Rif2 provide weak multivalent binding modules for Rap1 thereby conferring plasticity to the telosome - rapid disassembly in S phase and stability in other phases of the cell cycle. Interestingly, Rif1 and Rif2 structural motifs, which form a part of the Velcro architecture, seem to directly and functionally compete with Sir3 binding to Rap1 (Shi et al., 2013).

Like Rap1, Abf1 is an essential protein. It is involved in DNA replication initiation, transcriptional regulation of many metabolic gene and nucleotide excision repair (Yu et al., 2009).

Finally, ORC's main function is to bind replication origins in a process called origin licensing that primes and prepares origins for replication (Hoggard, Shor, Müller, Nieduszynski, & Fox, 2013).

ORC also recruits Sir1 to silencers. Unlike the other Sir subunits, which are the structural building blocks of heterochromatin, Sir1 functions as a molecular adaptor, that facilitates heterochromatin establishment mostly at silent mating type loci. Experimental evidence suggests that Sir1 promotes the establishment of the silent state but does not appear to be necessary for its transmission to subsequent cell generations. The loss of Sir1 disrupts silencing at silent mating type loci, resulting in a phenotypically mixed population of cells. Some cells within the population are able to silence one or both mating type loci, while others fail to silence either. These findings illustrate perfectly why yeast heterochromatin has been considered ever since its discovery as a prime example of epigenetic regulation of gene expression (Gardner & Fox, 2001; Pillus & Rine, 1989a).

Some heterochromatin regions also contain specific sequences called proto-silencers that can enhance silencer function. Proto-silencers include individual binding sites for Rap1, Abf1 and ORC, which in isolation and in the absence of a silencer do not contribute to Sir recruitment (Lebrun et al., 2001). *PAU* (seripauperin) genes seem to act as proto-silencers aiding Sir recruitment at some subtelomeric regions. Interestingly, the expression of these genes is induced in stressful conditions which coincide with Sir3 hyperphosphorylation and subsequent delocalization from telomeres. These findings further demonstrate the plasticity of heterochromatin and its responsiveness to environmental changes (Radman-Livaja et al., 2011).

Despite the differences in structure and localization, silencers of silent mating type loci and (sub)telomeric regions share the same Sir-recruitment function (Figure 5).

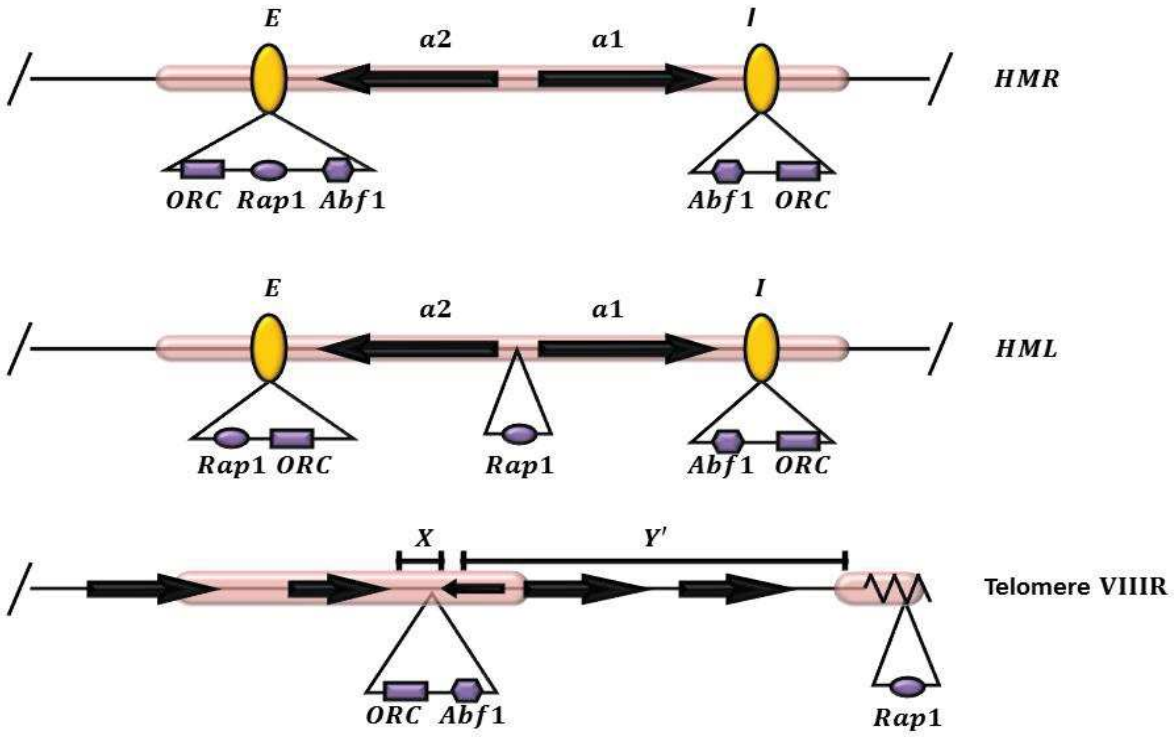

Figure 5: Silencers and silencer-bound factors at silent mating type loci and telomeres (modified from Gartenberg & Smith, 2016). At silent mating type loci, E and I silencers contain binding sites for Rap1, Abf1 and ORC. On the other hand, at telomeres, Rap1 binds telomeric repeats, while ORC and Abf1 bind X elements. Both telomeric repeats and X elements function as silencers. Peak repression is found at the autonomously replicating sequence of the X element.

In early experiments, the two silencers from each silent mating type locus were named E ("essential") and I ("important") based on their "importance" in the establishment of the silent state. This is somewhat misleading because the E silencer is sufficient for Sir recruitment to HMR, but either one is sufficient for Sir recruitment to HML. Silencers from both loci contain binding sites for at least two silencer-binding factors (Rap1, Abf1 or ORC). Telomeres, on the other hand, contain two distinct Sir-recruitment sites: $TG_{1\text{-}3}$ repeats enriched for the telomere-maintaining Rap1 and subtelomeric X elements enriched for Abf1 and ORC. Sir-mediated silencing is at its peak at the autonomously replicating sequence of X elements (Pryde & Louis, 1999; Radman-Livaja et al., 2011; Weber & Ehrenhofer-Murray, 2010).

In conclusion, silencers and their binding factors represent the first critical step of heterochromatin assembly, which is the recruitment of the Sir complex.

2.2 Sir complex

Each Sir subunit provides a unique activity necessary for the establishment and maintenance of heterochromatin domains as described below (Kueng, Oppikofer, & Gasser, 2013).

2.2.1 Sir2

Sir2 is a NAD^+ (**n**icotinamide **a**denine **d**inucleotide)-dependent histone deacetylase which belongs to a conserved family of proteins called sirtuins. Sirtuins are ubiquitous in all domains of life and implicated in a variety of processes, including genomic maintenance, aging, stress response and metabolic regulation (Dang, 2014). In yeast, Sir2 associates with partner proteins to form either the Sir or the RENT complex. The inherently weak Sir2 deacetylase activity is enhanced through conformational changes induced by interactions with the other subunits of the Sir or the RENT complex. This allosteric control of Sir2 activity ensures that its histone deacetylase activity is restricted to heterochromatin (reviewed in Gartenberg & Smith, 2016).

Sir2 consists of two distinct, independently folded domains. The N-terminal helical domain interacts with Sir4 and contains the regulatory module that targets Sir2 to heterochromatin loci. The C-terminal domain is the catalytic module responsible for substrate transformation by coupling NAD^+ breakdown to the removal of the acetyl group from lysine 16 on histone 4 (H4K16). The NAD^+-binding cleft is wedged in between the N-terminal and the C-terminal domains (Figure 6) (Hsu et al., 2013; Min, Landry, Sternglanz, & Xu, 2001).

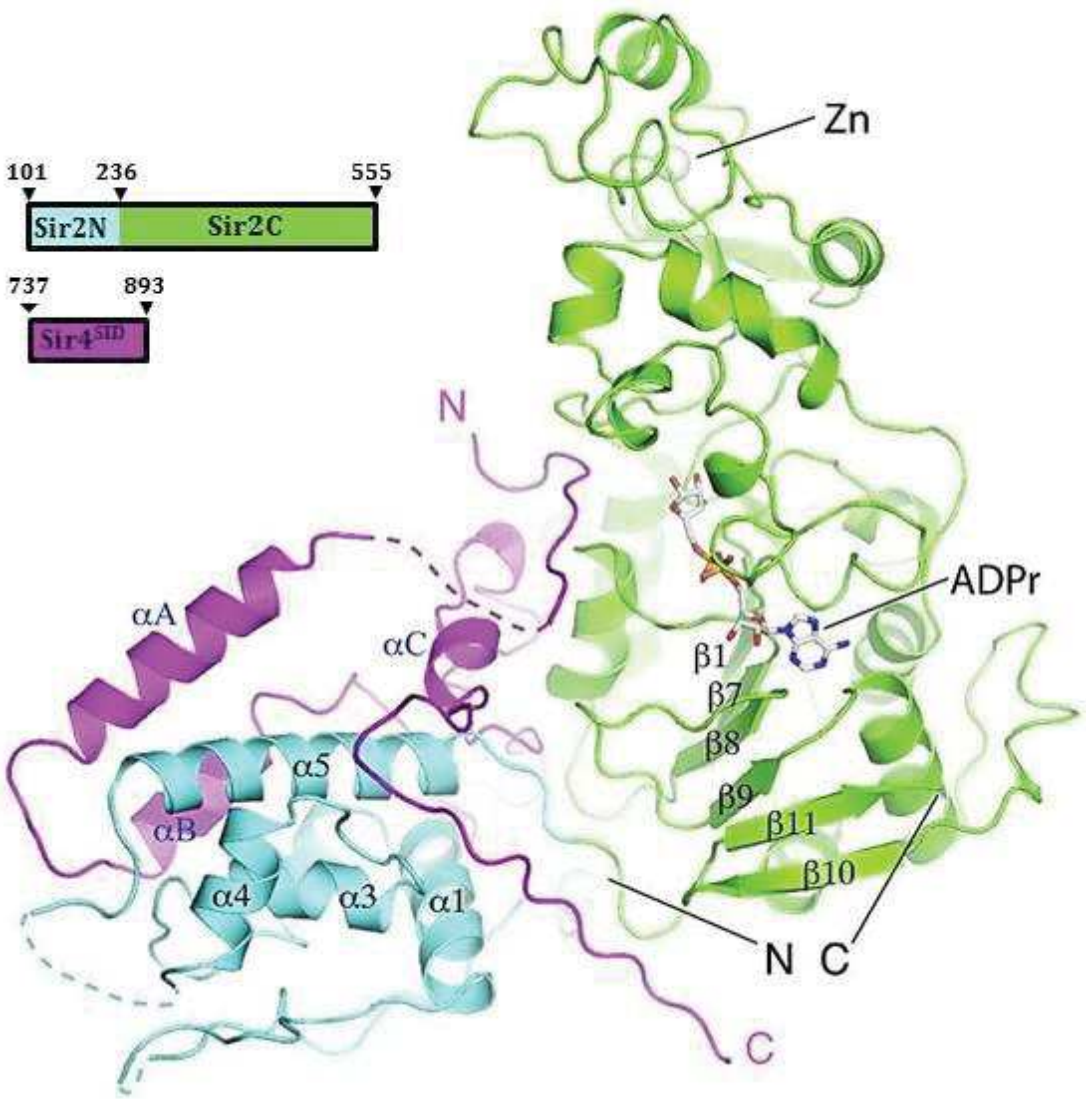

Figure 6: Sir2 structure **(Hsu et al., 2013).** The N-terminal domain (cyan) interacts with Sir4 (magenta). The C-terminal catalytic domain (green) binds and transforms reaction substrates (NAD+ and acetylated H4K16), ADP ribose (ADPr) appears in the crystal in the NAD+ binding site due to nicotinamide hydrolysis during crystallization. Additionally, the C-terminal domain contains a zinc ion pocket important for substrate positioning and transition state stabilization.

The Sir2-mediated deacetylation of H4K16ac is a group transfer reaction. The acceptor of the acetyl group is the ADP-ribose moiety of NAD+. The transfer of the acetyl group to ADP-ribose is coupled to the thermodynamically favorable NAD^+ hydrolysis, which ultimately yields three products: NAM (**n**icotin**am**ide), OAADPr (**O**-**a**cetyl-**A**DP-**r**ibose) and the deacetylated H4K16 (Figure 7) (Sauve, 2010; Tanny, Dowd, Huang, Hilz, & Moazed, 1999).

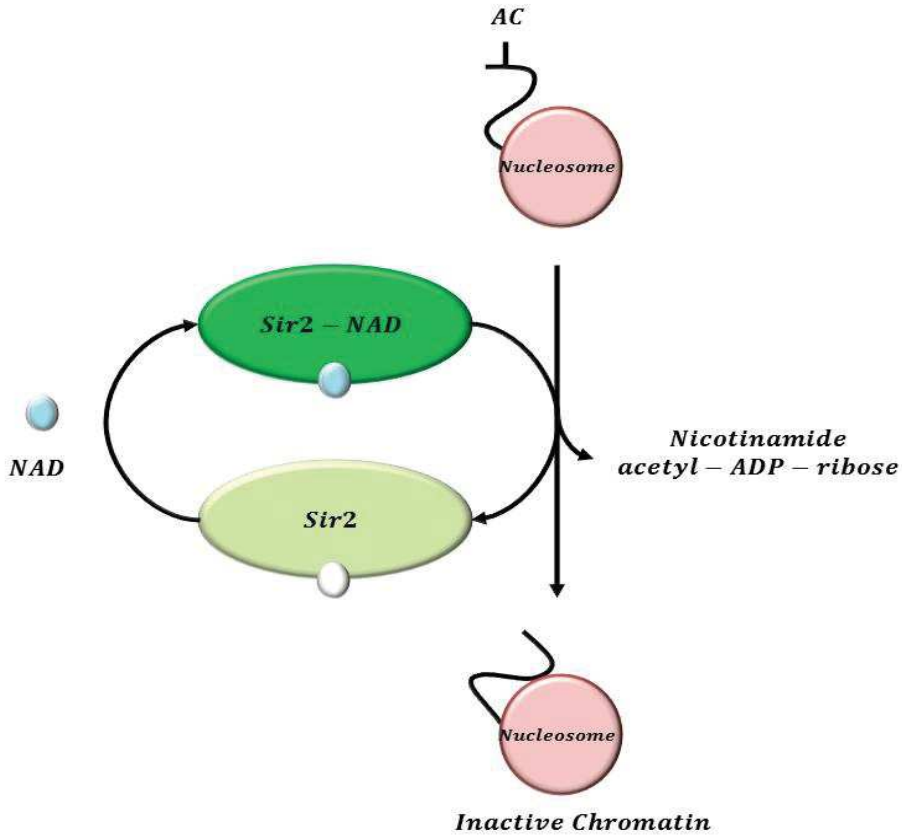

Figure 7: Sir2-mediated histone deacetylation (modified from Imai & Wilson, 2002). Sir2 facilitates the transfer of the acetyl group from H4K16 to ADP-ribose by coupling it to the thermodynamically favorable NAD^+ hydrolysis. In the end, three products are formed: NAM, OAADPr and the deacetylated histone.

NAM is a non-competitive inhibitor of Sir2 both *in vitro* and *in vivo*. The yeast nucleus is enriched for NAD^+ salvage pathway enzymes which are able to convert NAM into NAD^+, thereby restoring Sir2 activity. Pnc1 (pyrazinamidase / nicotinamidase) is responsible for converting NAM into NA (**n**icotinic **a**cid). Afterwards, Npt1 (**n**icotinate **p**hosphoribosyl**t**ransferase) converts NA into NaMN (nicotinic acid mononucleotide) before merging with the *de novo* NAD^+ synthesis

pathway (Kato & Lin, 2014; Sauve, Moir, Schramm, & Willis, 2005). The cross-talk between the *de novo* and salvage pathways regulates intracellular NAD^+ levels and, indirectly, Sir2-mediated silencing. Deleting any of the salvage pathway enzymes can completely abolish Sir2 function, further demonstrating the critical link between Sir2, NAD^+ and associated derivatives (Kato & Lin, 2014; Sauve, Moir, Schramm, & Willis, 2005).

The importance of NAM in feedback inhibition of Sir2 activity raised the question whether OAADPr might have a similar function. Initial, *in vitro*, binding experiments suggested that OAADPr contributes to the efficient binding of Sir complex to nucleosome arrays (Liou, Tanny, Kruger, Walz, & Moazed, 2005). *In vivo* studies observed defects in Sir3 binding and diminished Sir3-Sir3 and Sir3-Sir4 interactions in a strain carrying mutations of the putative OAADPr Sir3 binding site. Furthermore, when the heterochromatin boundary deacetylase Rpd3 (**R**educed **P**otassium **D**ependency 3) was targeted to heterochromatin regions, Sir complex spreading was halted. Due to the removal of the Sir2 substrate (H4K16ac) by Rpd3, no OAADPr could be produced, thus rendering Sir complex unable to effectively spread (Ehrentraut, Weber, Dybowski, Hoffmann, & Ehrenhofer-Murray, 2010). However, heterochromatin formation was not compromised when an NAD^+-independent deacetylase fusion with Sir3 was used instead of Sir2 in a strain that lacks all OAADPr-generating enzymes (including Sir2), thus casting doubt on the importance of OAADPr in modulating Sir complex activity (Chou, Li, & Gartenberg, 2008).

The role of the enzymatic activity of Sir2 is to generate high-affinity binding sites for Sir3 and consequently promote the spreading of heterochromatin domains (Kueng et al., 2013). On the other hand, the deacetylase activity of Sir2 induces structural changes in the underlying chromatin template that are necessary for silencing, but it is not required for RENT binding (Hoppe et al., 2002). Sir2 is also implicated in the extension of the cellular lifespan caused by caloric restriction (CR). Empirically, CR is defined as the reduction of glucose concentration in yeast-growth media from 2% to 0,5%. In response to CR, Pnc1 levels increase, consequently

elevating NAD^+ levels, decreasing NAM levels and ultimately stimulating Sir2 activity. However, the exact mechanism by which Sir2 activity causes the longevity effect is still unknown (Imai & Guarente, 2016; Kato & Lin, 2014).

In conclusion, Sir2 is an important NAD^+-dependent histone deacetylase linking cellular metabolism, genomic maintenance and aging.

2.2.2 Sir3

Unlike Sir2, Sir3 functions primarily at heterochromatin domains, where it serves as a nucleosome-binding protein (Kuenget al., 2013). Sir3 consists of three well-defined domains: the N-terminal BAH (bromo-adjacent) domain- the domain with the highest similarity to the corresponding Orc1 BAH domain (Ehrentraut et al., 2011), the central AAA^+ ATP-ase-like domain and the C-terminal winged-helix domain (Bell, Mitchell, Leber, Kobayashi, & Stillman, 1995) (Figure 8) .

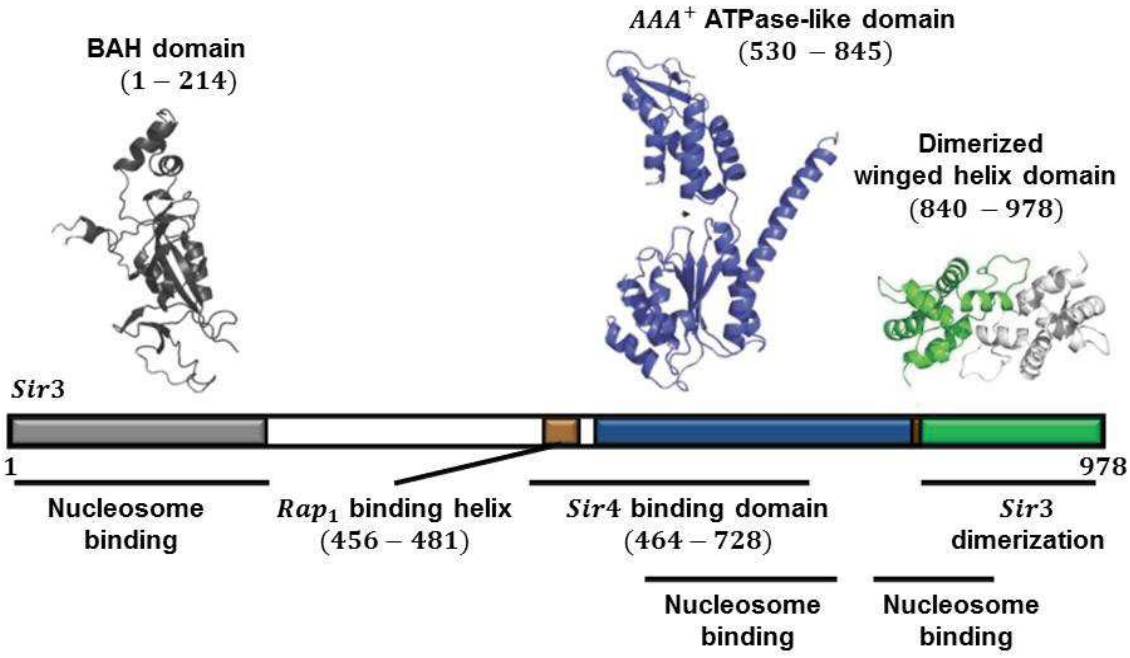

Figure 8: Structure and function of Sir3 domains (modified from Gartenberg & Smith, 2016). The BAH domain is the nucleosome binding domain of Sir3, while the AAA+ ATPase domain mediates the interaction between Sir3 and Sir4/Rap1 at heterochromatin loci. The winged-helix domain enables Sir3 homodimerization.

Initial mutational studies revealed the BAH domain's central role as the mediator of nucleosome binding (Onishi, Liou, Buchberger, Walz, & Moazed, 2007). It was discovered later on that the BAH domain has the highest binding affinity for nucleosomes lacking acetylated H4K16. As previously discussed, the acetylation of H4K16 is removed by the catalytic activity of Sir2, which enables Sir3 binding and spreading of heterochromatin domains (Sampath et al., 2009).

Sir3 binding to H4K16 is greatly enhanced in the absence of methylation marks on H3K4 and H3K79. These modifications, generated by Set1 and Dot1 respectively, are associated with transcriptionally active regions. Paradoxically Set1 and Dot1 deletions actually reduce heterochromatin silencing because the absence of H3K4 and H3K79 methylation creates high affinity binding sites for Sir3 in euchromatic regions and titers the low abundance Sir3 proteins away from heterochromatic loci (Bernstein et al., 2002; Wood, Tellier, & Murphy, 2018b). Overexpressing Sir3 extends heterochromatin domains beyond the boundaries found in naturally limiting Sir3 conditions (Radman-Livaja et al., 2011). These findings suggest that Sir3 dosage and genomic methylation are tightly regulated in order to restrict heterochromatin domains within well-defined regions with discrete boundaries. However, a recent study revealed that Sir3 spreading at subtelomeric regions can reach saturation when Sir3 is overexpressed between 9x and 16x, indicating the presence of fixed borders which limit H3K79me and H3K79me2heterochromatin spreading (Hocher et al., 2018). Furthermore, telomeric regions, which normally form clusters at the nuclear periphery in limiting Sir3 conditions, aggregate into hyperclusters and move to the center of the nucleus when Sir3 is overexpressed. Interestingly, the silencing and clustering function of Sir3 are mediated by two different domains: the BAH and the winged helix domain, respectively. The formation of hyperclusters seems to further increases the local concentration of silencing factors and stabilize (sub)telomeric silencing (Ruault, De Meyer, Loïodice, & Taddei, 2011).

In addition to the BAH domain, Sir3 contains an AAA^+ ATPase-like domain. Unlike conventional AAA^+ domains found in ATP-binding enzymes, the Sir3 AAA^+ ATPase-like domain is catalytically inactive due to noncanonical amino acid residues that block the ATP-binding pocket. The domain is still critical for heterochromatin establishment because it provides a Sir4-interacting module. Although Sir3 can bind to naked DNA *in vitro*, it is found almost exclusively on deacetylated nucleosomes in vivo where it is stabilized through interactions with Sir4. Additionally, Sir3 is recruited to silencers through an interaction between a small region of the AAA^+ ATPase-like domain with Rap1 (Ehrentraut et al., 2011).

Lastly, Sir3 contains a winged-helix domain implicated in Sir3 dimerization. Sir3 dimerization is essential for stable loading of the Sir complex and repression of target genomic loci. The winged-helix domain can be replaced with another self-associating domain without compromising heterochromatin establishment. It is still unclear whether Sir3 dimers bind to one nucleosome or bridge two neighboring nucleosomes (Oppikofer et al., 2013).

2.2.3 Sir4

Sir4 is the least evolutionarily conserved subunit of the Sir complexes from the *Saccharomycetaceae* yeast family. Sir4 is essential for Sir complex assembly and the perinuclear localization of heterochromatin domains (Faure et al., 2019). It is composed of three structural domains: the N-terminal domain, the central domain and the C-terminal domain (Figure 9).

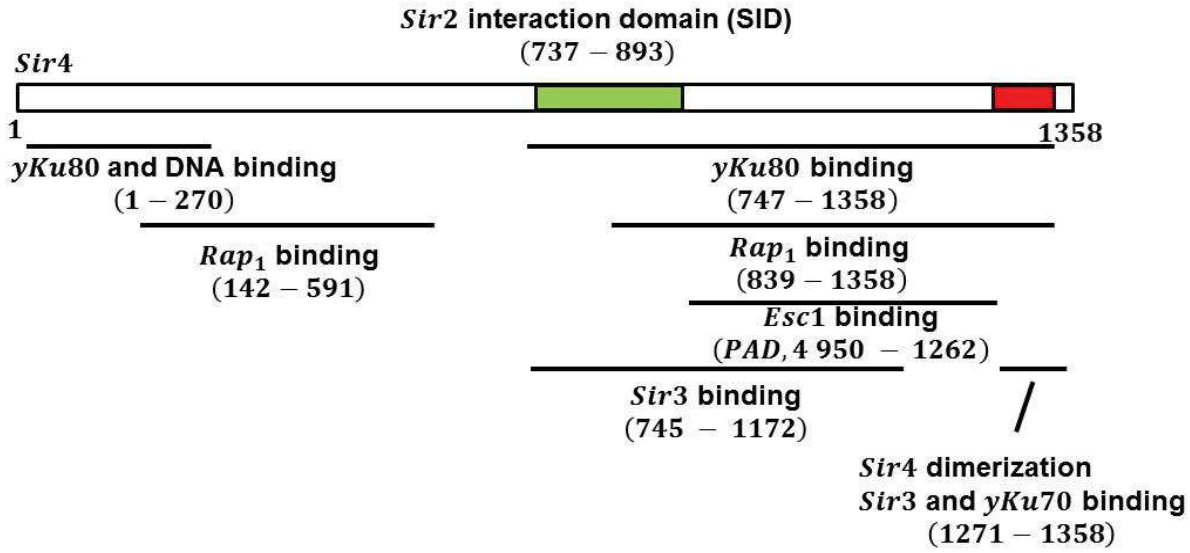

Figure 9: Functional organization of Sir4 domains (modified from Gartenberg & Smith, 2016). All three functional domains contain binding sites for various partner proteins. Unlike Sir2 and Sir3, Sir4 has a DNA binding domain, which is located in the N-terminal domain. The C-terminal coiled-coil domain interacts with Sir3 and mediates Sir4 dimerization.

Each one of these domains contains interaction modules for association with different partners, including yKu70/80 at telomeres, Rap1 at silencers and telomeric repeats, Sir1 at silent mating type loci, and finally Sir2 and Sir3. The central domain is responsible for interaction with Sir2, while the C-terminal coiled-coil interacts with Sir3 and enables Sir4 dimerizations, which are both critical for proper heterochromatin establishment. Sir4 facilitates Sir complex nucleation at silencers thanks to its DNA binding domain (Faure et al., 2019; Xu, 2003).

Sir4 functions as a scaffold for Sir2 and Sir3. It is also an allosteric regulator of Sir2's enzymatic activity and Sir3's binding to nucleosomes. Sir4 mutations that affect Sir4 dimerization and its interaction with Sir2 and Sir3 abolish silencing at silent mating type loci and subtelomeric regions but have no effect on rDNA silencing where only Sir2 is necessary for repression (Faure et al., 2019).

Sir4 also recruits the Sir complex to silencers through interactions with Sir1 and Rap1. Sir4 binding to silencers is independent of Sir2 and Sir3. Telomeric Rap1 and Ku proteins enrich Sir4 at telomeres through direct interactions (Hass & Zappulla, 2015; Luo, Vega-Palas, & Grunstein, 2002).

Sir4 contributes to the specific subnuclear localization of heterochromatin domains by anchoring them to the nuclear envelope. As previously discussed, the sequestration of heterochromatin domains at the nuclear periphery is thought to regulate the pool of available silencing proteins by keeping them away from the rest of the genome. In order to achieve functional heterochromatin tethering, Sir4 interacts with three docking proteins at the nuclear envelope: Esc1 (**E**stablishes **S**ilent **C**hromatin), Nup170 (**NU**clear **P**ore) and Mps3 (**M**ono **P**olar **S**pindle). In addition to Sir4, an alternative anchoring pathway is mediated by Ku. The two pathways are co-dependent due to direct Sir4-Ku interactions (Gartenberg & Smith, 2016; Taddei, Hediger, Neumann, Bauer, & Gasser, 2004).

Considering Sir4's central role in the heterochromatin interaction network, its cellular levels would be the logical target of cellular mechanisms that regulate heterochromatin formation in response to environmental signals. A relatively recent study showed that Sir4 levels temporarily drop after releasing cells from extended α-factor arrest, and are restored after two cell doublings (Larin et al., 2015).

In conclusion, Sir4 recruits Sir2 and Sir3 to subtelomeric and silent mating type loci and provides a scaffolding interface for other heterochromatic proteins that help the localization of heterochromatin to the nuclear periphery.

3 The Formation of Heterochromatin Domains

All the aforementioned heterochromatin components (summarized in Table 1) come together to form a dynamic and tightly regulated structure that has to keep its functional and structural integrity throughout the perturbations caused by cell cycle progression or environmental challenges as discussed below (Young & Kirchmaier, 2012).

Table 1: Summary of heterochromatin-associated DNA sequences and proteins.

Name	Role in Heterochromatin Assembly
Silencers	Sites of Sir complex recruitment and nucleation.
Silencer-bound factors	Adaptors between silencers and the Sir complex.
Sir2	Catalyzes the deacetylation of H4K16.
Sir3	Binds deacetylated H4K16.
Sir4	Scaffold of the Sir complex, which targets the complex to silencers and anchors heterochromatin domains at the nuclear periphery.

Two types of definitions are commonly and, sometimes, interchangeably used when discussing the assembly of heterochromatin domains and their cell cycle progression. Both types of definitions will be used in their appropriate context.

Operational definitions include global processes:

a) Establishment - *de novo* repression of a locus.
b) Maintenance – retention of the silent state within the cell cycle.
c) Inheritance – propagation of the silent state through genomic replication.

On the other hand, molecular definitions include more discrete assembly steps:

a) Nucleation – initial step when the Sir complex is recruited to silencers.
b) Spreading – extension of the heterochromatin domain.
c) Maturation – acquisition of complete heterochromatin functionality by the action of histone-modifying enzymes and conformational changes (Gartenberg & Smith, 2016; T. J. Young & Kirchmaier, 2012).

3.1 The sequential model of heterochromatin establishment

The sequential model is akin to a linear polymerization reaction and describes the establishment of heterochromatin domains by examining each molecular step (nucleation, spreading and maturation) separately (Hoppe et al., 2002). Even though the sequential model cannot be applied to the discontinuous loop-back structure of telomeric regions, it is still useful for understanding the general principles of heterochromatin formation in yeast (Lynch & Rusche, 2009) (Figure 10).

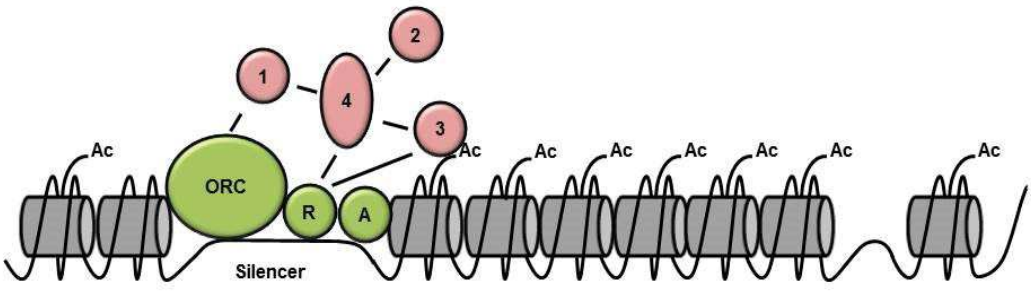

A) Nucleation

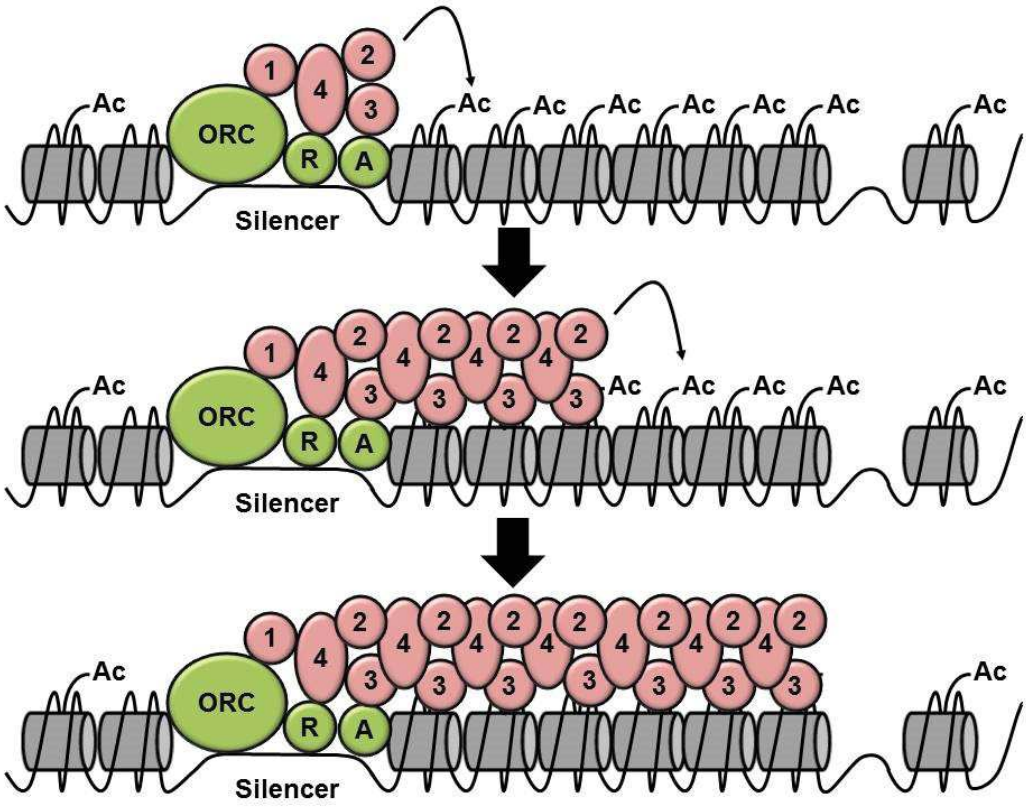

B) Spreading

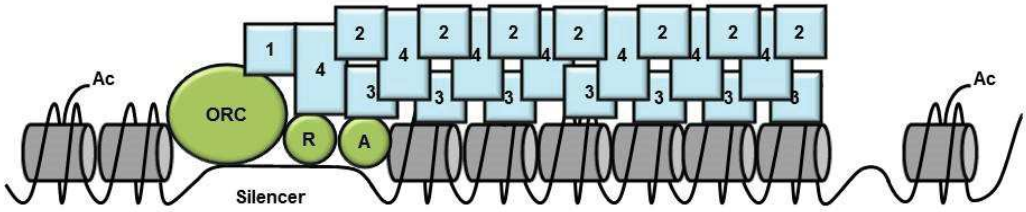

C) Maturation

Figure 10: The three-step sequential model of heterochromatin assembly (modified from Gartenberg & Smith, 2016). (A) Nucleation involves the recruitment of the Sir complex by a network of interactions between silencers and silencer-binding factors. (B) Spreading of heterochromatin is initialized after adjacent nucleosomes are deacetylated by Sir2, thereby creating high-affinity binding sites for the Sir3-Sir4 dimer. Heterochromatin then extends through repeated cycles of Sir2 mediated H4K16ac deacetylation and Sir3/Sir4 binding until it reaches an active barrier. (C) Maturation includes the removal of specific methylation marks in order to stabilize heterochromatin.

The establishment of heterochromatin domains begins with nucleation. This initial step includes the recruitment of the Sir complex to silencers by the network of interactions between silencers and silencer-binding factors. Sir4, initially recruited by Sir1 (bound to ORC) and Rap1, brings in Sir2 and Sir3 to silencers. The assembly of this “nuclear” Sir complex stimulates the catalytic activity of Sir2, which then deacetylates adjacent nucleosomes. The removal of the acetyl group from H4K16 generates Sir3-binding sites for another round of Sir complex recruitment, nucleosome deacetylation and Sir complex binding. The successive steps of Sir complex binding and deacetylation spread heterochromatin domains across the nucleosomal array until a barrier is reached or Sir subunits are locally depleted (Moretti & Shore, 2001; T. J. Young & Kirchmaier, 2012). A reconstituted heterochromatin study reaffirmed the importance of H4K16 deacetylation for Sir complex spreading and, ultimately, formation of a uniform and condensed heterochromatin fiber (Swygert et al., 2018). However, as previously discussed, methyl groups on H3K79 (by Dot1) and H3K4 (by Set1) destabilize Sir3 binding and are consequently removed in a final maturation step. H3K4 methylation is actively demethylated by Jhd2 (**J**mjC domain-containing **H**istone **D**emethylase) and passively removed via dilution after DNA replication since newly synthesized histones do not carry the mark (T. J. Young & Kirchmaier, 2012). On the other hand, H3K79 methylation is thought to be removed only passively, although an H3K79 demethylase has recently been characterized in mammalian cells (Kang et al., 2018).

Mature heterochromatin domains display several unique properties, most of which were discussed in previous chapters. To summarize, heterochromatin domains repress transcription of underlying genes and recombination of repetitive sequences, protect DNA against unwanted cleavage (by HO at silent mating type loci) and concentrate silencing factors in a separate subnuclear compartment (Allshire & Madhani, 2017; Grewal & Moazed, 2003). Furthermore, the established silent state is maintained through the cell cycle and stably inherited through multiple cell generations. Heterochromatin gene silencing in yeast was first described as a phenomenon called telomere position effect (TPE) and is one of the first examples of epigenetic inheritance of a cellular phenotype (Gottschling, Aparicio, Billington, & Zakian, 1990; Sandell & Zakian, 1992).

Normally, yeast colonies that have a wt *ADE2* (phosphoribosylaminoimidazole carboxylase) are white. However, when the reporter gene *ADE2* is placed in close proximity to a heterochromatinized artificial telomere, the expression of *ADE2* is repressed and yeast accumulate a red pigment in the absence of adenine in the media. The repressive state of the reporter gene is stably transmitted through a series of cell division, until occasional silencing failures restore the reporter's expression and white pigmentation. Therefore, the localization of the reporter close to heterochromatin results in variegated expression in a cell population. Since ON and OFF states are being passed on from one cell generation to the next for dozens of cell divisions yeast colonies end up sectored into red and white sections. This phenomenon is similar to position effect variegation in *Drosophilla* (Figure 11) (Gottschling, Aparicio, Billington, & Zakian, 1990; Sandell & Zakian, 1992).

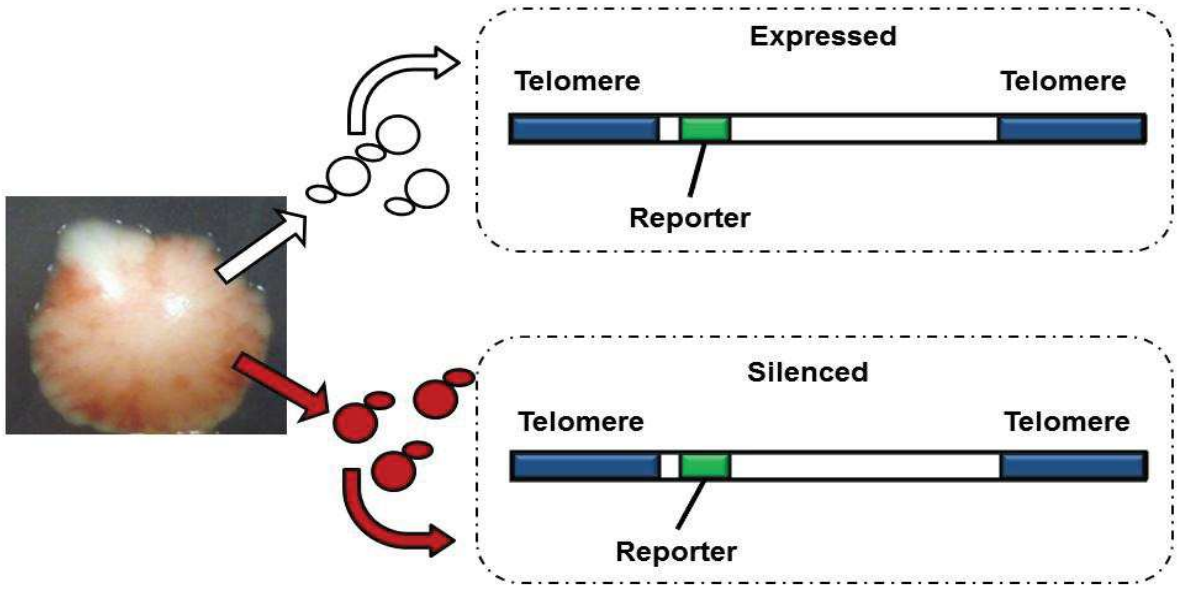

Figure 11: Variegated expression of the *ADE2* reporter gene and the epigenetic propagation of ON and OFF states to subsequent generations (modified from Gartenberg & Smith, 2016). Placing the reporter at an artificial telomere results in epigenetic repression and yields red yeast cells. However, not all cells are able to successfully repress the reporter, thus remaining white. The pattern of red and white sectors reflects the expression state of the reporter gene (reminiscent of the *Drosophilla* position effect variegation) which is stably propagated through successful cell divisions.

The same positional effect can be observed at the silent mating type loci. However, these domains derepress less often and seem to be more stable, thus requiring genetic manipulation (such as mutations in the silencer sequence or Sir1) in order to observe changes in expression patterns of reporter genes (Pillus & Rine, 1989b).

In conclusion, the sequential model describes the three steps of heterochromatin establishment: nucleation (recruitment of the Sir complex to target loci), spreading (extension of heterochromatin across nucleosome arrays) and maturation (removal of methylation marks). Heterochromatin functions include repression of transcription and DNA recombination as well as protection from endonucleases. Finally, heterochromatic states are stably and epigenetically inherited from one cell generation to the next.

3.2 Barriers and anti-silencing factors

The unchecked spread of heterochromatin is a threat to genome integrity, and needs to be constrained to specific genomic loci by limiting the pool of available silencing factors and the action of antisilencing mechanisms. Antisilencing can be defined as a set of interconnected, genome-wide mechanisms that prevent heterochromatin delocalization. These mechanisms are most critical at heterochromatin edges where discrete antisilencing zones (called barriers) locally antagonize heterochromatin spreading (Noma & Grewal, 2002; Oki & Kamakaka, 2005).

The antisilencing properties of barriers are a product of complementary activities of DNA-binding factors, chromatin remodelers and histone modifying enzymes. Together, these effectors actively alter the chromatin template by rapidly exchanging histones, adding or removing histone modifications and creating regions completely devoid of nucleosomes (Oki & Kamakaka, 2005; Simms et al., 2008a).

One common class of barriers is represented by tRNA genes. tRNA genes are dispersed throughout the genome either organized into small clusters or as single copies. The transcription of tRNA genes by Pol III is initialized by the binding of transcription factor III C (TFIIIC) to conserved promoter sequences (named box A and box B) inside the gene body. The stable TFIIIC-promoter interaction recruits the transcription factor III B (TFIIIB) to an AT-rich region upstream of the transcription start site. The binding of both transcription factors ultimately recruits Pol III. Extensive research data on the $tRNA^{Thr}$ barrier adjacent to HMR suggests that Pol III transcription is not necessary for a functional barrier, but Pol III binding to tRNA genes may contribute to tDNA's antisilencing capacity by creating a nucleosome-free region which interrupts the spread of heterochromatin. Mutations that impair TFIIIC and TFIIIB binding to tRNA weaken its barrier function, suggesting that the binding of these factors is critical for the antisilencing role of tRNA genes. Surprisingly, genome-wide mapping of TFIIIC, TFIIIB and Pol III binding sites revealed nine additional loci called ETC (**E**xtra **T**FIII**C**) which bind either TFIIIC alone or TFIIIC and TFIIIB, but not Pol III and act as functional heterochromatin barriers (Oki & Kamakaka, 2005; Simms et al., 2008b).

Although Pol III transcription is not necessary for TFIIIC/B-mediated barriers, the action of chromatin-modifying enzymes and active remodelers is critical for barrier function. As previously discussed, Sir2-mediated deacetylation of H4K16 is necessary for heterochromatin establishment because it creates binding sites for Sir3. In contrast, tRNA barriers recruit a complex which contains the H4K16 acetyltransferase Sas2 (**S**omething **A**bout **S**ilencing). Sas2 and cofactor acetyl-CoA (acetyl-coenzyme A) catalyze the genome-wide acetylation of H4K16 featured prominently in transcriptionally-active regions and tRNA barriers. The barrier function of Sas2 is evident in deletion strains where heterochromatin domains extend beyond their usual limits into euchromatin (Oki & Kamakaka, 2005). The previously discussed histone deacetylase Rpd3 could also contribute to barrier activity by removing H4K16ac, thus halting the production of OAADPr, a possible heterochromatin spreading effector (Ehrentraut et al., 2010). Additionally, Sas2-mediated acetylation facilitates the incorporation of another antisilencing factor -the histone variant H2A.Z- into nucleosomes (Shia, Li, & Workman, 2006).

The methyltransferase Dot1 catalyzes the mono-, di- and trimethylation of H3K79 and interacts with H4K16ac regulated by Sir2 and Sas2 activities. The observed hypermethylation of euchromatin compared to heterochromatin could imply a potential antisilencing function of Dot1 in countering heterochromatin spreading (Altaf et al., 2007; van Leeuwen, Gafken, & Gottschling, 2002). However, studies with *dot1*Δ strains revealed that the loss of Dot1 does not globally alter Sir2 and Sir3 occupancy at subtelomeric regions and silent mating type loci. Slightly reduced Sir2/3 occupancy was reported only on specific subtelomeric regions, suggesting H3K79 methylation could have a context-dependent effect on Sir binding (Takahashi et al., 2011b). Similarly, ChIP (**Ch**romatin **I**mmuno**p**recipitation) revealed uncompromised Sir2 and Sir4 binding at two telomeres in a *dot1*Δ strain (Rossmann, Luo, Tsaponina, Chabes, & Stillman, 2011). Taken together, these results suggest H3K79 methylation is not required to counter heterochromatin spreading at least when Sir subunits are expressed at endogenous levels. However, when Sir3 is overexpressed in *dot1*Δ, mutants acquire growth defects proportional to the dose of Sir3. These defects could be remedied when silencing was abolished by Sir2 inhibition. Furthermore, the methylation of H3K4 and H3K36 and the deacetylation by Rpd3 were dispensable for maintaining growth when Sir3 was present at high levels in *dot1*Δ. By comparing overexpressed Sir3 binding patterns in *dot1*Δ with methylation levels deposited by Dot1 in wt cells, Sir3 enrichment was observed at loci enriched for H3K79me3 and depleted for H3K79me and H3K79me2. These results suggest H3K79me3 is necessary to counter the extension of heterochromatin domains and serve as an antisilencing factor when Sir3 is overexpressed (Hocher et al., 2018).

In addition to transcription factor binding and H4K16 acetylation, barriers are characterized by fast histone turnover rates and nucleosome free regions (**NFR**s), which are created by chromatin remodelers, such as RSC (**R**emodel the **S**tructure of **C**hromatin) (Angus-Hill et al., 2001). RSC mutations also compromise the recruitment of the cohesin complex to chromatin. Interestingly, yeast with defective cohesion-recruitment mechanisms demonstrate a significant loss of the $tRNA^{Thr}$ barrier activity (Simms et al., 2008b).

In conclusion, the additive effects of histone turnover, nucleosome eviction and targeted histone modifications create powerful barriers that restrict heterochromatin spreading and represent a demarcation zone between heterochromatin and euchromatin.

3.3 Heterochromatin and the cell cycle

Heterochromatin domains are stably maintained through the various phases of the cell cycle and are faithfully transmitted to daughter cells. Although the sequential model provides a molecular description of *de novo* heterochromatin establishment, it does not explain how the structure survives perturbations caused by DNA replication and cell division. For decades, researchers have been struggling to elucidate the cell cycle timing and specific cellular circumstances that promote *de novo* establishment and inheritance of silent states. Early experiments utilized a variety of techniques in order to induce the expression of Sir subunits at specific stages of the cell cycle and observe heterochromatin reconstitution. Interestingly, heterochromatin domains were re-established only in cells went through S phase, leading scientists to conclude that S phase-related events were necessary to effectively restore silencing (Miller & Nasmyth, 1984; T. J. Young & Kirchmaier, 2012).

The central molecular event of S phase is DNA replication, which perturbs the chromatin template while producing a faithful copy of the genome. The disruption and reconstitution of chromatin following replication could, therefore, provide a logical time window for heterochromatin establishment. Although, only some steps in the replication process seem to contribute to heterochromatin formation (Gartenberg & Smith, 2016; T. J. Young & Kirchmaier, 2012).

As previously discussed, ORC is a critical protein complex implicated in both the initiation of replication and silencing. The decoupling of ORC's silencing and replication functions using different mutants for each function in the same strain did

not affect ORC's silencing function, suggesting that ORC does not need to initiate replication at silencers to recruit the Sir complex. (Dillin & Rine, 1997). Interestingly, the replication origins in silencers were also not necessary for silencing when Sir1 was tethered directly to DNA (Fox, Ehrenhofer-Murray, Loo, & Rine, 1997). Finally, silencing could be successfully established on an unreplicative, extrachromosomal DNA containing only a partial silencer (Li, Cheng, & Gartenberg, 2001). Together, these findings argue against a role of replication origins and fortk progression in heterochromatin establishment. However, they do not eliminate the possibility that another S-phase process is required for heterochromatin establishment (T. J. Young & Kirchmaier, 2012).

Some fork-associated factors that could be involved in silencing include the sliding clamp PCNA (**P**roliferating **C**ell **N**uclear **A**ntigen), DNA helicases and the histone chaperones CAF-1 (**C**hromatin **A**ssembly **F**actor) and Asf-1 (**A**nti-**S**ilencing **F**unction). Many of these factors are directly or indirectly involved in the replication-coupled deposition of histones. Mutations in these factors could therefore compromise the establishment of heterochromatin by for example incorporating acetylated or methylated maternal histones into heterochromatic loci and consequently inhibiting Sir complex binding. They might also fail to recruit appropriate histone-modifying enzymes, which could result in an enrichment of hypoacetylated histones and create Sir3 binding regions away from heterochromatic loci (T. J. Young & Kirchmaier, 2012).

Strains lacking the fork-associated helicase Rrm3 (**r**DNA **R**ecombination **M**utation) promote Sir3 and Sir4 recruitment to the sites of replication fork pausing. These sites are usually generated by stable DNA-protein interactions that are normally removed by Rrm3 to facilitate the progression of the replication fork (Dubarry, Loïodice, Chen, Thermes, & Taddei, 2011). Such transient fork pausing was observed at the silent mating type loci, telomeres and tRNA genes (Ivessa et al., 2003).

In addition to fork-associated factors, cohesin seems to play an important role in heterochromatin establishment as a cell cycle-dependent antisilencing regulator. As previously discussed, cohesin is a critical contributor to the $tRNA^{Thr}$ barrier function. Interestingly, tethering cohesin directly to DNA creates an artificial barrier to heterochromatin spreading (Dubey & Gartenberg, 2007). Cohesin does not bind to HMR locus in strains with the $tRNA^{Thr}$ deletion and silencing at HMR is established in any phase of the cell cycle in this strain. When the $tRNA^{Thr}$ gene and cohesin were transferred to HML, the establishment of silencing was again dependent on cell cycle progression (Lazarus & Holmes, 2011). These findings seem to suggest that cohesin at the $tRNA^{Thr}$ barrier not only prevents heterochromatin spreading, but also conditions heterochromatin establishment on cell cycle progression.

One of the most striking features of heterochromatin is its ability to propagate the established silent state to subsequent cell generations. This form of epigenetic inheritance is conceptually different from *de novo* establishment. *De novo* establishment is usually not required for epigenetic inheritance once heterochromatin is assembled. Nevertheless, following replication-induced perturbations, heterochromatin needs to be quickly and efficiently restored on both daughter chromatids. This faithful re-establishment and replication-coupled transmission of the silent state is usually defined as inheritance and differs from *de novo* establishment in speed and efficiency (Gartenberg & Smith, 2016).

Although various inheritance models exist, the most prevalent one is based on the *cis*-maintenance of histone modifications after DNA replication. According to this model, parental nucleosomes distribute randomly between daughter chromatids in the wake of the replication fork and recruit modifying enzymes to generate the same modification patterns on newly deposited histones. In the case of heterochromatin, the association of the Sir complex with parental nucleosomes could facilitate the deacetylation of newly synthesized histones that were mixed in with the old histones during assembly on replicated daughter strands. This would ensure that newly-deposited histones quickly become optimal binding targets for the Sir complex

and would thus enable the quick re-establishment of heterochromatin domains. Experimental data do suggest that re-establishment is more efficient if silencer-proximal regions inherit the deacetylated parental nucleosomes but silencers still appear to be continuously needed for silencing, as evidenced by silencer deletion strains where heterochromatin is disrupted after only one cell division. These findings seem to indicate that cooperative Sir complex recruitment to silencer regions works in tandem with Sir-mediated deacetylation to ensure the efficient restoration of silent states after replication (Moazed, 2011).

In conclusion, the search for elusive cell cycle events driving heterochromatin establishment and inheritance still continues, with the most likely contributors chromatin assembly events during DNA replication. Although origin firing and replication fork progression do not seem to be required for *de novo* establishment, fork-associated factors and replication-induced perturbations profoundly affect the composition of chromatin which, ultimately, influences both *de novo* establishment and inheritance (T. J. Young & Kirchmaier, 2012).

4 Heterochromatin Maintenance in Stationary Phase

In order for the intricate web of metabolic pathways to sustain life it requires a constant influx of matter and energy. Yeast share the same carbon and energy requirements as other eukaryotic organisms for all their cellular processes, including the maintenance and inheritance of heterochromatin domains. The central carbon and energy source for yeast is glucose. In nutrient-rich conditions, glucose is preferentially metabolized by anaerobic glycolysis, which produces ATP and releases ethanol to the surrounding environment. However, when glucose availability becomes limited, cells are able to switch metabolism from anaerobic glycolysis to the aerobic oxidation of ethanol in a process called diauxic shift. Once ethanol is exhausted and no other carbon source is available, haploid cells arrest growth and enter the stationary phase (Figure 12). Yeast can thus preserve viability for extended periods of time when nutrients are scarce and resume growth once favorable conditions are restored. Unlike haploid cells, nutrient-deprived diploid cells usually enter meiosis and sporulate into four haploid spores. Afterwards, spores are able to reform diploids via conjugation (mating) once nutrients are available again.

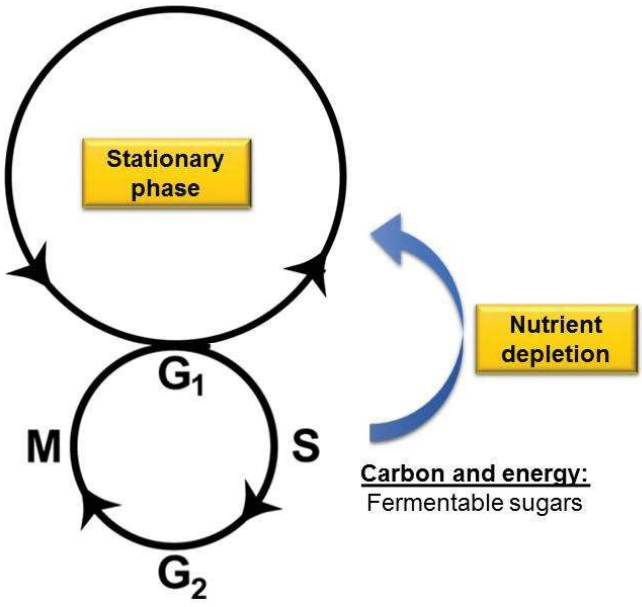

Figure 12: The cell cycle and stationary phase in yeast. Under nutrient-rich conditions, yeast can seamlessly proceed through the various phases of the cell cycle. However, when nutrients are depleted, haploid cells arrest growth and enter the stationary phase until nutrients are restored. In addition to carbon source deprivation, yeast can enter the stationary phase when deprived of nitrogen or phosphate, although they do not display the same molecular and physiological characteristics (Galdieri, Mehrotra, Yu, & Vancura, 2010).

4.1 Features of stationary-phase cells

Initially, stationary phase cells were thought to produce a phenotypically homogenous population. However, density centrifugation experiments revealed that stationary phase cells differentiate into two distinct subsets termed Q (**Q**uiescent) and NQ (**N**on-**Q**uiescent). Q cells were found to be denser, accumulating in the bottom fraction of the centrifugation tube. NQ cells were less dense and remained in the upper fraction of the tube (Figure 13) (Allen et al., 2006).

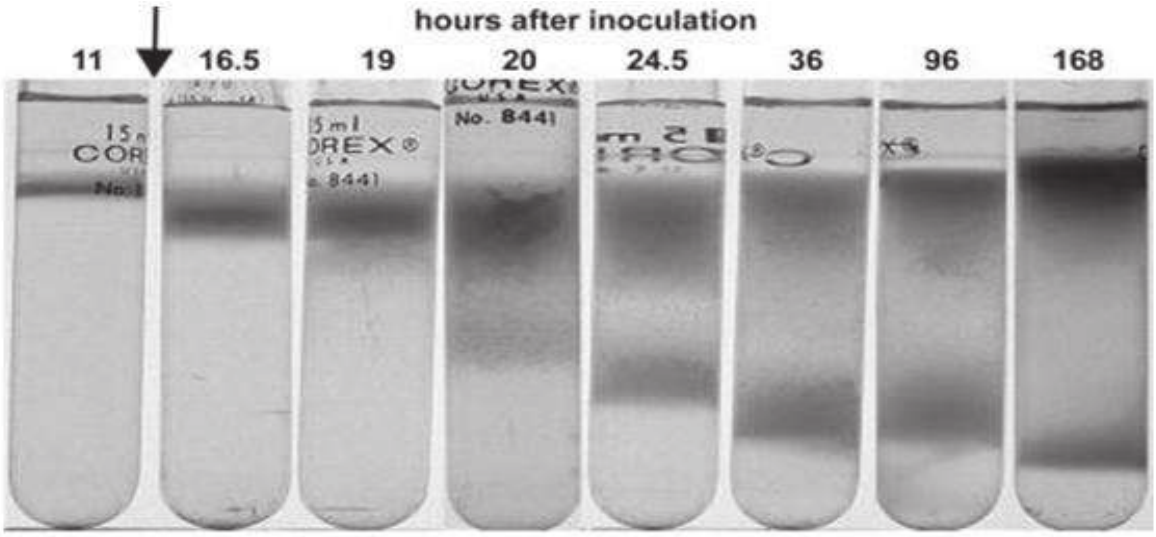

Figure 13: Density-gradient separation of Q and NQ cells. As time progresses following glucose depletion, two distinct fractions of cells are formed: the lower (denser) fraction of Q cells and upper (less dense) fraction of NQ cells.

In addition to density, Q and NQ cells differ in other features, most notably in their propensity to reenter the cell cycle after re-adding glucose to their growth medium. Q cells are unbudded and replicatively younger cells which retain their ability to reenter the cell cycle. NQ cells are enriched in reactive oxygen species and less likely to reenter the cell cycle. Both Q and NQ cells seem to have significantly reduced transcription and translation rates and decreased proteosomal activity and a more active lysosomal degradation pathway. A study using purified Q cells identified a ~ 30-fold decrease in mRNA levels compared to a ~ 2-fold decrease at diauxic

shift. This global transcriptional shutdown could be attributed to the global deacetylation activity of Rpd3 which was shown to be recruited to thousands of gene promoter in Q cells. Deletion of Rpd3 limits the transcriptional shutdown to the one observed in cells undergoing diauxic shift, suggesting prolonged nutrient depletion leads to an adaptive and global transcriptional reprogramming mediated by Rpd3 (McKnight, Breeden, & Tsukiyama, 2015). Although global transcriptional rates might vary, both Q and NQ cells seem to accumulate storage polysaccharides, including glycogen and trehalose. Trehalose serves an additional protective function at cell walls where it increases the resistance to heat and osmotic stressors (Allen et al., 2006; Galdieri et al., 2010).

Stationary phase entry and exit are both regulated by interconnected pathways serving as cellular nutrient sensors. These pathways include PKA (**P**rotein **K**inase **A**), TOR (**T**arget **O**f **R**apamycin), SNF1 (**S**ucrose **N**on**F**ermenting) and related downstream effectors. Once nutrients are depleted, the transition from exponential growth to stationary phase is triggered by activating signal transduction cascades which result in the transcription of stress-related genes, stationary phase genes and genes involved in the catabolism of nonfermentable sugars. Following the restoration of nutrients, these signaling pathways can also mediate the reversal of the stationary phenotype and the return to exponential growth, although the referenced experiments generalized the stationary phase population without differentiating Q and NQ cells. Both PKA and TOR pathways seem to primarily be negative regulators of stationary phase entry. Mutants with diminished PKA activity can enter the stationary phase even in the presence of glucose in the growth medium. A similar stationary phase entry is also observed when the TOR pathway is inhibited by rapamycin. Interestingly, cells treated with rapamycin display similar features as cells deprived of a nitrogen source, implicating TOR in the regulation of nitrogen starvation. Unlike the negative regulation imposed by TOR and PKA, the SNF1-mediated pathway acts as a positive regulator of stationary phase entry. Snf1 usually forms a complex which recruits transcription factors and chromatin remodelers to induce the expression of target genes, including genes necessary for processing nonfermentable carbon sources. The complex is only active in the absence of glucose (Galdieri et al., 2010).

In addition to physiologically-induced changes in gene expression patterns, heterochromatin domains also seem to acquire specific stationary phase features. DNA FISH and chromosome conformation capture experiments revealed that telomeres in Q cell reorganize into a distinct hypercluster positioned in the center of the nucleus. The formation of the hypercluster seems to be induced by reactive oxygen species originating from mitochondrial respiration and mediated by Sir3. This particular telomere organization could serve as a more efficient way to sequestrate silencing factors and hinder DNA transactions in Q cells (Guidi et al., 2015). Chip on chip assays revealed that Sir3 localization changes in early-stationary phase cells compared to exponentially growing cells, although Q and NQ cells were not analyzed separately. In early-stationary phase cells, Sir3 seems to redistribute to unconventional genomic regions, including stress-related genes and genes implicated in aging, while also remaining bound to conventional heterochromatin domains, but at decreased levels (Tung et al., 2013).

Similar to the global cellular and genomic changes upon nutrient depletion, cells respond globally once nutrients are restored. A microarray and RT-qPCR study analyzed expression patterns of a variety of genes up to 55 minutes after re-feeding a stationary phase population. The results of this study indicate that dramatic changes in mRNA levels occur within the first 35 minutes after re-feeding. The mRNA of growth-related genes (including ribosomal genes and permeases) displays a 64-fold increase in the first 10 minutes, while the mRNA of stationary phase genes displays a 4-fold decrease within 15-25 minutes. Similarly, mRNA of amino acid transporters and genes related to cell wall biosynthesis increases 16-fold in the first 5 minutes, but decreases to levels of exponentially growing cells by 35 minutes. On the other hand, mRNA of DNA repair and secretion genes seems to increase in a slow, linear manner during the course of the experiment. These findings suggest cells initiate a quick global response once glucose is reintroduced by increasing the expression of genes necessary for growth and protein biosynthesis, while decreasing the expression of stationary phase genes (Martinez et al., 2004). An additional study revealed Pol II seems to be pre-loaded on promoters of multiple stationary-exit genes, possibly in preparation for a fast transcriptional response after re-feeding (Radonjic et al., 2005).

In conclusion, the stationary phase induces cells to differentiate into two stress-resistant phenotypes with varying propensities to re-enter the cell cycle once nutrients become available. The acquisition of the stationary phenotype is accompanied by global cellular and genomic changes mediated by three interconnected pathways. Heterochromatin domains do not remain immune to these global changes, but rather reorganize telomeres into a distinct hypercluster and seemingly redistribute a portion of Sir3 proteins to other genomic locations.

4.2 Fate of histone modifications in the stationary phase

During stationary phase, cells seem to rewire their transcriptome in order to increase survivability until favorable conditions are restored. These molecular adaptations need to be reversed for cells to resume growth. The transitions between metabolic states imply changes in local and/or global histone modification patterns which influence the availability of chromatin and gene expression. The methyl-transferase activity of Dot1 and Set1, important for heterochromatin establishment and maturation, depends on the availability of the cofactor SAM (**S**-**a**denosine **m**ethionine), normally generated by cellular metabolism (Mentch & Locasale, 2016). Similarly, Sir2-mediated deacteylation and Sas2-mediated acetylation both contribute to the generation of heterochromatin domains and their containment to appropriate genomic loci. Sir2 and Sas2 are enzymatically active only in the presence of their respective cofactors, NAD^+ and acetyl-CoA. These cofactors and their derivatives are usually found at the crossroads of anabolic and catabolic pathways. The unconventional metabolic context of stationary cells could therefore indirectly influence the structure of heterochromatin domains by modulating the availability of cofactors involved in H3K4 and H3K79 methylation patterns and H4K16 (de)acetylation (Denu, 2003; Galdieri, Zhang, Rogerson, Lleshi, & Vancura, 2014; Shia et al., 2006; C. P. Young et al., 2017).

Recent studies aimed to map histone methylation patterns in stationary phase and upon reentry to the cell cycle. During stationary phase (7 and 14 days after glucose inoculation), both Q and NQ cells seem to retain most forms of H3 methylation. However, H3K4me3 seems to decrease by 50%, while H3K79me3

increases in both Q and NQ cells compared to log cells. Q cells could be further distinguished from NQ and log cells by their selective loss of H3K79me and H3K79me2. The methylation landscape of Q cells together with the presence of untranslated mRNAs and Pol II occupancy at growth genes suggest Q cells are poised for a quick global response upon refeeding (C. P. Young et al., 2017). RNA seq and mass spectrometry experiments seem to further this notion by confirming that growth gene upregulation and stress gene dowregulation after refeeding are accompanied by a stable presence of methylation marks detected in stationary phase. Despite dramatic metabolic changes, histone methylation seems to retain a generally stable presence during and after stationary phase (Mews et al., 2014).

Contrary to histone methylation, mass spectrometry results confirmed that H3 and H4 are generally hypoacetylaed in the stationary phase (Ngubo, Kemp, & Patterton, 2011). Furthermore, the general empirical consensus seems to agree that global levels of acetyl-CoA dramatically decrease in stationary cells, while NAD^+ levels increase, despite occasional fluctuations due to the dynamic interplay of the *de novo* and salvage pathways (Galdieri et al., 2014; Minard & McAlister-Henn, 2009). The observed decrease in acetyl-CoA can be correlated with low global histone acetylation levels in stationary phase, which implies transcriptional inactivity (Galdieri et al., 2014). As previously discussed, a variety of genes seem to however be upregulated upon entering stationary phase. Additional experimental data revealed transcriptional activation of a group of heat shock proteins during diauxic shift when acetyl-CoA levels started decreasing and could not maintain promoter acetylation, suggesting hypoacetylation activates genes relevant for metabolic states with low acetyl-CoA production (Mehrotra et al., 2014). After nutrients are restored, a quick burst in acetyl-CoA synthesis seems to be the predominant factor that activates the transcription of growth genes and restarts exponential growth (Cai, Sutter, Li, & Tu, 2011). Low levels of acetyl-CoA and global histone hypoacetylation suggest that H4K16 stays hypoacetylated within heterochromatin during stationary phase. This could weaken barriers and promote promiscuous Sir binding beyond heterochromatin in stationary cells (Ngubo et al., 2011). Further research is necessary to uncover additional mechanistic links and implications of histone acetylation patterns on heterochromatin maintenance in the stationary phase.

5 ARTICLE

The budding yeast heterochromatic SIR complex resets upon exit from stationary phase

Hrvoje Galic[1,2], Pauline Vasseur[1,2,3] and Marta Radman-Livaja[1,2*]

[1] *Institut de Génétique Moléculaire de Montpellier, UMR 5535 CNRS, 1919 route de Mende, 34293 Montpellier cedex 5, France;*

[2]*Université de Montpellier, 163 rue Auguste Broussonnet, 34090 Montpellier, France*.

[3] *current address* : *CIRAD, Campus international de Baillarguet, UMR 117- ASTRE "Animal, Santé, Territoires, Risques & Écosystèmes", TA A-117/E, Bât. G bureau 212, 34398 Montpellier cedex 5, France*

*Corresponding author

Abstract

The budding yeast SIR complex (Silent Information Regulator) is the principal actor in heterochromatin formation, which causes epigenetically regulated gene silencing phenotypes. The maternal chromatin bound SIR complex is disassembled during replication. Consequently, if heterochromatin is to be restored on both daughter strands, the SIR complex has to be reformed on both strands to pre-replication levels. The dynamics of SIR complex maintenance and re-formation during the cell-cycle and in different growth conditions are however not clear. Understanding exchange rates of SIR subunits during the cell cycle and their distribution pattern to daughter chromatids after replication has important implications for how heterochromatic states may be inherited and therefore how epigenetic states are maintained from one cellular generation to the next. We used the tag switch RITE system to measure genome wide turnover rates of the SIR subunit Sir3 before and after exit from stationary phase and show that maternal Sir3 subunits are completely replaced with newly synthesized Sir3 at subtelomeric regions during the first cell cycle after release from stationary phase. The SIR complex is therefore not “inherited” and the silenced state has to be established *de novo* upon exit from stationary phase. Additionally, our analysis of genome-wide transcription dynamics shows that precise Sir3 dosage is needed for the optimal up-regulation of “growth” genes during the first cell-cycle after release from stationary phase.

Introduction

Budding yeast heterochromatin is a repressive structure located at the silent mating type loci (*HMR* and *HML*), telomeres and rDNA repeats. The essential component of the structure is the non-histone protein complex SIR (Silent Information Regulator), which consists mainly of Sir2, Sir3 and Sir4. Sir4 scaffolds the complex while Sir2 functions as an NAD-dependent H4K16 deacetylase, providing a high-affinity binding site for Sir3 which recruits Sir4 and so on (for review see (Grunstein and Gasser 2013)). In the classical polymerization model, SIR components are first recruited to silencer regions by a combination of silencer-binding factors (ORC – Origin Recognition Complex, Rap1 and Abf1). The SIR complex then spreads from the nucleation site (silencer) through cycles of deacetylation and nucleosome binding, which continue until the SIR complex reaches boundary elements that prevent unwanted spreading to transcriptionally active regions (for review see (Gartenberg and Smith 2016)). For example, one well-characterized boundary element is the threonine tRNA gene in the telomere-proximal region of HMR (Donze and Kamakaka 2001). Recent studies have shown that the SIR complex can also be recruited to unconventional binding sites, including tRNA genes. SIR binds to these sites mostly during genomic replication. Since these loci are tightly bound by non-histone proteins such as transcription factors which may cause replication fork stalling, it has been proposed that SIR may play a role in releasing stalled forks or preventing fork stalling (Dubarry et al. 2011; Nikolov and Taddei 2016).

It has been shown that over-expressed Sir3p can be incorporated into existing heterochromatin(Cheng and Gartenberg 2000). However, beyond this bulk measurement, the locus-specific dynamics of the chromatin bound SIR complex within and from one cell generation to another have not yet been measured. How heterochromatic SIR complexes exchange their components during the cell cycle and how they are distributed to daughter chromatids after replication has important implications for how heterochromatic states are maintained and whether they may be inherited. The maternal SIR complex has to be disassembled during replication and if heterochromatin is to be restored on both daughter strands, the SIR complex has to be reformed on both strands to pre-replication levels.

Another open question is how chromatin bound complexes that epigenetically determine gene expression states, like the SIR complex, respond to environmental challenges such as nutrient depletion. Indeed, under unfavorable conditions, yeast cells stop growing and enter the stationary phase, which lasts until depleted nutrients are restored. Molecular hallmarks of the stationary phase include transcriptional reprogramming, spatial reorganization of the genome and a 300-fold decrease in protein synthesis rates(McKnight et al. 2015). While the organization of the SIR complex in stationary phase has been described, the dynamics of the SIR complex during and following exit from the stationary phase are still poorly understood(Guidi et al. 2015). These questions have motivated us to investigate the dynamics of the SIR complex during and upon release from the stationary phase. Our strategy was to use the Recombination-Induced Tag Exchange (RITE) method(Verzijlbergen et al. 2010; Terweij et al. 2013) to map genome wide Sir3 turnover rates with the goal to better understand the mechanisms of heterochromatin maintenance and find out whether the SIR complex is "inherited" on newly replicated daughter chromatids. We chose to focus on the Sir3 subunit because Sir3 is the limiting factor that determines the extent of SIR complex polymerization and the location of SIR complex boundaries.(Renauld et al. 1993; Hecht et al. 1996; Radman-Livaja et al. 2011).

Our results show that during stationary phase, subtelomeric Sir3 occupancy is reduced 4-fold and Sir3 turnover is undetectable. Sir3 bound to chromatin is then completely replaced with newly synthesized Sir3 subunits at the end of the first cell cycle upon release from stationary phase, suggesting that at least the Sir3 subunit of the SIR complex is not inherited and therefore does not contribute to the epigenetic inheritance of the silenced state in these conditions. Heterochromatic complexes are instead completely "reset" after exit from quiescence. Additionally, average Sir3 occupancy at subtelomeric loci decreases rapidly before the first cell division after release from stationary phase and then increases gradually over multiple cell divisions. We propose that the observed transient instability of the SIR complex after release from stationary phase is a functional adaptation that allows the cell to rapidly respond to changing growth conditions and upregulate genes involved in carbon source metabolism and cellular growth.

Results

Sir3 subunit exchange dynamics during and after release from stationary phase

We used the RITE tag switch system developed by Fred van Leeuwen(Verzijlbergen et al. 2010) to construct the Sir3 “tag switch” module. The genomic *Sir3* locus was engineered with a C-terminal tag switch cassette containing loxP sites, and the HA and T7 tags, separated by a transcription termination signal, and the hygromycin resistance gene (**Figure 1A**). The host strain carries the CreEBD78 recombinase, which is activated upon estradiol addition. After Cre-mediated recombination of LoxP sites, the HA tag on Sir3 is switched to the T7 tag. Recombination efficiency is assessed by growth on hygromycin plates, and is typically ~97% if arrested cells are treated with estradiol for at least 16hrs.

Cells were grown in glucose rich medium (YPD) for 48hrs until they reached the stationary phase. Since it has been shown that after 48hrs the majority of cells in the population have the characteristics of quiescent cells i.e. the ability to retain viability and reproductive capacity in the absence of nutrients, we consider that our experiments record the average behavior of quiescent cells upon exit from stationary phase(Allen et al. 2006). Stationary phase cells were incubated with estradiol for 16hrs to induce the Cre mediated tag switch. Anti-HA (old Sir3) and anti-T7 (new Sir3) chromatin immuno-precipitations were performed in parallel at regular intervals before and after Cre activation. Formaldehyde cross-linked chromatin was sonicated to 300-500bp fragments before immune precipitation and DNA isolated from immune-precipitated chromatin fragments was analyzed with deep-sequencing.

ChIP-seq of old and new Sir3 showed that Sir3 dynamics are similar at all heterochromatic loci, including silent mating type loci and subtelomeric regions (**Figure 1 B-C, E-F**). Namely, the old Sir3 is maintained in stationary phase cells even after the tag switch, although overall Sir3 occupancy is decreased 4 fold compared to the pre-stationary midlog phase (**Supplementary Figure S1 B-C)**. After

release into fresh media old Sir3 completely disappears at the time of the first cell doubling and is replaced by new Sir3. New Sir3 enrichment is however still low even after the twelfth doubling: 3 fold lower than old Sir3 immediately after release and ~7 fold lower than Sir3 in mid-log cells (Radman-Livaja et al. 2011) (**Figure 1 B-C and Supplementary Figure S1 B-C**). While the differences in Sir3 enrichment levels between new Sir3 after several divisions following the exit from stationary phase and old Sir3 in mid-log before stationary phase could be due to differences in binding affinities of the anti-T7 (new Sir3) and anti-HA (old Sir3) antibodies to their respective epitopes, it is nevertheless apparent that new Sir3 binding to subtelomeric loci does not reach saturation even after several doublings. The observed pattern of Sir3 binding dynamics in cell populations after exit from stationary phase suggests that the existing Sir3 is rapidly removed from chromatin when cells resume growth before the first cell division and is gradually replaced with new Sir3 over several cell division cycles. Interestingly, Sir3 replacement at silent mating type loci is faster than at subtelomeric loci and new Sir3 occupancy reaches a plateau after 1-3 doublings, probably as a consequence of the stronger SIR complex nucleation capacity of HML and HMR silencers compared to subtelomeric silencers (**Figure 1 E-F, Supplementary Figure S1 E-F**).

Sir3 removal, heterochromatin instability and "growth" genes up-regulation upon release from stationary phase

The SIR complex appears to be unstable in the first cell cycle after exit from stationary phase, thus making heterochromatin potentially permissive to transcription during that period. The rapid decrease in chromatin occupancy of old Sir3 during the first cell cycle after release coincides with a fast decline in total cellular old Sir3 levels resulting in the complete disappearance of old Sir3 by the time of the first cellular doubling accompanied by a slow and gradual increase in new Sir3 which starts around 90min after release (**Figure 2A**). Since the rapidly declining levels of old Sir3 and the slow synthesis of new Sir3 could compromise heterochromatin function we tested the silencing potential of SIR complexes after exit from stationary phase using the "α-factor test", described below (**Figure 2B**).

MATa (Mating Type a) cells will respond to the presence of α-factor (mating pheromone α) by arresting in G1 and forming a “shmoo” if the silent mating type locus *HML* (containing the genes for mating type α) is stably heterochromatinized with the SIR complex. If *HML* is not fully silenced, cells will behave like pseudo-diploids and will not respond to α-factor. Log-phase cells should therefore predominantly respond to α-factor and become shmoo. On the other hand, we expect that populations exposed to α-factor immediately upon exit from quiescence will have a higher fraction of cells that form buds. This is exactly what we observe: there are ~two times more cells that divide and don’t form shmoon in populations exiting stationary phase than in mid-log populations. If cells are allowed to divide even just once after release and are then exposed to α-factor they arrest normally and form stable “shmoon” like mid-log cells (**Figure 2B**).

The inability to form shmoon in a subpopulation of cells exiting quiescence is not due to a Sir3 independent defect since cells that can shmoo in log phase in the absence of α-factor irrespective of the presence Sir3 due to a *HMLα/MATa* double deletion, also shmoo with 100% efficiency upon release from stationary phase even in the absence of Sir3 (**Figure 2C**). The transient decrease in Sir3 amount at subtelomeric regions during the first cell cycle upon exit from quiescence can however be overcome with Sir3 overexpression (**Figure 3**). In a galactose inducible overexpression system, Sir3 occupancy starts increasing immediately upon release of stationary cells into galactose even before the first cell division, suggesting that SIR complex renewal does not directly depend on DNA replication or cell division but is likely driven by the rate of accumulation of newly synthesized Sir3. Overexpression of Sir3 can therefore compensate for the rapid removal of old Sir3 that was bound to chromatin in stationary phase. It is however important to note that the process of old Sir3 removal occurs independently of Sir3 synthesis as evidenced by the complete disappearance of chromatin bound old Sir3 by the second doubling upon release into dextrose or raffinose in which new Sir3 is not expressed (**Figure 3 F, N**). In other words, the removal of old Sir3 from chromatin is not “driven” by its replacement with new Sir3.

We have also tested the effects of Sir3 dynamics during the stationary to growth phase transition on genome wide gene expression levels. Changes in mRNA enrichment relative to a genome-wide average in the wt Sir3 (strain used in Figures 1 and S1), Sir3Δ or oeSir3 (used in Figure 3) strains show that wt Sir3 levels are needed to maintain the up-regulation of 710 genes during the first cell cycle after release from stationary phase (**Figure 4**). The up –regulated genes are enriched for "growth" genes involved in ribosome synthesis, mitochondrial processes and amino-acid and carbon metabolism (Table S1). These genes are all upregulated in stationary phase but their expression starts to decrease immediately after release from stationary phase either in the absence of Sir3 (Sir3Δ strain) or in the presence of excess total Sir3 (oe Sir3 strain). In wt cells on the other hand, they are further upregulated immediately after release and their mRNA levels stay high until the first division when they drop abruptly down to approximately mid-log levels (**Figure 4C-D**). An analysis of median Sir3 enrichment in the coding regions of these genes suggests that the observed transcription up-regulation may be a direct consequence of low level Sir3 enrichment at these genes (**Figure 4 E**). The observed Sir3 enrichment values are relative to average genome-wide Sir3 enrichment in each time-point since our ChIP-seq experiments were not normalized to a spike-in control. Even though we cannot measure absolute changes in Sir3 occupancy at these genes, we do detect a trend in relative Sir3 occupancy upon release from stationary phase. The median Sir3 enrichment over the time course is proportional to transcription levels with the highly expressed cluster 1 having the highest Sir3 occupancy, as has been documented before (Radman-Livaja et al. 2011). Unlike at subtelomeric regions where old Sir3 levels decrease abruptly immediately after release, old Sir3 enrichment at induced genes appears to be mostly constant although with a slight drop immediately after release in clusters 2 and 3 (**Figure 4E**). On the other hand Sir3 dynamics after the first cell division are similar on subtelomeric regions and on these "growth" response genes: the exchange of old Sir3 subunits with new Sir3 starts with the first cell division after release with similar rates as in subtelomeric regions (**Figure 4 F-G**). When Sir3 is over-expressed however, Sir3 enrichment drops immediately after release (except for cluster 1 where there is an initial increase 1hr after release) and continues to decrease with each cell division. Since Sir3 enrichments are calculated relative to a genome-wide average, the apparent depletion of Sir3 at these genes is a consequence of Sir3 accumulation

in subtelomeric regions after release and its spreading beyond heterochromatin boundaries found in wt cells (compare Figures 1B and 3B). The correlation between relative Sir3 depletion and impaired up-regulation of "growth" response genes in cells with over expressed Sir3 as well as the correlation between constant Sir3 occupancy and up-regulation of these same genes in wt cells, suggest that controlled and potentially transcription dependent Sir3 binding may have a direct effect on gene expression.

Sir2 binding during and after release from stationary phase

Genome-wide Sir2 binding dynamics during the stationary to growth phase transition are similar to Sir3 dynamics with some quantitative differences as shown in **Figure 5**. Like for Sir3, we observe a decrease in Sir2 occupancy at subtelomeres, silent mating type loci and rDNA in stationary phase, although the decrease is more modest: 50% (silent mating type loci; **Figure 5E-F**) to ~2 fold (subtelomeric regions, **Figure 5C** and rDNA, **Figure 5G**). Also, the return to (subtelomeric regions) or even above pre-stationary phase levels (silent mating type loci and rDNA) is observed immediately after the first cell division after release, while Sir3 has not reached saturation even after 12 doublings.

Sir3 and Sir2 binding to tDNA

Our results have unexpectedly uncovered non-canonical Sir3 binding to tRNA genes (**Figures 1D, S1D, 3G-J**). New, T7 tagged Sir3 is significantly enriched at all but 20 tRNA genes immediately upon release from stationary phase and this high Sir3 occupancy persists at least for 5 subsequent doublings (**Figure 1D**). The source of the gradual increase in Sir3-HA binding to tRNA genes is likely originating from the fraction of cells (~2.5%) that did not complete the tag switch. A replicate experiment using a different anti-T7 antibody (a monoclonal one versus the polyclonal one in Figure 1) does confirm Sir3-T7 binding to tDNAs upon release (**Figure S1 D**) but with

Sir3 enrichment levels that are 8 to 16 fold lower than with the polyclonal antibody used in Figure 1. Unlike their dynamics at subtelomeric loci, new Sir3-T7 and old Sir3-HA in the replicate experiment seem to follow the same binding dynamics with the same level of occupancy: no binding during the stationary phase followed by a "jump" in occupancy after the first doubling and constant binding for at least twelve doublings afterwards. The discrepancies in Sir3-T7 enrichment at tDNAs between the two replicates are puzzling and are possibly a consequence of different affinities of the polyclonal and the monoclonal antibodies for the T7 epitope in the context of different Sir3 configurations found at tDNAs and subtelomeres. The monoclonal and the polyclonal anti-T7 antibodies seem to bind with comparable efficiency to Sir3 when it is present in multiple subunits in the densely packaged configuration of a SIR polymer at subtelomeric and silent mating type loci. The polyclonal anti-T7 is on the other hand more efficient than the monoclonal antibody when Sir3 stoichiometry is low as it is likely to be at tDNAs.

The signal clearly correlates with Sir3 presence in the cell: 1. only Sir3-HA is detected in midlog cells before the tag switch from HA to T7, while Sir3-T7 and Sir3-HA are both detected after release from stationary phase following the tag switch (Figure S1 D, the Sir3-HA signal comes probably from cells that did not recombine the two tags); 2. The Sir3-HA signal from the Sir3 overexpression system is undetectable in the 12^{th} doubling after release into dextrose or raffinose media where Sir3 is not expressed while it is still there in the 12^{th} doubling after release into galactose when Sir3 is overexpressed (Figure 3G-J). Consequently, the enrichment of tDNA sequences in our Sir3 ChIP-seq datasets cannot be due to non-specific binding of these sequences to antibodies or protein A beads as has been proposed previously(Teytelman et al. 2013), nor is it likely to be a tag artefact since tDNA sequences were isolated with the anti-HA (Figures 1D, S1D, and 3G-J) and the anti-T7 antibodies (Figures 1D, S1D). We cannot, however exclude the possibility that Sir3 binding to tDNAs has no biological significance and is merely a consequence of transient and non-specific "stickiness" of nucleoplasmic Sir3 to tDNA sequences in vivo or even after cell fixation.

Sir2 also binds to tDNAs although the binding pattern and kinetics are somewhat different from Sir3. While Sir3 occupies a footprint from -100bp to 200bp around the start of the tRNA gene throughout the time course, Sir2's footprint spreads progressively from +-150bp around the tRNA gene start in the first cell cycle to +-400bp by the 12th cycle (compare the top panels of Figures 1D, S1D and 5D). Also, while the position of peak binding immediately downstream of the tRNA gene start is common to both Sir3 and Sir2, the rate of peak height changes is different for the two proteins. Peak height already reaches a plateau after the first cell cycle for Sir3, while it is still growing (although slowly) after the 12th doubling for Sir2 (**Figure 6D**). The timing of the binding signals and the footprint patterns of the two proteins suggest that Sir3 might be binding first and might then recruit Sir2 which then spreads to the nucleosomes immediately adjacent to the tRNA gene.

It is curious that the enrichment signal at tDNAs disappears in stationary phase for both Sir3 tag switch replicates and in the Sir3 overexpression system as well as Sir2 (Figures 1D, S1D, 3G-J and 5D, respectively) even though Sir3 and Sir2 still bind to silent mating type loci and subtelomeric regions although at reduced levels, and may reflect the scarcity of nucleoplasmic Sir3 and possibly Sir2 in stationary cells. The fluctuations in Sir3 occupancy at tDNAs coincide with changes in growth conditions: 1.low level binding in mid-log (Figure S1D); 2. no binding in stationary phase; 3. increased binding upon release from stationary phase that reaches a plateau after the first cell division and stays higher than the previous midlog phase even twelve doublings after release from stationary phase. This suggests that Sir3 binding may be linked to changes in the chromatin configuration and/or gene expression state of tRNA genes.

TFIIIC is a transcription factor responsible for the recruitment of the RNApolIII transcription machinery and its binding sites are verified heterochromatin boundary and chromatin insulator elements (Simms et al. 2008). We therefore mapped the TAP-tagged TFC3 (a subunit of TFIIIC) genome wide binding pattern upon release from stationary phase to find out whether there is a correlation between TFIIIC and Sir3 binding to tDNAs (**Figure 6**).

We have identified three tRNA gene clusters with specific TFIIIC binding dynamics (**Figure 6B-C**). Sir3 and Sir2 binding dynamics correlate with TFIIIC binding in less than 50% of all tRNA genes (124 tRNA genes in cluster 1 out of a total of 273 tRNA genes) (**Figure 6 D-F**). Consequently Sir3 and Sir2 are not likely to bind to tDNAs in response to tRNA gene activation but they may be "recognizing" structural chromatin features common to all tRNA genes independently of their gene expression state.

Discussion

Our results suggest that yeast heterochromatin is reprogrammed upon exit from stationary phase. We observe a ~4 fold and ~2 fold drop in Sir3 and Sir2 subtelomeric occupancy, respectively, when cells enter the stationary phase that is followed by an even steeper drop of Sir3 occupancy during the first cell cycle after release from stationary phase. All Sir3 proteins bound to subtelomeric and silent mating type loci are replaced with newly synthesized Sir3 after the first division following release. Surprisingly, the enrichment of new Sir3 subunits in subtelomeric regions increases slowly and appears to not reach saturation even after 12 cell divisions. Even though we have not measured Sir2 turnover rates, our Sir2 ChIP-seq time-course experiment clearly shows that Sir2, unlike Sir3, comes back to pre-stationary levels by the first cell division after release, suggesting that heterochromatin function is potentially regulated by modulating Sir3 dosage. Further experiments will be necessary to understand how the differences in the stoichiometry of Sir2 and Sir3 in this "reset" form of heterochromatin in which Sir2 levels are constant and Sir3 gradually increases over multiple cell generations affect the functionality and stability of heterochromatin.

The biological significance of this kind of heterochromatic "clean slate" upon exit from quiescence and the slow rebuilding of heterochromatin structure is not clear. The apparent depletion of Sir3 before the first cell division after release can be

overcome with Sir3 overexpression, bringing up the possibility that the naturally limiting amount of Sir3 has a regulatory function. It opens up the question of the function of Sir3 stoichiometry at heterochromatic loci. Are there different higher order conformations of heterochromatin that depend on the amount of Sir3 and does heterochromatin that contains less Sir3 have greater plasticity that would facilitate the cell's response to environmental changes and stressful growth conditions?

Sir3 appears to be actively kept at low levels in the first two divisions after release as our Western blot results suggest, even though global protein synthesis is greatly increased (for review see(Valcourt et al. 2012)). Heterochromatin formation may be impaired to potentially prevent mating during first divisions when the cell is replenishing its protein content or to allow expression of subtelomeric genes or both. Sir3 also becomes hyperphosphorylated in stress conditions, such as nutrient depletion, following the inactivation of the TOR pathway(Stone and Pillus 1996). Sir3 hyperphosphorylation in turn causes the derepression of subtelomeric PAU genes involved in cell wall restructuring (Ai et al. 2002). Since TOR activity is necessary for growth, an alternative pathway to Sir3 phosphorylation that insures the expression of subtelomeric genes upon exit from quiescence may be necessary and may involve targeted degradation of Sir3 proteins and/or reduced synthesis of Sir3 proteins. A small increase in relative mRNA abundance of low expressed genes cannot be detected in our RNA-seq experiment because mRNA enrichment is normalized to average genome-wide sequencing read density. We were therefore unable to detect changes in subtelomeric gene expression that are likely to be subtle. We do detect, however, Sir3 dependent up–regulation of ~700 "growth" response genes localized throughout the genome. Indeed, a precise control of genome-wide Sir3 density upon exit from stationary phase appears to be necessary for sustained up-regulation of "growth" genes, which presumably enables optimal cell growth in the first cell cycle after release (**Figure 4**). Cells without Sir3 or with excessive amounts of Sir3 both fail to maintain high levels of up-regulation of these genes in the first cell cycle after release. Moreover, the correlation between mRNA and Sir3 levels and the specific pattern of Sir3 turnover at these genes suggest that Sir3 may play a direct role in transcription regulation. Interestingly, (Weiner et al. 2012) also proposed that Sir3

might play a direct role in the regulation of ribosomal protein gene expression during the stress response. There is therefore an intriguing possibility that apparently transcription dependent low level Sir3 binding to gene bodies of environmentally responsive genes directly regulates transcription of these genes in response to environmental signals.

Our genome-wide maps of Sir3 dynamics have also unexpectedly revealed a potentially new function of the Sir complex at tDNA loci. Even though the pervasive binding of Sir3 and Sir2 to tRNA genes may be an experimental artefact with no biological function, the dynamics of Sir3 and Sir2 binding during stationary to growth phase transitions do raise some intriguing possibilities. Sir3 binding may precede TFIIIC binding to reorganize the nucleosome configuration that may have been altered in stationary phase and thus prepare tRNA genes for optimal activation. tRNA genes have a specific nucleosome organization that somewhat resembles a yeast RNApol2 gene promoter (**Supplementary Figure S2A**). There is a nucleosome free region (NFR) covering the entire tRNA gene (-100bp to 150bp around the tRNA gene start site (datasets used for the analysis were taken from (Weiner et al. 2010; Ziane et al. 2019)), and the nucleosomes surrounding the NFR on either side are enriched for H3K56ac (a mark of newly synthesized histone H3, dataset from (Ziane et al. 2019)) and the H2A variant Htz (dataset from (Watanabe et al. 2013)), both characteristics of high nucleosome turnover rates (Dion et al. 2007). The nucleosomal organization of tRNA genes is a dynamic structure as is evident from nucleosome and H3K56ac tDNA profiles from replicating mid-log cells (Figure S2B). Replicated tRNA genes have a wider and shallower NFR that seems to be partially populated with nucleosomes (compare the MNAse-seq profiles from bulk and nascent chromatin in the left panel) and an asymmetric H3K56ac distribution with less H3K56ac downstream of the tRNA gene that is more pronounced in early S-phase compared to mid-S-phase. Thus, DNA replication disrupts chromatin organization of tRNA genes which needs to be subsequently restored. This is supported by evidence that shows that concerted activity of DNA polymerase epsilon, the H3K56 acetylase rtt109 and the chromatin remodeler Rsc is needed to create the nucleosome positioning pattern of the tRNA insulator at HMR(Dhillon et al. 2009).

tRNA genes are also known “obstacles” for replication forks (Deshpande and Newlon 1996) but not all tRNA genes have the same capacity to slow forks down in optimal growth conditions(Ivessa et al. 2003). It will therefore be interesting to see whether the chromatin structure of tRNA genes is altered in stationary phase and whether the Sir complex functions to reorganize nucleosomes at tRNA genes after exit from quiescence to prevent dangerous fork stalling in the first S-phase after release and/or prime tRNA genes for transcription activation or insulator function.

Our results have revealed the dynamic nature of yeast heterochromatin that changes in response to environmental challenges that cells face in variable growth conditions. Future studies should explore the regulatory mechanisms that ensure heterochromatin plasticity while preserving its functionality. We have also uncovered two potential new roles for Sir3: one in gene expression regulation of genes involved in the stationary to growth phase transition and the other in tDNA binding. Our study joins the growing body of work that delves into the dynamics of chromatin structure in different organisms and is yet another reminder that chromatin organization is not a static structure that reaches some sort of final stable state that just needs to be maintained once cells have differentiated. It is instead an active element in the cell’s response to its environment that has to be continuously shaped and reshaped by specialized cellular processes in order to ensure the survival and preserve the function of each cell.

Materials and Methods

Yeast Strains

The strain used in Figures 1, 2, and S1 is MRL9.1 (S288C: *MATa his3d200 leu2d0 lys2d0 met15d0 trp1d63 ura3d0 bar1::HisG HIS3 Pgpd_CRE_EBD78 Sir3Histag-LoxP-3xHA-Hygro-LoxP-3xT7*) that was constructed by transforming NKI12318 (*MATa his3d200 leu2d0 lys2d0 met15d0 trp1d63 ura3d0 bar1::HisG HIS3 Pgpd_CRE_EBD78*; courtesy of Fred van Leeuwen) with the RITE-switch (*LoxP-3xHA-Hygro-LoxP-3xT7*) cassette amplified from the pFvL159 plasmid (Fred van Leeuwen) with primers (

forward:
5'GCCTTTTCGATGGATGAAGAATTCAAAAATATGGACTGCATTCATCACCATCAC
CATCACGGTGGATCTGGTGGATCT;

reverse:
5'CATAGGCATATCTATGGCGGAAGTGAAAATGAATGTTGGTGGTGATTACGCCA
AGCTCG) compatible for homologous recombination with the C-terminal end of the Sir3 gene. Cassette incorporation was verified by PCR.

The Sir3 over-expression strain in Figure 3 is THC70 (W303: *MATa HMLa HMRa ade2-1 can1-100 his3-11,15 leu2-3,112 trp1-1 matΔ::TRP1 hmr::rHMRa hmlΔ::kanMX ura3-1::GAL10P–Sir3HA::URA3 bar1Δ::hisG lys2Δ sir3Δ::HIS3*) (courtesy of K.Struhl (Cheng and Gartenberg 2000; Katan-Khaykovich and Struhl 2005)). TAP-tagged Sir2 (YDL042C) and TFC3 (YAL001C, subunit TFIIIC) (S288C: *MATa his3Δ1 leu2Δ0 met15Δ0 ura3Δ0 ORF-TAP:HIS3MX6*) strains were both obtained from the yeast TAP-tagged ORF library (Dharmacon). The Sir3D strain from Figure 6 is MRL5.1 (S288C: *MATa ura3D leu2D his3D met15D sir3D:KANR*).

Cell culture

Sir3 tag exchange time course:

All cultures were incubated at 30˚C in an incubator shaker at 220 rpm, crosslinked for 20 min with 1% formaldehyde and quenched for 5 min with 125mM Glycine, unless indicated otherwise. Two 10 ml cultures were grown overnight in YPD (2% glucose). One culture contained hygromicin (0,3 mg/mL; the Hyg+ culture). Hyg+ and Hyg- saturated cultures were then transferred to flasks with 90 ml YPD and hygromicin was added to the Hyg+ culture and incubated for 24h until glucose was depleted and they entered the stationary phase. A 20 ml aliquot from the Hyg+ culture was fixed, pelleted and flash frozen in liquid nitrogen and kept at -80°C as the "before switch" stationary phase sample. The rest of the Hyg+ and Hyg- cultures were pelleted and 80 ml of the Hyg- supernatant was used to resuspend the Hyg+ pellet, and the Hyg+ supernatant and Hyg- pellet were discarded. The resuspended 80 ml culture was inoculated with 1 μM estradiol (Sigma) in order to induce tag exchange, and and incubated overnight for at least 16h. An aliquot for the "after switch" stationary phase sample was processed as above. The remaining culture was diluted to OD 0.3 with fresh YPD (total volume: 1600-2000 ml) and incubated at 30°C to release the culture from stationary phase. 400 ml aliquots were taken at 0, 30 and 1h 30 min after release and after indicated cell doublings (monitored by OD measurements; the first doubling typically takes place 3.5 hours after release and each subsequent doubling takes 1.5hrs). Aliquots for each time point were processed as above and fresh YPD was added to the rest of the culture in order to keep cell density constant (constant OD) maintain cells in exponential growth.

Small cell aliquots (50ul of from a 1:100000 dilution) before and after tag switch were plated on YPD plates and replica-plated on YPD+hygromycin to estimate recombination efficiency. The average recombination efficiency in our cell culture conditions is 96.9% (from 11 independent experiments).

Sir2-TAP and TFC3-TAP time course :

Cultures were done as above except without the Hyg+ culture and estradiol addition, and cells were released from stationary phase after a 48h incubation in YPD.

Western blot

10 mL aliquots from time points above were mixed with 2 mL 100% TCA and kept on ice for 10 min. Cells were then pelleted and washed twice with 500 µL 10% cold TCA. Pellets were resuspended in 300 µL 10% cold TCA and bead beated with Zirconium Sillicate beads (0.5 mm) in a bullet blender (Next Advance) for 3 times x 3 min (intensity 8). Zirconium beads were removed from the cell lysate by centrifugation and the entire cell lysate was washed twice with 200 µL 10% cold TCA. The cells lysate was then pelleted and re-suspended in 70 µL 2xSDS loading buffer (125 mM Tris pH 6.8, 20% glycerol; 4% SDS, 10% β-mercaptoethanol, 0,004% bromophenol blue) preheated at 95˚C. Approximately 30 µL Tris (1M, pH 8,7) was added to each sample to stabilize the pH. Samples were heated for 10 min at 95˚C, pelleted and the soluble protein extract in the supernatant was transferred to new tubes. Protein concentrations were measured by Bradford test kit (Sigma, B6916) and 40 µg/sample was loaded on a 7% polyacrylamide SDS-PAGE gel (30:1 acrylamide/bis-acrylamide). Proteins were transferred after electrophoresis to a PDVF membrane (Bio-Rad, 1620177). The membrane was incubated for 1h at room temperature with either anti-HA (Abcam, ab9110 (lot# GR3245707-3)) or anti-T7 (Bethyl A190-117A (lot# A190-117A-7)) antibodies to detect Sir3 and anti-α-tubulin (Sigma T6199 (lot#116M48C2V)) to detect the α-tubulin loading control. Secondary goat anti-rat-HRP (Santa Cruz Biotechnology G2514), goat anti-rabbit-HRP (Santa Cruz Biotechnology sc-2054) and bovine anti-mouse-HRP (Santa Cruz Biotechnology sc-2375) were added after the corresponding primary antibody and incubated for 1h at room temperature. All antibodies (primary and secondary) were diluted 1/10000 in 5% milk/TBS. The membrane was washed 3x in 1xTBS-10%Tween after each antibody incubation step. The blot was then covered with 500

µL Immobilon Forte Western HRP substrate (Millipore WBLUF0500) for 2 min and protein bands were detected on a high-performance chemiluminescent film (Amersham 28906837).

Microscopy and image analysis

Cells were grown as above and concentrated by centrifugation. 3ul of the cell pellet was injected under the 0.8% agarose/YPD layer that had been poured into each well of an 8-well glass bottom microscopy plate (BioValley).

We used a wide field inverted microscope for epifluorescence and TIRF acquisition (Nikon) under the HiLo setting, with a 60X water objective with a water dispenser, and a EMCCD Evolve 512 Photometrics camera (512*512, 16µm pixel size). The time courses on growing cells were performed at 30°C. Pictures in bright field (Exposure time= 300ms and the Hilo angle= 62°) were taken every 10 or 20min for 6.5hrs.

Shmoon and budding cells were counted manually using the Image J software for visualization.

Chromatin Sonication

Cross-linked frozen cell pellets were re-suspended in 500 µL cell breaking buffer (20% glycerol, 100 mM Tris pH 7.5, 1xEDTA-free protease inhibitor cocktail (Roche)). Zirconium Sillicate beads (400 µL, 0.5 mm) were then added to each aliquot and cells were mechanically disrupted using a bullet blender (Next Advance) for 5 times x 3 min (intensity 8). Zirconium beads were removed from the cell lysate by centrifugation and the entire cell lysate was subject to sonication using the Bioruptor-Pico (Diagenode) for 3x10 cycles of 30 seconds ON/OFF each for a 500bp final median size of chromatin fragments. Cellular debris was then removed by centrifugation and the supernatant was used for ChIP.

ChIP

All steps were done at 4˚C unless indicated otherwise. For each aliquot, Buffer L (50 mM Hepes-KOH pH 7.5, 140 mM NaCl, 1 mM EDTA, 1% Triton X-100, 0.1% sodium deoxycholate) components were added from concentrated stocks (10-20X) for a total volume of 0.8 ml per aliquot. For anti-Ha and anti-T7 ChIP, each aliquot was rotated for 1 hour with 100 µL 50% Sepharose Protein A Fast-Flow bead slurry (IPA400HC, Repligen) previously equilibrated in Buffer L. The beads were pelleted at 3000 X g for 30sec, and approximately 200 µl of the supernatant was set aside for the input sample. The reminder (equivalent to 200 ml of cell culture of 0.5 OD) was separated into anti-HA and anti-T7 fractions. 10 µL anti-HA (Abcam, ab9110 (lot# GR3245707-3) and 10 µL polyclonal anti-T7 (Bethyl A190-117A (lot# A190-117A-7) (Figure 1) or 10 µL monoclonal anti-T7 (Cell Signaling Technology, DSE1X (lot#1)) (Supplementary Figure S1) were added to the corresponding aliquots. Immunoprecipitation, washing, protein degradation, and DNA isolation were performed as previously described (Liu et al., 2003).

Purified DNA was treated with RNAse A (Qiagen) (5µg per sample 1hr at 37°C) and purified once more with Phenol-Chloroform. Purified fragments were used for NGS library construction (Input, ChIP) and subsequent NGS library construction.

For anti-TAP ChIP, aliquots were incubated directly with 10 µL anti-TAP antibodies (Thermo Scientific, CAB10001 (lot# TA261224) overnight with rotation. 50 µL of Dynabeads protein G (Thermo Scientific, 30 mg/mL) were added to each aliquot and incubated for 2h. All the following steps were as above with the following modifications: cross-links were removed after DNA elution, with a 65°C overnight incubation without proteinase K. After RNAse A treatment as above, 1mg/ml of proteinase K was added for 2hrs ate 65°C. DNA was purified with Phenol-Chloroform and further processed as above.

Cell culture and RNA isolation for RNA-seq

MRL9.1 (Sir3wt) and MRL5.1 (Sir3D) were grown as above in YPD and MRL9.1 was not subject to tag switching with estradiol. THC70 (oeSir3) were grown in conditions of Sir3 over-expression in YPGalactose. Cells were flash frozen in liquid N2 and total RNA was isolated from frozen cell pellets with Trizol. Frozen cell pellets were re-suspended directly in Trizol and bead beated in the Bullet Blender (Next Advance) for 4 times x3 min (intensity 8). RNA was then purified and DNAseI treated with the RNAeasy Column purification kit (Qiagen). Extracted total RNA amounts were measured on the Qubit and the Nanodrop and the quality was checked in a Bioanalyzer scan (Agilent). The RNA samples were then used for NGS library preparation using the Illumina TruSeq Stranded mRNA kit according to the manufacturer's protocol. Libraries were sequenced on the Illumina NextSeq550 (2x75bp) (Plateforme Transcriptome, IRMB, Montpellier, France).

GS Input and ChIP library construction and Illumina sequencing

DNA fragments were blunt ended and phosphorylated with the Epicentre End-it-Repair kit. Adenosine nucleotide overhangs were added using Epicentre exo-Klenow. Illumina Genome sequencing adaptors with in line barcodes (

PE1-NNNNN: PhosNNNNNAGATCGGAAGAGCGGTTCAGCAGGAATGCCGAG

PE2-NNNNN: ACACTCTTTCCCTACACGACGCTCTTCCGATCTNNNNNT

, NNNNN indicates the position of the 5bp barcode, (IDT)) were then ligated over night at 16°C using the Epicentre Fast-Link ligation kit. Ligated fragments were amplified as above using the Phusion enzyme (NEB) for 18 PCR cycles with Illumina PE1 (AATGATACGGCGACCACCGAGATCTACACTCTTTCCCTACACGACGCTCTTCCGATCT) and PE2 (CAAGCAGAAGACGGCATACGAGATCGGTCTCGGCATTCCTGCTGAACCGCTCTTCCGATCT) primers (IDT). Reactions were cleaned between each step using MagNa beads.

Libraries were mixed in equimolar amounts (12 to 21 libraries per pool) and library pools were sequenced on the HiSeq 2000 (2x75bp) (Illumina) at the CNAG, Barcelona, Spain or the NextSeq550 (2x75bp) (Plateforme Transcriptome, IRMB, Montpellier, France).

ChIP-seq data analysis

All analysis was done using in house Perl and R scripts available upon request.

Sequences were aligned to S. Cerevisiae genome using BLAT (Kent Informatics, http://hgdownload.soe.ucsc.edu/admin/). We kept reads that had at least one uniquely aligned 100% match in the paired end pair. Read count distribution was determined in 1bp windows and then normalized to 1 by dividing each base pair count with the genome-wide average base-pair count. Forward and reverse reads were then averaged and ChIP reads were normalized to their corresponding input reads.

The repetitive regions map was constructed by “BLATing” all the possible 70 bp sequences of the yeast genome and parsing all the unique 70bp sequences. All the base coordinates that were not in those unique sequences were considered repetitive.

RNA-seq data analysis

Reads were aligned and normalized as above. Normalized read densities for each gene were aligned by the transcription start site and divided into sense and antisense transcripts. The median read density for each gene (from the tss to the end of the coding sequence) was then determined for each transcript. Intron regions were excluded from the calculation.

Author Contributions

HG performed all the experiments except the microscopy part of the experiment in Figure 2B , which was performed by PV. MRL designed the experiments, analyzed the NGS data and wrote the manuscript with input from HG.

Acknowledgments

We thank Fred van Leeuwen and Kevin Struhl for yeast strains and plasmids. Thank you to Marta Gut and Julie Blanc from CNAG (Barcelona, Spain) and Véronique Pantesco (IRMB, Montpellier, France) for deep-sequencing services. We thank Virginie Georget (MRI, Biocampus, Montpellier) for her assistance with the microscope set-up. This work was supported by the ERC-Consolidator grant (NChIP 647618) (MRL).

References

Ai W, Bertram PG, Tsang CK, Chan TF, Zheng XF. 2002. Regulation of subtelomeric silencing during stress response. *Mol Cell* **10**: 1295-1305.

Allen C, Buttner S, Aragon AD, Thomas JA, Meirelles O, Jaetao JE, Benn D, Ruby SW, Veenhuis M, Madeo F et al. 2006. Isolation of quiescent and nonquiescent cells from yeast stationary-phase cultures. *J Cell Biol* **174**: 89-100.

Cheng TH, Gartenberg MR. 2000. Yeast heterochromatin is a dynamic structure that requires silencers continuously. *Genes Dev* **14**: 452-463.

Deshpande AM, Newlon CS. 1996. DNA replication fork pause sites dependent on transcription. *Science* **272**: 1030-1033.

Dhillon N, Raab J, Guzzo J, Szyjka SJ, Gangadharan S, Aparicio OM, Andrews B, Kamakaka RT. 2009. DNA polymerase epsilon, acetylases and remodellers cooperate to form a specialized chromatin structure at a tRNA insulator. *Embo J* **28**: 2583-2600.

Dion MF, Kaplan T, Kim M, Buratowski S, Friedman N, Rando OJ. 2007. Dynamics of replication-independent histone turnover in budding yeast. *Science* **315**: 1405-1408.

Donze D, Kamakaka RT. 2001. RNA polymerase III and RNA polymerase II promoter complexes are heterochromatin barriers in Saccharomyces cerevisiae. *Embo J* **20**: 520-531.

Dubarry M, Loiodice I, Chen CL, Thermes C, Taddei A. 2011. Tight protein-DNA interactions favor gene silencing. *Genes Dev* **25**: 1365-1370.

Gartenberg MR, Smith JS. 2016. The Nuts and Bolts of Transcriptionally Silent Chromatin in Saccharomyces cerevisiae. *Genetics* **203**: 1563-1599.

Grunstein M, Gasser SM. 2013. Epigenetics in Saccharomyces cerevisiae. *Cold Spring Harb Perspect Biol* **5**.

Guidi M, Ruault M, Marbouty M, Loiodice I, Cournac A, Billaudeau C, Hocher A, Mozziconacci J, Koszul R, Taddei A. 2015. Spatial reorganization of telomeres in long-lived quiescent cells. *Genome Biol* **16**: 206.

Hecht A, Strahl-Bolsinger S, Grunstein M. 1996. Spreading of transcriptional repressor SIR3 from telomeric heterochromatin. *Nature* **383**: 92-96.

Ivessa AS, Lenzmeier BA, Bessler JB, Goudsouzian LK, Schnakenberg SL, Zakian VA. 2003. The Saccharomyces cerevisiae helicase Rrm3p facilitates replication past nonhistone protein-DNA complexes. *Mol Cell* **12**: 1525-1536.

Katan-Khaykovich Y, Struhl K. 2005. Heterochromatin formation involves changes in histone modifications over multiple cell generations. *Embo J* **24**: 2138-2149.

McKnight JN, Boerma JW, Breeden LL, Tsukiyama T. 2015. Global Promoter Targeting of a Conserved Lysine Deacetylase for Transcriptional Shutoff during Quiescence Entry. *Mol Cell* **59**: 732-743.

Nikolov I, Taddei A. 2016. Linking replication stress with heterochromatin formation. *Chromosoma* **125**: 523-533.

Radman-Livaja M, Ruben G, Weiner A, Friedman N, Kamakaka R, Rando OJ. 2011. Dynamics of Sir3 spreading in budding yeast: secondary recruitment sites and euchromatic localization. *Embo J* **30**: 1012-1026.

Renauld H, Aparicio OM, Zierath PD, Billington BL, Chhablani SK, Gottschling DE. 1993. Silent domains are assembled continuously from the telomere and are defined by promoter distance and strength, and by SIR3 dosage. *Genes Dev* **7**: 1133-1145.

Simms TA, Dugas SL, Gremillion JC, Ibos ME, Dandurand MN, Toliver TT, Edwards DJ, Donze D. 2008. TFIIIC binding sites function as both heterochromatin barriers and chromatin insulators in Saccharomyces cerevisiae. *Eukaryot Cell* **7**: 2078-2086.

Stone EM, Pillus L. 1996. Activation of an MAP kinase cascade leads to Sir3p hyperphosphorylation and strengthens transcriptional silencing. *J Cell Biol* **135**: 571-583.

Terweij M, van Welsem T, van Deventer S, Verzijlbergen KF, Menendez-Benito V, Ontoso D, San-Segundo P, Neefjes J, van Leeuwen F. 2013. Recombination-induced tag exchange (RITE) cassette series to monitor protein dynamics in Saccharomyces cerevisiae. *G3 (Bethesda)* **3**: 1261-1272.

Teytelman L, Thurtle DM, Rine J, van Oudenaarden A. 2013. Highly expressed loci are vulnerable to misleading ChIP localization of multiple unrelated proteins. *Proc Natl Acad Sci U S A* **110**: 18602-18607.

Valcourt JR, Lemons JM, Haley EM, Kojima M, Demuren OO, Coller HA. 2012. Staying alive: metabolic adaptations to quiescence. *Cell Cycle* **11**: 1680-1696.

Verzijlbergen KF, Menendez-Benito V, van Welsem T, van Deventer SJ, Lindstrom DL, Ovaa H, Neefjes J, Gottschling DE, van Leeuwen F. 2010. Recombination-induced tag exchange to track old and new proteins. *Proc Natl Acad Sci U S A* **107**: 64-68.

Watanabe S, Radman-Livaja M, Rando OJ, Peterson CL. 2013. A histone acetylation switch regulates H2A.Z deposition by the SWR-C remodeling enzyme. *Science* **340**: 195-199.

Weiner A, Chen HV, Liu CL, Rahat A, Klien A, Soares L, Gudipati M, Pfeffner J, Regev A, Buratowski S et al. 2012. Systematic dissection of roles for chromatin regulators in a yeast stress response. *PLoS Biol* **10**: e1001369.

Weiner A, Hughes A, Yassour M, Rando OJ, Friedman N. 2010. High-resolution nucleosome mapping reveals transcription-dependent promoter packaging. *Genome Res* **20**: 90-100.

Ziane R, Camasses A, Radman-Livaja M. 2019. Mechanics of DNA Replication and Transcription Guide the Asymmetric Distribution of RNAPol2 and New Nucleosomes on Replicated Daughter Genomes. *bioRxiv*: 553669.

Figure Legends

Figure 1: A. Diagram of the Sir3 tag switch construct used in ChIP-seq experiments (top left). Bottom: Experiment outline. Cells were arrested by glucose depletion before the tag switch, induced with estradiol addition to stationary cells (recombination efficiency :98.1%). Cells were then released from arrest with addition of fresh media and allowed to grow for one to five doublings (monitored by OD measurements). Cell aliquots were fixed with 1% formaldehyde for 20min at times indicated below the diagrams and anti-HA and anti-T7 (polyclonal) ChIPs were performed on sonicated chromatin. **B**. Heat map of new Sir3 (T7 tag) enrichment over old Sir3 (HA tag) during and after exit from quiescence, at all yeast telomeres (30kbp from chromosomes ends). Time points are aligned by the ARS Consensus Sequence (ACS) located in telomeric silencer regions, which are Sir complex nucleation sites at telomeres. White arrows show tRNA genes where new Sir3 binds after exit from quiescence. Silent mating type loci HML and HMR, on 3L and 3R, respectively, are framed with a white rectangle. Sir3 is enriched in a small 1kb region upstream of the ACS at all telomeres. Repetitive and unmapped regions are shown in grey. The HMLa reads have been eliminated as repetitive sequences during alignment to the reference genome which is MATa. **C-D**. Old (top) and new (middle) Sir3 enrichment around ACS averaged for all 32 telomeres (C) or tRNA genes averaged for all 274 genes (D) at indicated time points during the stationary and the renewed growth phases. The bottom panel shows average enrichment around the ACS (C) or tRNA genes (D) for old and new Sir3 over time. **E-F**. Old (top left) and new (bottom left) Sir3 enrichment at HML (E) and HMR (F) at indicated time points (same color code for E and F) during the stationary and the renewed growth phase. The right panel shows average enrichment over the entire silent mating type locus for old and new Sir3 over time.

Figure 2: Heterochromatin is destabilized before the first division following exit from stationary phase. **A**. Western blot of old Sir3-HA (anti-HA antibody) and new Sir3-T7 (anti T7 antibody) from total cell extracts during and after release from stationary phase. The top panel shows the experimental outline and describes the time points

shown in the blot (marked by arrows above the blot). * marks a non-specific band detected with the anti-T7 antibody. The graph below the blot shows the quantification of the bands from the blot. Sir3 band intensities were first normalized to the a-tubulin loading control and then divided by the normalized Sir3-HA intensity from mid-log cells (bar graph). The line plot inset shows the same normalized Sir3-HA and Sir3-T7 band intensities for all time points after mid-log. **B**. α-factor heterochromatin stability test. The diagram on top shows the expected response of MATa cells to α-factor added after release from stationary phase. If the SIR heterochromatic complex is unstable HMLα and HMRa will be transcribed along with MATa, thus creating pseudo-diploid cells that don't respond to α-factor and consequently do not become shmoo but start budding instead. The bottom panel shows examples of frames from a live cell imaging experiment that follows log phase cells (top), stationary phase cells in the first cell cycle after release (middle) or stationary phase cells that have undergone one cell division after release (bottom) in the presence of 0.2mg/ml α-factor 0 and 380min after the beginning of the time course. The bar graph on the right shows the fraction of budding cells in all cells (budding and shmoo) for each cell population. The p-values for the null-hypothesis between released stationary phase cells and log-phase cells shown above the bars are calculated from the Z score obtained using Z-test statistics with significance cutoff a=0.05:

$$Z = \frac{(p1 - p2) - 0}{\sqrt{(p(1-p)(\frac{1}{n1} + \frac{1}{n2}))}}$$

where p1 and p2 are n(budding)/n(shmoon +budding) in cells released from stationary phase and log-phase cells respectively, n1 and n2 are n(shmoon+budding) in stationary phase and mid-log cells respectively and p is (n(budding)stationary + n(budding)midlog) / (n1+n2). **C.** α-factor test with the OE Sir3 strain which shmooes independently of Sir3 in the presence of α-factor because of the deletion of HML and MAT loci.

Figure 3: A. Diagram of the Sir3 gene construct controlled by a Galactose inducible promoter in the Sir3 OE strain (OverExpression) (top left). Bottom: Experiment outline. Cells were arrested by galactose depletion, and released of fresh media with the indicated carbon source (2%) and allowed to grow for 2 and 12 doublings (monitored by OD measurements). Cell aliquots were fixed with 1% formaldehyde for 20min at times indicated below the diagrams and anti-HA ChIPs were performed on sonicated chromatin. **B**. Heat map of Sir3 (HA tag) enrichment over input during and after exit from quiescence, at all yeast telomeres (30kbp from chromosomes ends). Time points are aligned by the ARS Consensus Sequence (ACS) located in telomeric silencer regions, which are Sir complex nucleation sites at telomeres. Silent mating type loci HML (HML is deleted in this strain) and HMR, on 3L and 3R, respectively, are framed with a white rectangle. Repetitive and unmapped regions are shown in grey. **C-E**. Sir3 enrichment around ACS averaged for all 32 telomeres after release into Galactose- over expression of Sir3 (C), Dextrose- inhibition of Sir3 expression (D) or Raffinose- low Sir3 expression (E). **F-G**. Average Sir3 enrichment around the ACS (E) or tRNA genes (F) over time in indicated carbon sources. **H-J**. Average Sir3 enrichment at tRNA genes for all 274 genes after release into Galactose (H), Dextrose (I) or Raffinose (J). K-M. Sir3 enrichment at HMR after release into Galactose (K), Dextrose (L) or Raffinose (M). N Average Sir3 enrichment over the entire HMR over time.

Figure 4: Gene expression upregulation upon release from stationary phase is impaired in the absence of Sir3 depletion. A. Left: Genotypes of yeast strains used in the RNA-seq experiment outlined on the right. **B.** Heat map of median mRNA enrichment (normalized to the genome average per time point) in wtSir3, Sir3D and oeSir3 strains before and after release from stationary phase for 710 genes that are upregulated before the first division after release from stationary phase in the wtSir3 strain. The genes are divided into three clusters based on average mRNA abundance in midlog (bar graph on the left). GO analysis shows enrichment for “growth” genes: ribosome biogenesis, metabolic processes, mitochondrial proteins (Table S1) **C.** Line plot of average median mRNA enrichment (over all 710 genes from B) for wtSir3, Sir3D and oeSir3 at each time point. **D.-E.** Box plot distributions of median mRNA per cluster from B (D) compared to the median wt Sir3 (dataset from

Figure S1) and oeSir3 (Figure 3) CDS enrichment (E). **F.** Sir3 exchange rates after release from stationary phase at genes from clusters in B and D. The new/old Sir3 ratios are calculated from the medians of the log2(median Sir3 CDS enrichment) distributions from **E.** G. Sir3 exchange rates after release from stationary phase at subtelomeric regions and HMR and HML from Figure S1. The new/old Sir3 ratios are calculated from the average Sir3 enrichment shown in Figure S1**.**

Figure 5: A. Diagram of the Sir2-TAP tag construct used in ChIP-seq experiments shown here (top left). Bottom: Experiment outline. Cells were grown for 48hrs until they reached stationary phase by glucose depletion . Cells were then released from arrest with addition of fresh media and allowed to grow for one to twelve doublings (monitored by OD measurements). Cell aliquots were fixed with 1% formaldehyde for 20min at times indicated below the diagrams and anti-TAP ChIPs were performed on sonicated chromatin. **B.** Heat map of Sir2 (TAP tag) enrichment over input during and after exit from quiescence, at all yeast telomeres (30kbp from chromosomes ends). Time points are aligned by the ARS Consensus Sequence (ACS) located in telomeric silencer regions i.e. Sir complex nucleation sites at telomeres. Silent mating type loci HML and HMR, on 3L and 3R, respectively, are framed with a white rectangle. Sir2 is enriched in a small 1kb region upstream of the ACS at all telomeres. Repetitive and unmapped regions are shown in grey. The HMLa reads have been eliminated as repetitive sequences during alignment to the reference genome which is MATa. **C-D**. Sir2 enrichment around ACS averaged for all 32 telomeres (C) or tRNA genes averaged for all 274 genes (D) at indicated time points during the stationary and the renewed growth phases. The bottom panel shows average enrichment around the ACS (C) or tRNA genes (D) for Sir2 over time. **E-G**. Sir2 enrichment at HML (E), HMR (F) and rDNA (G) (NTS1-2 is the non-transcribed region of the rDNA repeat between the 3' ETS and RDN5) at indicated time points during the stationary and the renewed growth phase. The bottom panel shows average enrichment over the entire silent mating type locus or rDNA for Sir2 over time.

Figure 6: TFIIIC binding to tRNA genes upon release from stationary phase. **A**. Diagram of the TFC3-TAP tag construct used in ChIP-seq experiments shown here (top). Right: Experiment outline. Cells were grown for 48hrs until they reached stationary phase by glucose depletion. Cells were then released from arrest with addition of fresh media and allowed to grow for one to twelve doublings (monitored by OD measurements). Cell aliquots were fixed with 1% formaldehyde for 20min at times indicated below the diagrams and anti-TAP ChIPs were performed on sonicated chromatin. **B**. Average profiles of TFIIIC (TAP tag) enrichment over input at all 274 tRNA genes before, during and after exit from quiescence. **C**. K-means clustering of median TFIIIC enrichment at tRNA genes (-50 to +150 bp around the start of the gene) at indicated time points (columns). Cluster 1: tRNA genes with increased TFIIIC binding after release; Cluster 2:tRNA genes with reduced TFIIIC binding after release; Cluster 3:low binding TFIIIC tRNA genes with slow recovery after release. **D-F** box plot distributions of median read density enrichment comparing TFIIIC binding to old(HA)/new(T7) Sir3 (D: Figure 1, polyclonal anti-T7; E: Figure S1, monoclonal anti-T7) , over-expressed Sir3 (Galactose inducible, Figure S2) and Sir2 (F, Figure 3) at tRNA genes from clusters shown in C. Sir3 and Sir2 binding is independent of TFIIIC binding (and consequently tRNA expression) since binding dynamics of Sir3 and Sir2 before and after stationary phase are the same for all three clusters from C: Sir3 and Sir2 are depleted from tRNA genes in stationary phase and rebind gradually before the first doubling after release and stay stably bound through at least 12 doublings. The polyclonal anti-T7 antibody (D, Figure 1) appears to have a much higher affinity for the T7 tag than the monoclonal anti-T7 used in Figure S1 (E), at least in the Sir3 configuration bound to tRNA genes since a difference between these two antibodies is not detected at telomeres and silent mating type loci (compare Figures 1 and S1). It is therefore difficult to judge whether binding of old Sir3 detectable even at 12 doublings after release comes from cells that have not undergone tag switch (about 2% of the initial population in stationary phase) or from a fraction of old Sir3 that has “survived” since the stationary phase. Sir3 binding is not a “tag” artefact as untagged “wt Sir3” (custom ant-Sir3 antibody, dataset from(Radman-Livaja et al. 2011)) (F) and old-Sir3 HA (E) have similar enrichment distributions in midlog cells.

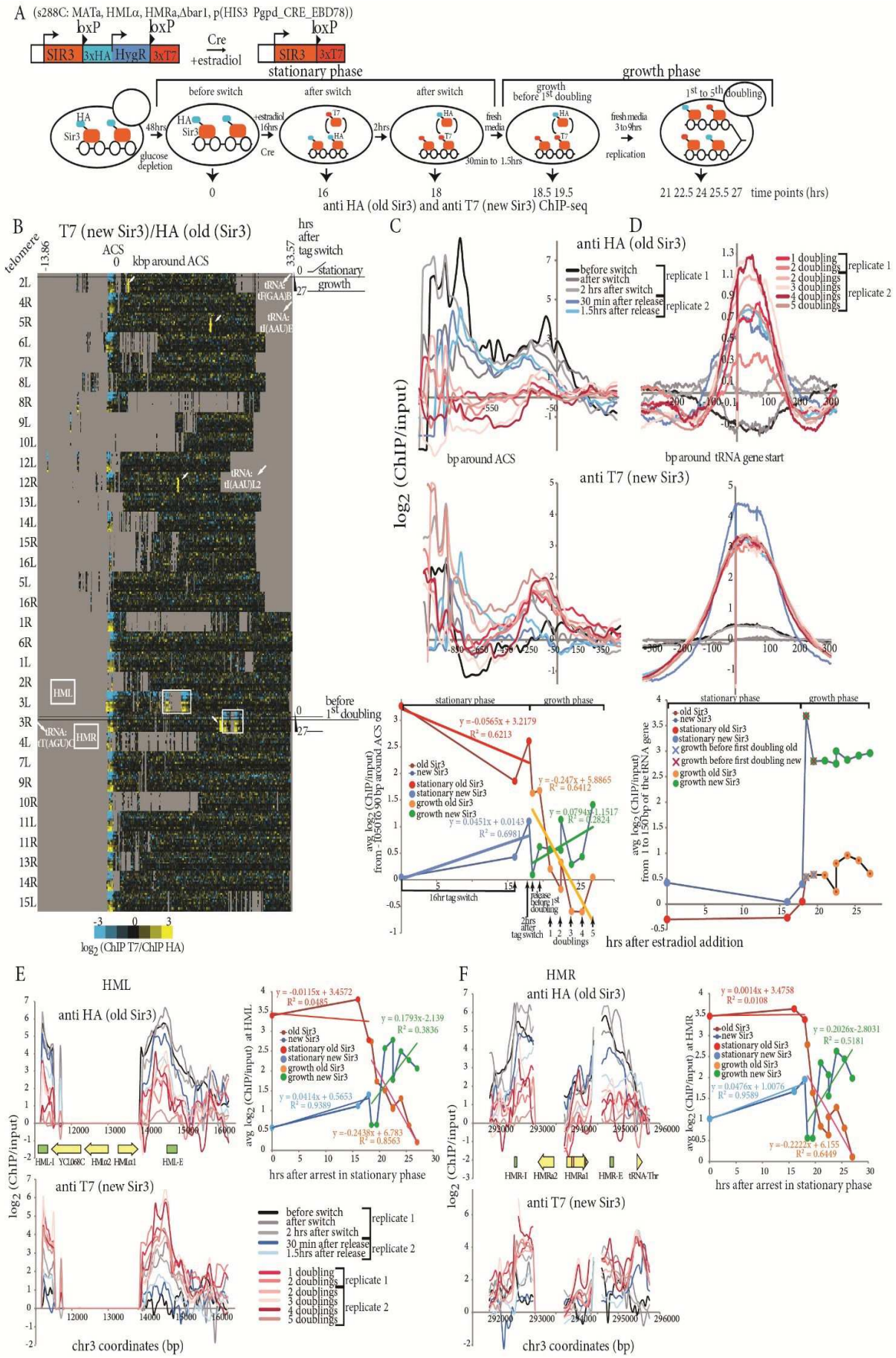
A
(s288C: MATa, HMLα, HMRa,Δbar1, p(HIS3 Pgpd_CRE_EBD78))
loxP
SIR3
3xHA
HygR
3xT7
Cre
+estradiol
stationary phase
growth phase
before switch
after switch
after switch
growth before 1st doubling
1st to 5th doubling
HA
Sir3
48hrs
glucose depletion
+estradiol 16hrs
Cre
2hrs
fresh media
30min to 1.5hrs
fresh media 3 to 9hrs
replication
0
16
18
18.5 19.5
21 22.5 24 25.5 27 time points (hrs)
anti HA (old Sir3) and anti T7 (new Sir3) ChIP-seq
B
T7 (new Sir3)/HA (old Sir3)
telomere
ACS
kbp around ACS
hrs after tag switch
stationary
growth
tRNA: tF(GAA)B
tRNA: tI(AAU)F
tRNA: tI(AAU)L2
HML
HMR
tRNA: tT(AGU)C
before 1st doubling
log2 (ChIP T7/ChIP HA)
C
anti HA (old Sir3)
before switch
after switch
2 hrs after switch
30 min after release
1.5hrs after release
replicate 1
replicate 2
log2 (ChIP/input)
bp around ACS
anti T7 (new Sir3)
D
anti HA (old Sir3)
1 doubling
2 doublings
3 doublings
4 doublings
5 doublings
bp around tRNA gene start
anti T7 (new Sir3)
stationary phase
growth phase
old Sir3
new Sir3
stationary old Sir3
stationary new Sir3
growth old Sir3
growth new Sir3
growth before first doubling old
growth before first doubling new
avg. log2 (ChIP/input) from -1050 to 90 bp around ACS
avg. log2 (ChIP/input) from 1 to 1500 bp of the tRNA gene
y = -0.0565x + 3.2179
R² = 0.6213
y = -0.247x + 5.8865
R² = 0.6412
y = 0.0794x - 1.1517
R² = 0.2824
y = 0.0451x + 0.0143
R² = 0.6981
16hr tag switch
release before 1st doubling
2hrs after tag switch
doublings
hrs after estradiol addition
E
HML
anti HA (old Sir3)
HML-I
YCL068C
HMLα2
HMLα1
HML-E
avg log2 (ChIP/input) at HML
y = -0.0115x + 3.4572
R² = 0.0485
y = 0.1793x - 2.139
R² = 0.3836
y = 0.0414x + 0.5653
R² = 0.9389
y = -0.2438x + 6.783
R² = 0.8563
hrs after arrest in stationary phase
anti T7 (new Sir3)
chr3 coordinates (bp)
F
HMR
anti HA (old Sir3)
HMR-I
HMRa2
HMRa1
HMR-E
tRNA-Thr
avg log2 (ChIP/input) at HMR
y = 0.0014x + 3.4758
R² = 0.0108
y = 0.2026x - 2.8031
R² = 0.5181
y = 0.0476x + 1.0076
R² = 0.9589
y = -0.2222x + 6.155
R² = 0.6449
anti T7 (new Sir3)
chr3 coordinates (bp)

Figure 1

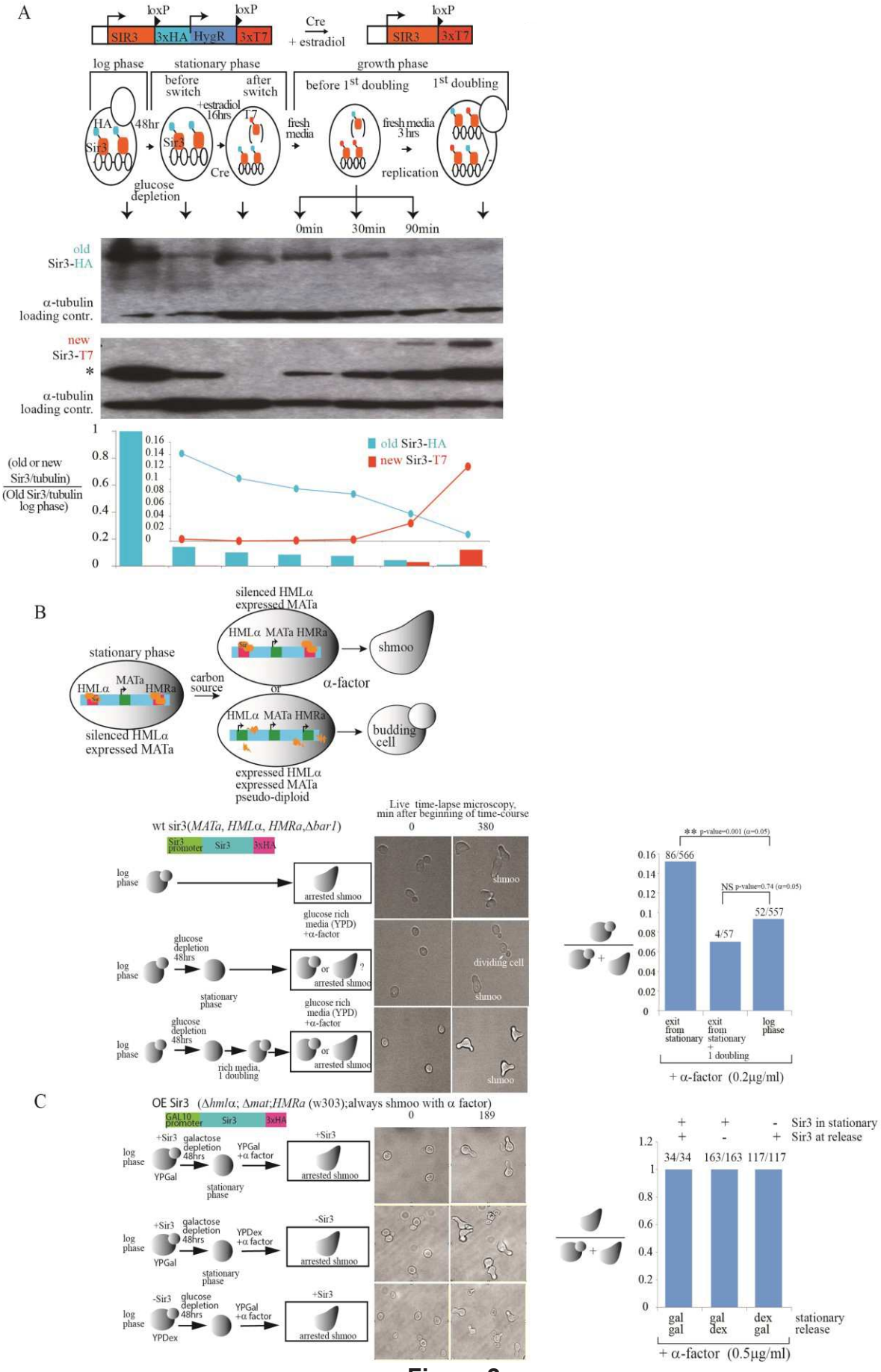
A
loxP
SIR3
3xHA
HygR
3xT7
Cre
+ estradiol
log phase
stationary phase
growth phase
before switch
after switch
before 1st doubling
1st doubling
HA
Sir3
48hr
+estradiol 16hrs
T7
Cre
fresh media
fresh media 3 hrs
replication
glucose depletion
0min
30min
90min
old Sir3-HA
α-tubulin loading contr.
new Sir3-T7
*
α-tubulin loading contr.
(old or new Sir3/tubulin) / (Old Sir3/tubulin log phase)
old Sir3-HA
new Sir3-T7
B
silenced HMLα expressed MATa
HMLα MATa HMRa
shmoo
α-factor
stationary phase
carbon source
or
budding cell
expressed HMLα expressed MATa pseudo-diploid
Live time-lapse microscopy, min after beginning of time-course
0
380
wt sir3(MATa, HMLα, HMRa,Δbar1)
Sir3 promoter
Sir3
3xHA
log phase
arrested shmoo
glucose rich media (YPD) +α-factor
glucose depletion 48hrs
stationary phase
dividing cell
rich media, 1 doubling
** p-value=0.001 (α=0.05)
NS p-value=0.74 (α=0.05)
86/566
4/57
52/557
exit from stationary
exit from stationary + 1 doubling
log phase
+ α-factor (0.2μg/ml)
C
OE Sir3 (Δhmlα; Δmat;HMRa (w303);always shmoo with α factor)
GAL10 promoter
Sir3
3xHA
0
189
+Sir3
galactose depletion 48hrs
YPGal
YPGal +α factor
-Sir3
YPDex +α factor
YPDex
Sir3 in stationary
Sir3 at release
34/34
163/163
117/117
gal gal
gal dex
dex gal
stationary release
+ α-factor (0.5μg/ml)

Figure 2

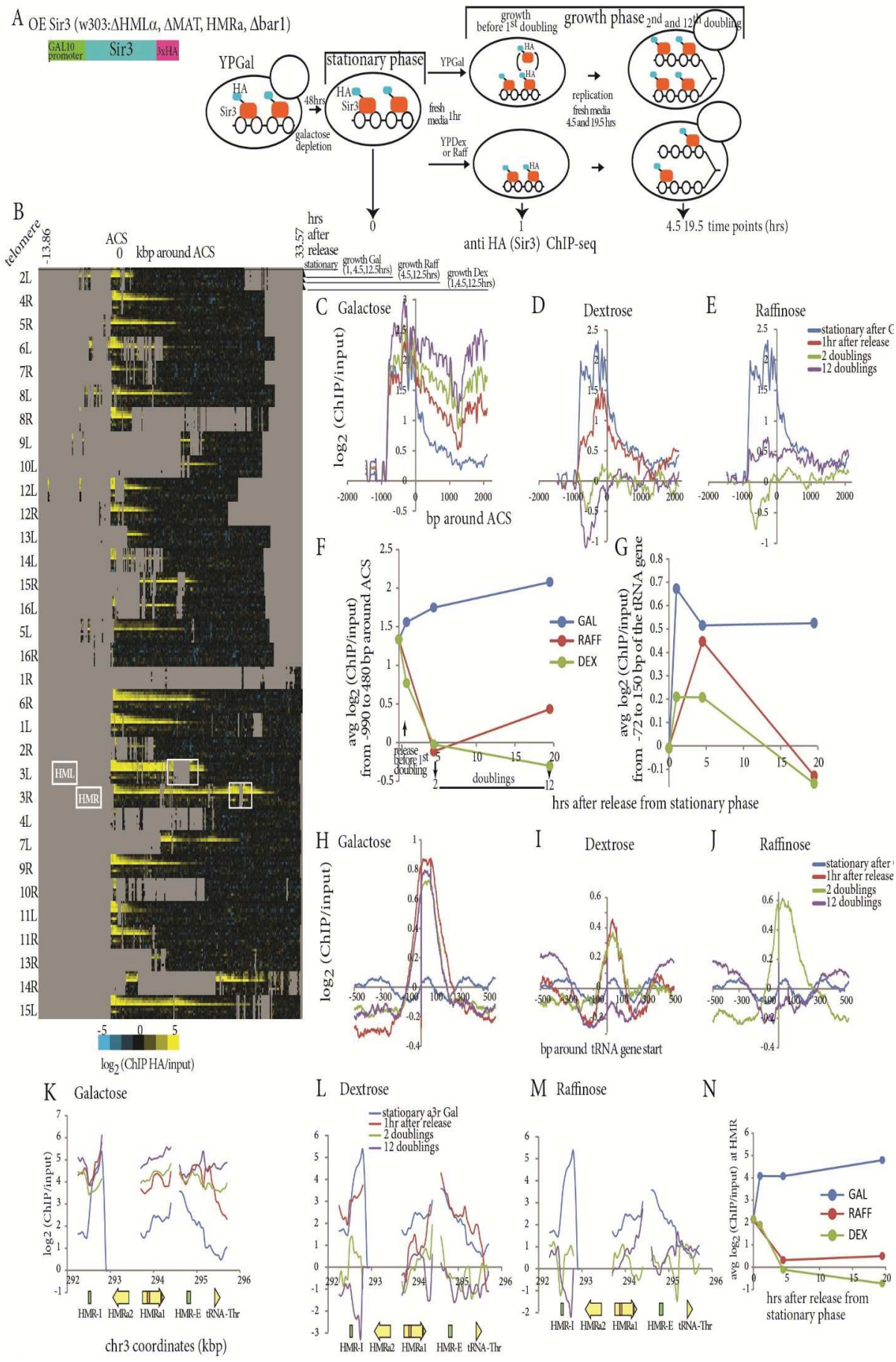
A OE Sir3 (w303:ΔHMLα, ΔMAT, HMRa, Δbar1)
GAL10 promoter
Sir3
3xHA
YPGal
HA
Sir3
48hrs
galactose depletion
stationary phase
fresh media 1hr
YPDex or Raff
growth before 1st doubling
growth phase 2nd and 12th doubling
replication fresh media 4.5 and 19.5 hrs
0
1
anti HA (Sir3) ChIP-seq
4.5 19.5 time points (hrs)
B
telomere
-13.86
ACS
0 kbp around ACS
33.57
hrs after release
stationary
growth Gal (1, 4.5, 12.5hrs)
growth Raff (4.5, 12.5hrs)
growth Dex (1,4.5,12.5hrs)
2L
4R
5R
6L
7R
8L
8R
9L
10L
12L
12R
13L
14L
15R
16L
5L
16R
1R
6R
1L
2R
3L
3R
4L
7L
9R
10R
11L
11R
13R
14R
15L
HML
HMR
log2 (ChIP HA/input)
C Galactose
D Dextrose
E Raffinose
log2 (ChIP/input)
bp around ACS
stationary after G
1hr after release
2 doublings
12 doublings
F
avg log2 (ChIP/input) from -990 to 480 bp around ACS
GAL
RAFF
DEX
release before 1st doubling
doublings
G
avg log2 (ChIP/input) from -72 to 150 bp of the tRNA gene
hrs after release from stationary phase
H Galactose
I Dextrose
J Raffinose
log2 (ChIP/input)
bp around tRNA gene start
K Galactose
log2 (ChIP/input)
HMR-I
HMRa2
HMRa1
HMR-E
tRNA-Thr
chr3 coordinates (kbp)
L Dextrose
stationary a3r Gal
1hr after release
2 doublings
12 doublings
M Raffinose
N
avg log2 (ChIP/input) at HMR
GAL
RAFF
DEX
hrs after release from stationary phase

Figure 3

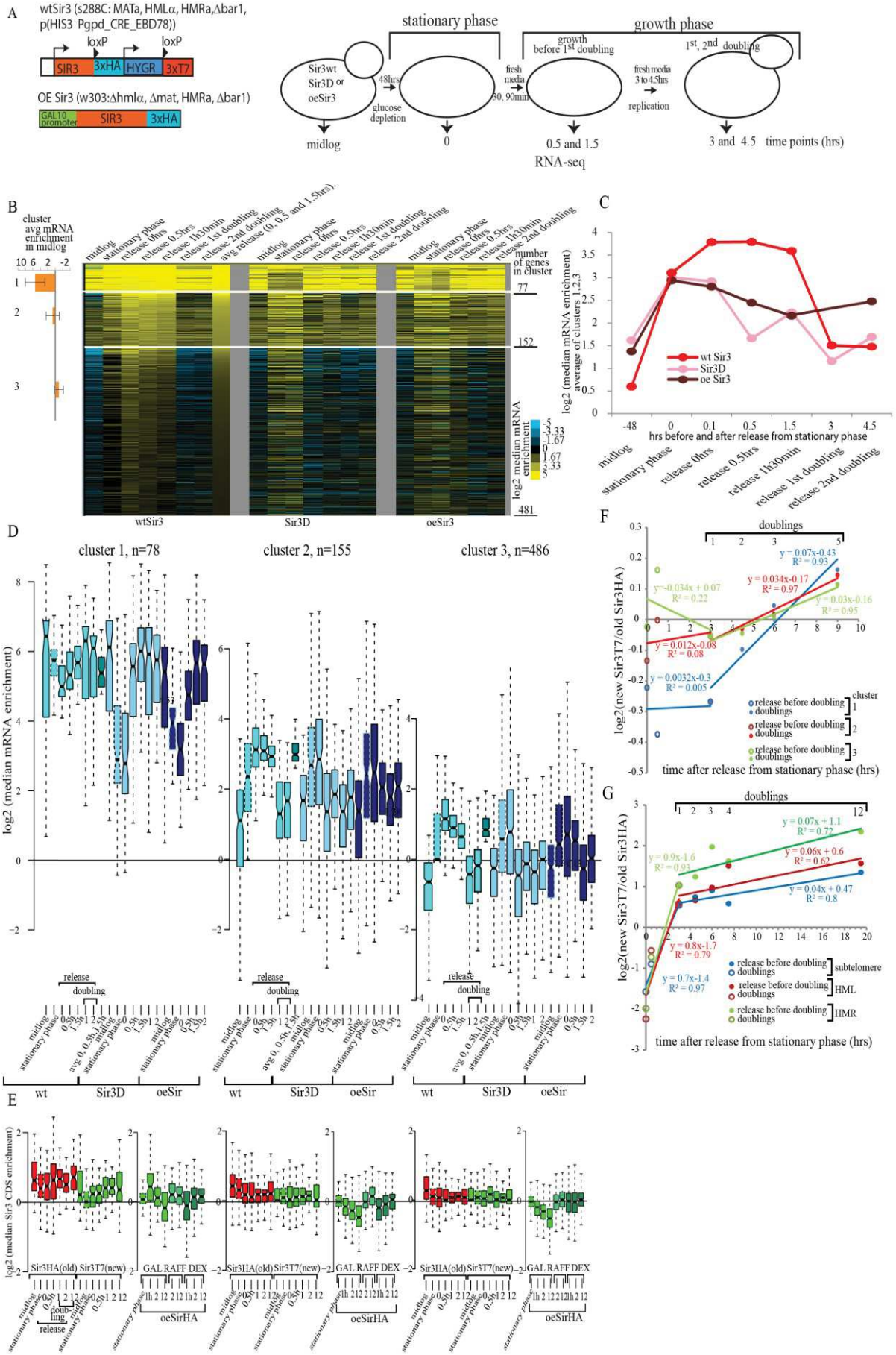
A
wtSir3 (s288C: MATa, HMLα, HMRa,Δbar1, p(HIS3 Pgpd_CRE_EBD78))
loxP
loxP
SIR3
3xHA
HYGR
3xT7
OE Sir3 (w303:Δhmlα, Δmat, HMRa, Δbar1)
GAL10 promoter
SIR3
3xHA
stationary phase
growth phase
Sir3wt
Sir3D or
oeSir3
48hrs
glucose depletion
fresh media
30, 90min
growth before 1st doubling
fresh media 3 to 4.5hrs
replication
1st, 2nd doubling
midlog
0
0.5 and 1.5
RNA-seq
3 and 4.5 time points (hrs)
B
cluster avg mRNA enrichment in midlog
number of genes in cluster
77
152
481
log2 median mRNA enrichment
wtSir3
Sir3D
oeSir3
C
log2 (median mRNA enrichment) average of clusters 1,2,3
wt Sir3
Sir3D
oe Sir3
hrs before and after release from stationary phase
midlog
stationary phase
release 0hrs
release 0.5hrs
release 1h30min
release 1st doubling
release 2nd doubling
D
cluster 1, n=78
cluster 2, n=155
cluster 3, n=486
log2 (median mRNA enrichment)
release
doubling
wt
Sir3D
oeSir
E
log2 (median Sir3 CDS enrichment)
Sir3HA(old) Sir3T7(new)
GAL RAFF DEX
oeSirHA
F
doublings
log2(new Sir3T7/old Sir3HA)
y = 0.07x-0.43 R² = 0.93
y = 0.034x-0.17 R² = 0.97
y=-0.034x + 0.07 R² = 0.22
y = 0.03x-0.16 R² = 0.95
y = 0.012x-0.08 R² = 0.08
y = 0.0032x-0.3 R² = 0.005
release before doubling
doublings
cluster
time after release from stationary phase (hrs)
G
doublings
log2(new Sir3T7/old Sir3HA)
y = 0.07x + 1.1 R² = 0.72
y = 0.9x-1.6 R² = 0.93
y = 0.06x + 0.6 R² = 0.62
y = 0.04x + 0.47 R² = 0.8
y = 0.8x-1.7 R² = 0.79
y = 0.7x-1.4 R² = 0.97
release before doubling
doublings
subtelomere
HML
HMR
time after release from stationary phase (hrs)

Figure 4

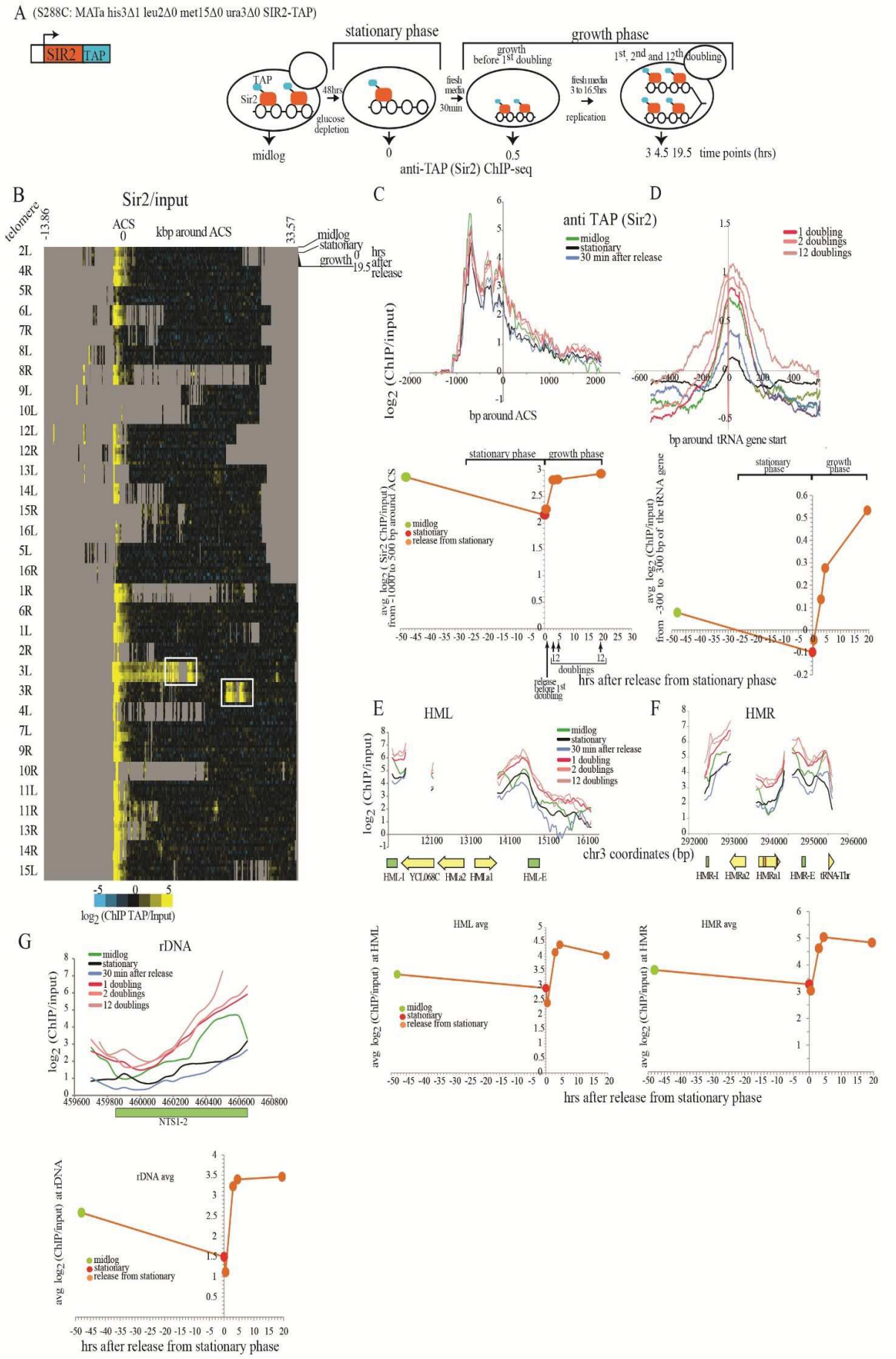
A (S288C: MATa his3Δ1 leu2Δ0 met15Δ0 ura3Δ0 SIR2-TAP)
SIR2 TAP
stationary phase
growth phase
TAP
Sir2
48hrs
glucose depletion
fresh media 30min
growth before 1st doubling
fresh media 3 to 16.5hrs
replication
1st, 2nd and 12th doubling
midlog
0
0.5
3 4.5 19.5 time points (hrs)
anti-TAP (Sir2) ChIP-seq
B
Sir2/input
telomere
-13.86
ACS
0
kbp around ACS
33.57
midlog
stationary
growth
hrs after release
0
19.5
2L
4R
5R
6L
7R
8L
8R
9L
10L
12L
12R
13L
14L
15R
16L
5L
16R
1R
6R
1L
2R
3L
3R
4L
7L
9R
10R
11L
11R
13R
14R
15L
-5
0
5
log2 (ChIP TAP/Input)
C
anti TAP (Sir2)
midlog
stationary
30 min after release
log2 (ChIP/input)
bp around ACS
D
1 doubling
2 doublings
12 doublings
bp around tRNA gene start
stationary phase
growth phase
midlog
stationary
release from stationary
avg log2 (Sir2 ChIP/input) from -1000 to 500 bp around ACS
avg log2 (ChIP/input) from -300 to 300 bp of the tRNA gene
release before 1st doubling
12 doublings
hrs after release from stationary phase
E
HML
midlog
stationary
30 min after release
1 doubling
2 doublings
12 doublings
log2 (ChIP/input)
chr3 coordinates (bp)
HML-I YCL068C HMLa2 HMLa1 HML-E
F
HMR
HMR-I HMRa2 HMRa1 HMR-E tRNA-Thr
G
rDNA
log2 (ChIP/input)
NTS1-2
rDNA avg
avg log2 (ChIP/input) at rDNA
HML avg
avg log2 (ChIP/input) at HML
HMR avg
avg log2 (ChIP/input) at HMR
hrs after release from stationary phase

Figure 5

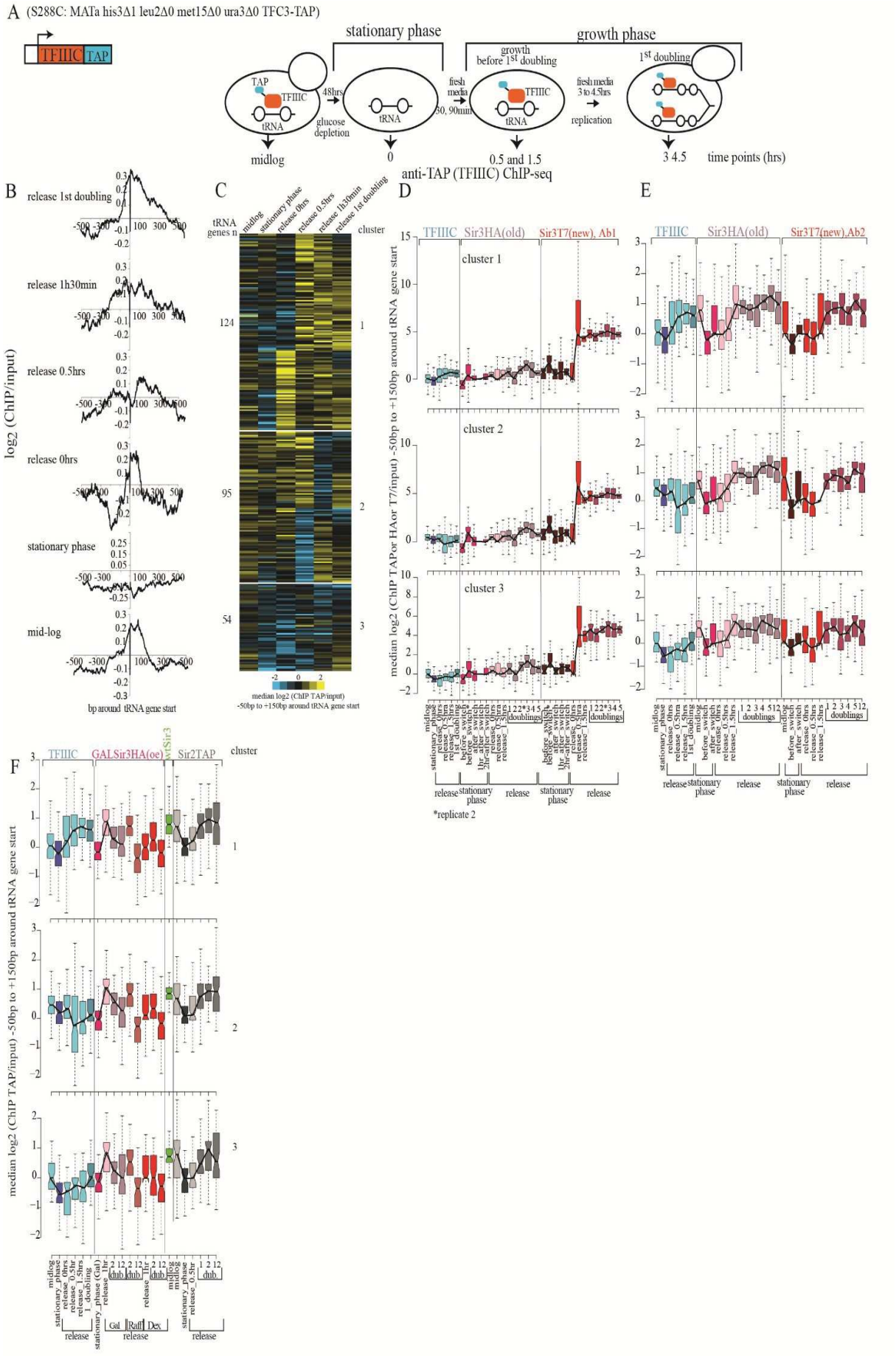
A (S288C: MATa his3Δ1 leu2Δ0 met15Δ0 ura3Δ0 TFC3-TAP)
TFIIIC TAP
stationary phase
growth phase
TAP
TFIIIC
tRNA
48hrs
glucose depletion
fresh media
30, 90min
growth before 1st doubling
fresh media 3 to 4.5hrs
replication
1st doubling
midlog
0
0.5 and 1.5
3 4.5
time points (hrs)
anti-TAP (TFIIIC) ChIP-seq
B
release 1st doubling
release 1h30min
release 0.5hrs
release 0hrs
stationary phase
mid-log
log2 (ChIP/input)
bp around tRNA gene start
C
tRNA genes n
midlog
stationary phase
release 0hrs
release 0.5hrs
release 1h30min
release 1st doubling
cluster
124
95
54
median log2 (ChIP TAP/input)
-50bp to +150bp around tRNA gene start
D
TFIIIC
Sir3HA(old)
Sir3T7(new), Ab1
cluster 1
cluster 2
cluster 3
median log2 (ChIP TAPor HAor T7/input) -50bp to +150bp around tRNA gene start
doublings
release
stationary phase
*replicate 2
E
TFIIIC
Sir3HA(old)
Sir3T7(new),Ab2
F
TFIIIC
GALSir3HA(oe)
wtSir3
Sir2TAP
cluster
median log2 (ChIP TAP/input) -50bp to +150bp around tRNA gene start
Gal
Raff
Dex
dub.

Figure 6

Supplementary Table S1: GO annotations of "growth response genes" from Figure 4

Supplementary Figure Legends

Figure S1: A. Diagram of the Sir3 tag switch construct used in ChIP-seq experiments shown here (top left). Bottom: Experiment outline. Cells were arrested by glucose depletion before the tag switch, which is induced with estradiol addition to arrested cells (recombination efficiency :97.5%). Cells were then released from arrest with addition of fresh media and allowed to grow for one to twelve doublings (monitored by OD measurements). Cell aliquots were fixed with 1% formaldehyde for 20min at times indicated below the diagrams and anti-HA and anti-T7 (monoclonal Cell Signaling Technology, DSE1X (lot#1)) ChIPs were performed on sonicated chromatin. **B.** Heat map of new Sir3 (T7 tag) enrichment over old Sir3 (HA tag) during and after exit from quiescence, at all yeast telomeres (30kbp from chromosomes ends). Time points are aligned by the ARS Consensus Sequence (ACS) located in telomeric silencer regions i.e. Sir complex nucleation sites at telomeres. Silent mating type loci HML and HMR, on 3L and 3R, respectively, are framed with a white rectangle. Sir3 is enriched in a small 1kb region upstream of the ACS at all telomeres. Repetitive and unmapped regions are shown in grey. The HMLα reads have been eliminated as repetitive sequences during alignment to the reference genome which is MATα**. C-D**. Old (top) and new (middle) Sir3 enrichment around ACS averaged for all 32 telomeres (C) or tRNA genes averaged for all 274 genes (D) at indicated time points during the stationary and the renewed growth phases. The bottom panel shows average enrichment around the ACS (C) or tRNA genes (D) for old and new Sir3 over time. **E-F.** Old (top left) and new (bottom left) Sir3 enrichment at HML (E) and HMR (F) at indicated time points (same color code for E and F) during the stationary and the renewed growth phase. The right panel shows average enrichment over the entire silent mating type locus for old and new Sir3 over time.

Supplementary Figure S2: Nucleosome features at tRNA genes. A. Average read density profiles for all tRNA genes from wt cells in mid-log: nucleosome positioning (red [1] and green[2]) from MNAse-seq datasets; H3K56ac (purple) [2] and Htz ChIP-seq (blue)[3]. Read densities were normalized to the average genomic read density for each dataset. Watson and Crick reads were treated separately and then averaged together. Datasets for analysis were taken from the articles indicated in the figure legened. **B.** Chromatin dynamics at tRNA genes during genome replication. Read density profiles of early replicating tRNA genes (76 genes with replication timing earlier than 35min after release from G1 arrest as measured in [4]) in early (left) and mid S-phase (right). The datasets were taken from[2]. Read densities were normalized to the average genomic read density for each dataset. Only Watson reads are shown. The solid line represents a 50bp moving window average of the dotted line.

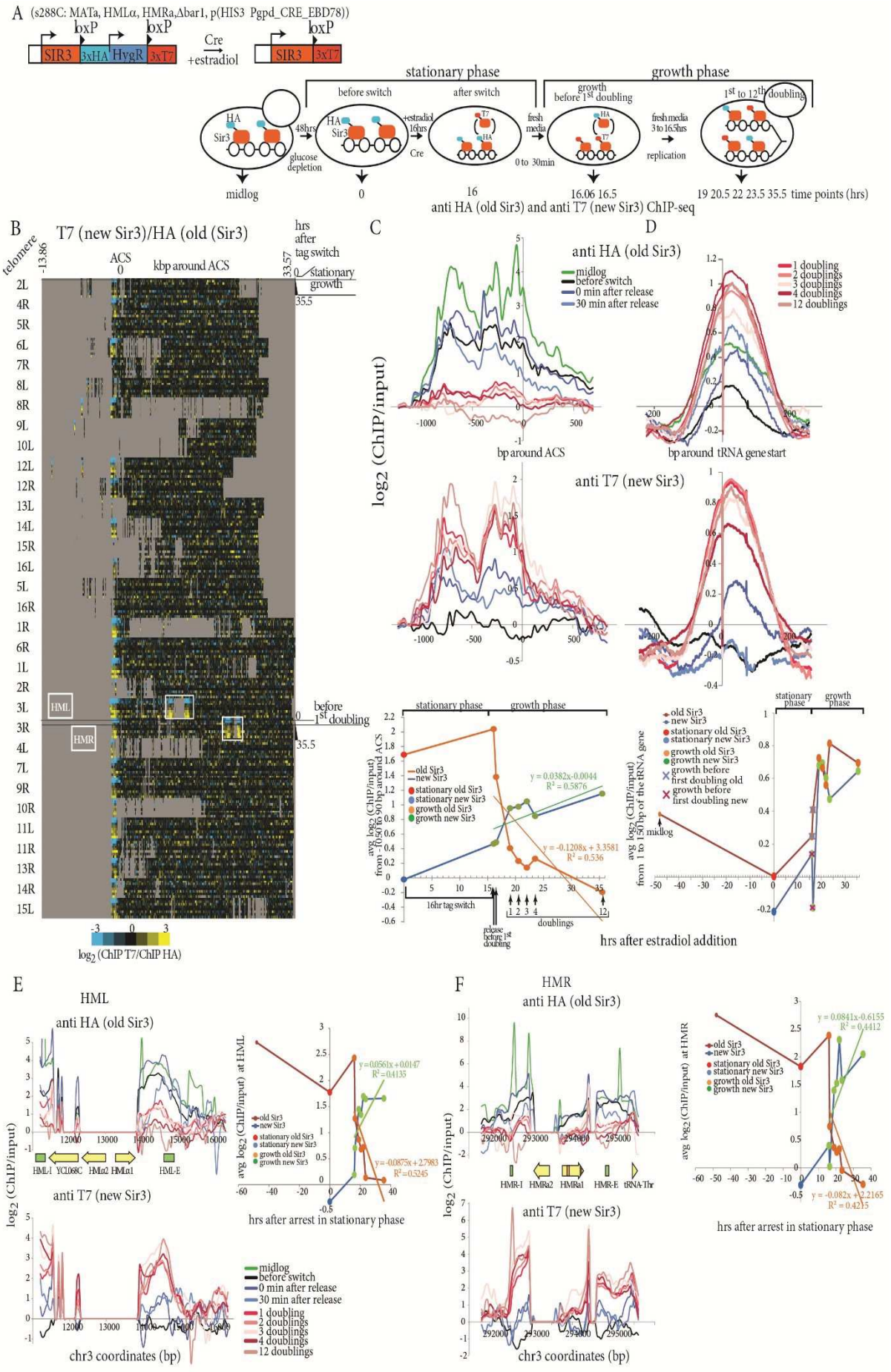
A
(s288C: MATa, HMLα, HMRa,Δbar1, p(HIS3 Pgpd_CRE_EBD78))
loxP
SIR3
3xHA
HygR
3xT7
Cre
+estradiol
stationary phase
growth phase
before switch
after switch
growth before 1st doubling
1st to 12th doubling
HA
Sir3
T7
48hrs
+estradiol 16hrs
Cre
fresh media
0 to 30min
fresh media 3 to 16.5hrs
replication
glucose depletion
midlog
0
16
16.06 16.5
19 20.5 22 23.5 35.5 time points (hrs)
anti HA (old Sir3) and anti T7 (new Sir3) ChIP-seq
B
T7 (new Sir3)/HA (old Sir3)
telomere
-13.86
ACS
kbp around ACS
hrs after tag switch
33.57
stationary
growth
35.5
HML
HMR
before 1st doubling
log2 (ChIP T7/ChIP HA)
C
anti HA (old Sir3)
midlog
before switch
0 min after release
30 min after release
log2 (ChIP/input)
bp around ACS
anti T7 (new Sir3)
D
1 doubling
2 doublings
3 doublings
4 doublings
12 doublings
bp around tRNA gene start
stationary phase
growth phase
old Sir3
new Sir3
stationary old Sir3
stationary new Sir3
growth old Sir3
growth new Sir3
y = 0.0382x-0.0044
R² = 0.5876
y = -0.1208x + 3.3581
R² = 0.536
avg. log2 (ChIP/input) from -150 to 90 bp around ACS
16hr tag switch
doublings
release before 1st doubling
avg. log2 (ChIP/input) from 1 to 150 bp of the tRNA gene
growth before first doubling old
growth before first doubling new
midlog
hrs after estradiol addition
E
HML
anti HA (old Sir3)
HML-I
YCL068C
HMLα2
HMLα1
HML-E
anti T7 (new Sir3)
avg. log2 (ChIP/input) at HML
y = 0.0561x + 0.0147
R² = 0.4135
y = -0.0875x + 2.7983
R² = 0.5245
hrs after arrest in stationary phase
chr3 coordinates (bp)
F
HMR
anti HA (old Sir3)
HMR-I
HMRa2
HMRa1
HMR-E
tRNA-Thr
anti T7 (new Sir3)
avg. log2 (ChIP/input) at HMR
y = 0.0841x-0.6155
R² = 0.4412
y = -0.082x + 2.2165
R² = 0.4215
hrs after arrest in stationary phase
chr3 coordinates (bp)

Figure S1

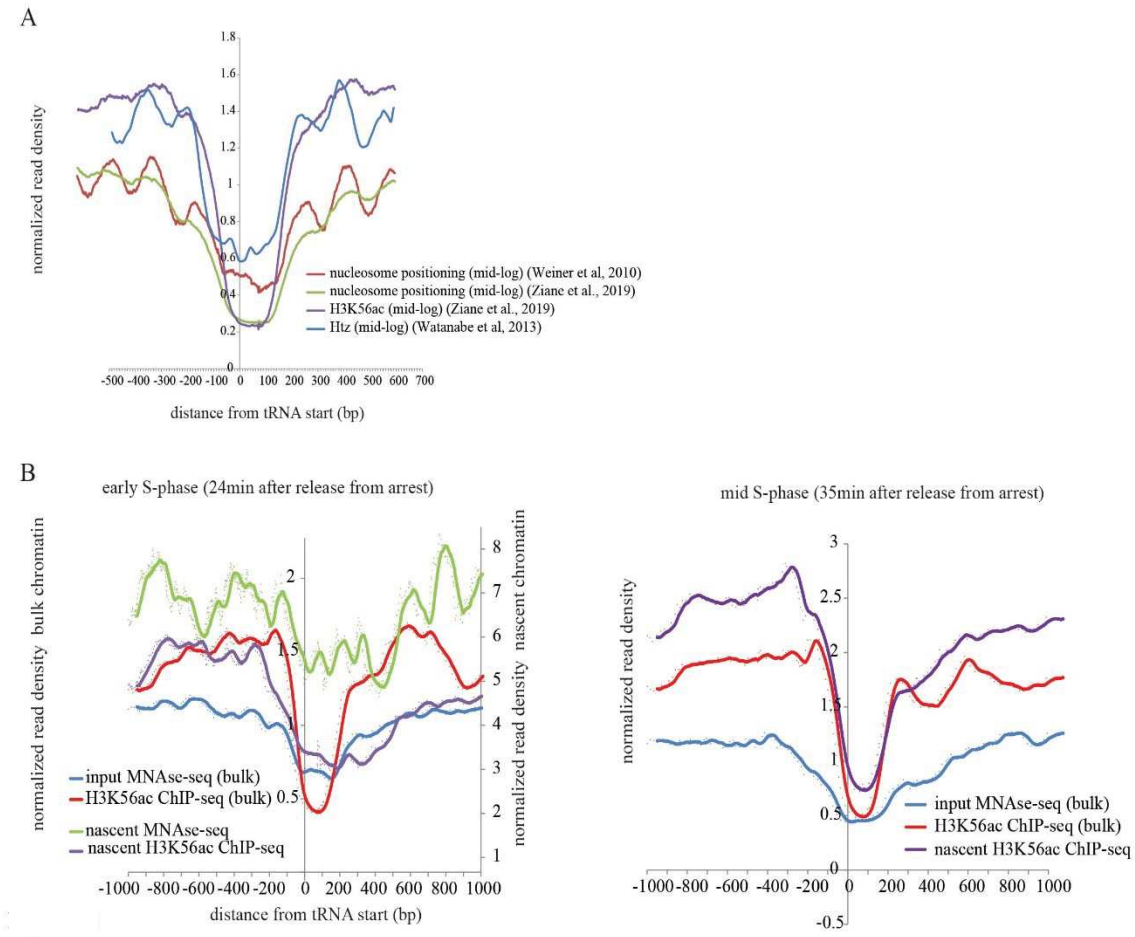
A
normalized read density
nucleosome positioning (mid-log) (Weiner et al, 2010)
nucleosome positioning (mid-log) (Ziane et al., 2019)
H3K56ac (mid-log) (Ziane et al., 2019)
Htz (mid-log) (Watanabe et al, 2013)
distance from tRNA start (bp)
B
early S-phase (24min after release from arrest)
normalized read density bulk chromatin
normalized read density nascent chromatin
input MNAse-seq (bulk)
H3K56ac ChIP-seq (bulk)
nascent MNAse-seq
nascent H3K56ac ChIP-seq
distance from tRNA start (bp)
mid S-phase (35min after release from arrest)
normalized read density
input MNAse-seq (bulk)
H3K56ac ChIP-seq (bulk)
nascent H3K56ac ChIP-seq

Figure S2

6 REFERENCES

Allen, C., Büttner, S., Aragon, A. D., Thomas, J. A., Meirelles, O., Jaetao, J. E., … Werner-Washburne, M. (2006). Isolation of quiescent and nonquiescent cells from yeast stationary-phase cultures. *The Journal of Cell Biology*, *174*(1), 89–100. https://doi.org/10.1083/jcb.200604072

Allshire, R. C., & Madhani, H. D. (2017). Ten principles of heterochromatin formation and function. *Nature Reviews Molecular Cell Biology*, *19*, 229.

Altaf, M., Utley, R. T., Lacoste, N., Tan, S., Briggs, S. D., & Côté, J. (2007). Interplay of chromatin modifiers on a short basic patch of histone H4 tail defines the boundary of telomeric heterochromatin. *Molecular Cell*, *28*(6), 1002–1014. https://doi.org/10.1016/j.molcel.2007.12.002

Angus-Hill, M. L., Schlichter, A., Roberts, D., Erdjument-Bromage, H., Tempst, P., & Cairns, B. R. (2001). A Rsc3/Rsc30 Zinc Cluster Dimer Reveals Novel Roles for the Chromatin Remodeler RSC in Gene Expression and Cell Cycle Control. *Molecular Cell*, *7*(4), 741–751. https://doi.org/10.1016/S1097-2765(01)00219-2

Bell, S. P., Mitchell, J., Leber, J., Kobayashi, R., & Stillman, B. (1995). The multidomain structure of Orc1 p reveals similarity to regulators of DNA replication and transcriptional silencing. *Cell*, *83*(4), 563–568. https://doi.org/10.1016/0092-8674(95)90096-9

Bernstein, B. E., Humphrey, E. L., Erlich, R. L., Schneider, R., Bouman, P., Liu, J. S., … Schreiber, S. L. (2002). Methylation of histone H3 Lys 4 in coding regions of active genes. *Proceedings of the National Academy of Sciences of the United States of America*, *99*(13), 8695–8700. https://doi.org/10.1073/pnas.082249499

Bi, X. (2014). Heterochromatin structure: Lessons from the budding yeast. *IUBMB Life*, *66*(10), 657–666. https://doi.org/10.1002/iub.1322

Botstein, D., & Fink, G. R. (2011). Yeast: an experimental organism for 21st Century biology. *Genetics*, *189*(3), 695–704. https://doi.org/10.1534/genetics.111.130765

Briggs, S. D., Bryk, M., Strahl, B. D., Cheung, W. L., Davie, J. K., Dent, S. Y., … Allis, C. D. (2001). Histone H3 lysine 4 methylation is mediated by Set1 and required for cell growth and rDNA silencing in Saccharomyces cerevisiae. *Genes & Development*, *15*(24), 3286–3295. https://doi.org/10.1101/gad.940201

Bühler, M., & Gasser, S. M. (2009). Silent chromatin at the middle and ends: lessons from yeasts. *The EMBO Journal*, *28*(15), 2149. https://doi.org/10.1038/emboj.2009.185

Cai, L., Sutter, B. M., Li, B., & Tu, B. P. (2011). Acetyl-CoA Induces Cell Growth and Proliferation by Promoting the Acetylation of Histones at Growth Genes. *Molecular Cell*, *42*(4), 426–437. https://doi.org/10.1016/j.molcel.2011.05.004

Chen, Y., Rai, R., Zhou, Z.-R., Kanoh, J., Ribeyre, C., Yang, Y., … Lei, M. (2011). A conserved motif within RAP1 has diversified roles in telomere protection and regulation in different organisms. *Nature Structural & Molecular Biology*, *18*(2), 213–221. https://doi.org/10.1038/nsmb.1974

Chou, C.-C., Li, Y.-C., & Gartenberg, M. R. (2008). Bypassing Sir2 and O-Acetyl-ADP-Ribose in Transcriptional Silencing. *Molecular Cell*, *31*(5), 650–659. https://doi.org/10.1016/j.molcel.2008.06.020

Croken, M. M., Nardelli, S. C., & Kim, K. (2012). Chromatin modifications, epigenetics, and how protozoan parasites regulate their lives. *Trends in Parasitology*, *28*(5), 202–213. https://doi.org/10.1016/j.pt.2012.02.009

Cuperus, G., Shafaatian, R., & Shore, D. (2000). Locus specificity determinants in the multifunctional yeast silencing protein Sir2. *The EMBO Journal*, *19*(11), 2641–2651. https://doi.org/10.1093/emboj/19.11.2641

Dang, W. (2014). The controversial world of sirtuins. *Drug Discovery Today. Technologies*, *12*, e9–e17. https://doi.org/10.1016/j.ddtec.2012.08.003

Denu, J. M. (2003). Linking chromatin function with metabolic networks: Sir2 family of NAD+-dependent deacetylases. *Trends in Biochemical Sciences*, *28*(1), 41–48. https://doi.org/10.1016/S0968-0004(02)00005-1

Dillin, A., & Rine, J. (1997). Separable Functions of ORC5 in Replication Initiation and Silencing in Saccharomyces cerevisiae. *Genetics*, *147*(3), 1053.

Dubarry, M., Loïodice, I., Chen, C. L., Thermes, C., & Taddei, A. (2011). Tight protein–DNA interactions favor gene silencing. *Genes & Development*, *25*(13), 1365–1370.

Dubey, R. N., & Gartenberg, M. R. (2007). A tDNA establishes cohesion of a neighboring silent chromatin domain. *Genes & Development*, *21*(17), 2150–2160. https://doi.org/10.1101/gad.1583807

Ehrentraut, S., Hassler, M., Oppikofer, M., Kueng, S., Weber, J. M., Mueller, J. W., … Ehrenhofer-Murray, A. E. (2011). Structural basis for the role of the Sir3 AAA+ domain in silencing: interaction with Sir4 and unmethylated histone H3K79. *Genes & Development*, *25*(17), 1835–1846. https://doi.org/10.1101/gad.17175111

Ehrentraut, S., Weber, J. M., Dybowski, J. N., Hoffmann, D., & Ehrenhofer-Murray, A. E. (2010). Rpd3-dependent boundary formation at telomeres by removal of Sir2 substrate. *Proceedings of the National Academy of Sciences of the United States of America*, *107*(12), 5522–5527. https://doi.org/10.1073/pnas.0909169107

Faure, G., Jézéquel, K., Roisné-Hamelin, F., Bitard-Feildel, T., Lamiable, A., Marcand, S., & Callebaut, I. (2019). Discovery and Evolution of New Domains in Yeast Heterochromatin Factor Sir4 and Its Partner Esc1. *Genome Biology and Evolution*, *11*(2), 572–585. https://doi.org/10.1093/gbe/evz010

Feldmann, E. A., & Galletto, R. (2014). The DNA-binding domain of yeast Rap1 interacts with double-stranded DNA in multiple binding modes. *Biochemistry*, *53*(48), 7471–7483. https://doi.org/10.1021/bi501049b

Fourel, G., Revardel, E., Koering, C. E., & Gilson, E. (1999). Cohabitation of insulators and silencing elements in yeast subtelomeric regions. *The EMBO Journal*, *18*(9), 2522–2537. https://doi.org/10.1093/emboj/18.9.2522

Fox, C. A., Ehrenhofer-Murray, A. E., Loo, S., & Rine, J. (1997). The Origin Recognition Complex, SIR1, and the S Phase Requirement for Silencing. *Science*, *276*(5318), 1547. https://doi.org/10.1126/science.276.5318.1547

Galdieri, L., Mehrotra, S., Yu, S., & Vancura, A. (2010). Transcriptional regulation in yeast during diauxic shift and stationary phase. *Omics : A Journal of Integrative Biology*, *14*(6), 629–638. https://doi.org/10.1089/omi.2010.0069

Galdieri, L., Zhang, T., Rogerson, D., Lleshi, R., & Vancura, A. (2014). Protein Acetylation and Acetyl Coenzyme A Metabolism in Budding Yeast. *Eukaryotic Cell*, *13*(12), 1472. https://doi.org/10.1128/EC.00189-14

Gardner, K. A., & Fox, C. A. (2001). The Sir1 protein's association with a silenced chromosome domain. *Genes & Development*, *15*(2), 147–157. https://doi.org/10.1101/gad.852801

Gartenberg, M. R., & Smith, J. S. (2016). The Nuts and Bolts of Transcriptionally Silent Chromatin in Saccharomyces cerevisiae. *Genetics*, *203*(4), 1563–1599. https://doi.org/10.1534/genetics.112.145243

Gottschling, D E. (1992). Telomere-proximal DNA in Saccharomyces cerevisiae is refractory to methyltransferase activity in vivo. *Proceedings of the National Academy of Sciences*, *89*(9), 4062. https://doi.org/10.1073/pnas.89.9.4062

Gottschling, Daniel E., Aparicio, O. M., Billington, B. L., & Zakian, V. A. (1990a). Position effect at S. cerevisiae telomeres: Reversible repression of Pol II transcription. *Cell*, *63*(4), 751–762. https://doi.org/10.1016/0092-8674(90)90141-Z

Gottschling, Daniel E., Aparicio, O. M., Billington, B. L., & Zakian, V. A. (1990b). Position effect at S. cerevisiae telomeres: Reversible repression of Pol II transcription. *Cell*, *63*(4), 751–762. https://doi.org/10.1016/0092-8674(90)90141-Z

Grewal, S. I. S., & Moazed, D. (2003). Heterochromatin and Epigenetic Control of Gene Expression. *Science*, *301*(5634), 798. https://doi.org/10.1126/science.1086887

Guidi, M., Ruault, M., Marbouty, M., Loïodice, I., Cournac, A., Billaudeau, C., … Taddei, A. (2015). Spatial reorganization of telomeres in long-lived quiescent cells. *Genome Biology*, *16*(1), 206. https://doi.org/10.1186/s13059-015-0766-2

Haber, J. E. (2012). Mating-type genes and MAT switching in Saccharomyces cerevisiae. *Genetics*, *191*(1), 33–64. https://doi.org/10.1534/genetics.111.134577

Hanson, S. J., & Wolfe, K. H. (2017). An Evolutionary Perspective on Yeast Mating-Type Switching. *Genetics*, *206*(1), 9. https://doi.org/10.1534/genetics.117.202036

Hass, E. P., & Zappulla, D. C. (2015). The Ku subunit of telomerase binds Sir4 to recruit telomerase to lengthen telomeres in S. cerevisiae. *ELife*, *4*, e07750. https://doi.org/10.7554/eLife.07750

Hocher, A., Ruault, M., Kaferle, P., Descrimes, M., Garnier, M., Morillon, A., & Taddei, A. (2018). Expanding heterochromatin reveals discrete subtelomeric domains delimited by chromatin landscape transitions. *Genome Research*, *28*(12), 1867–1881. https://doi.org/10.1101/gr.236554.118

Hoggard, T., Shor, E., Müller, C. A., Nieduszynski, C. A., & Fox, C. A. (2013). A Link between ORC-Origin Binding Mechanisms and Origin Activation Time Revealed in Budding Yeast. *PLOS Genetics*, *9*(9), e1003798. https://doi.org/10.1371/journal.pgen.1003798

Hoppe, G. J., Tanny, J. C., Rudner, A. D., Gerber, S. A., Danaie, S., Gygi, S. P., & Moazed, D. (2002). Steps in assembly of silent chromatin in yeast: Sir3-independent binding of a Sir2/Sir4 complex to silencers and role for Sir2-dependent deacetylation. *Molecular and Cellular Biology*, *22*(12), 4167–4180. https://doi.org/10.1128/MCB.22.12.4167-4180.2002

Hsu, H.-C., Wang, C.-L., Wang, M., Yang, N., Chen, Z., Sternglanz, R., & Xu, R.-M. (2013). Structural basis for allosteric stimulation of Sir2 activity by Sir4 binding. *Genes & Development*, *27*(1), 64–73. https://doi.org/10.1101/gad.208140.112

Imai, S.-I., & Guarente, L. (2016). It takes two to tango: NAD(+) and sirtuins in aging/longevity control. *NPJ Aging and Mechanisms of Disease*, *2*, 16017–16017. https://doi.org/10.1038/npjamd.2016.17

Ivessa, A. S., Lenzmeier, B. A., Bessler, J. B., Goudsouzian, L. K., Schnakenberg, S. L., & Zakian, V. A. (2003). The Saccharomyces cerevisiae Helicase Rrm3p Facilitates Replication Past Nonhistone Protein-DNA Complexes. *Molecular Cell*, *12*(6), 1525–1536. https://doi.org/10.1016/S1097-2765(03)00456-8

Jensen, R., Sprague, G. F., & Herskowitz, I. (1983). Regulation of yeast mating-type interconversion: feedback control of HO gene expression by the mating-type locus. *Proceedings of the National Academy of Sciences*, *80*(10), 3035. https://doi.org/10.1073/pnas.80.10.3035

Kang, J.-Y., Kim, J.-Y., Kim, K.-B., Park, J. W., Cho, H., Hahm, J. Y., … Seo, S.-B. (2018). KDM2B is a histone H3K79 demethylase and induces transcriptional repression via sirtuin-1–mediated chromatin silencing. *The FASEB Journal*, *32*(10), 5737–5750. https://doi.org/10.1096/fj.201800242R

Kato, M., & Lin, S.-J. (2014). Regulation of NAD+ metabolism, signaling and compartmentalization in the yeast Saccharomyces cerevisiae. *DNA Repair*, *23*, 49–58. https://doi.org/10.1016/j.dnarep.2014.07.009

Kueng, S., Oppikofer, M., & Gasser, S. M. (2013). SIR Proteins and the Assembly of Silent Chromatin in Budding Yeast. *Annual Review of Genetics*, *47*(1), 275–306. https://doi.org/10.1146/annurev-genet-021313-173730

Larin, M. L., Harding, K., Williams, E. C., Lianga, N., Doré, C., Pilon, S., … Rudner, A. D. (2015). Competition between Heterochromatic Loci Allows the Abundance of the Silencing Protein, Sir4, to Regulate de novo Assembly of Heterochromatin. *PLOS Genetics*, *11*(11), e1005425. https://doi.org/10.1371/journal.pgen.1005425

Lazarus, A. G., & Holmes, S. G. (2011). A cis-acting tRNA gene imposes the cell cycle progression requirement for establishing silencing at the HMR locus in yeast. *Genetics*, *187*(2), 425–439. https://doi.org/10.1534/genetics.110.124099

Lebrun, É., Revardel, E., Boscheron, C., Li, R., Gilson, E., & Fourel, G. (2001). Protosilencers in Saccharomyces cerevisiae Subtelomeric Regions. *Genetics*, *158*(1), 167.

Li, Y.-C., Cheng, T.-H., & Gartenberg, M. R. (2001). Establishment of Transcriptional Silencing in the Absence of DNA Replication. *Science*, *291*(5504), 650. https://doi.org/10.1126/science.291.5504.650

Liou, G.-G., Tanny, J. C., Kruger, R. G., Walz, T., & Moazed, D. (2005). Assembly of the SIR Complex and Its Regulation by O-Acetyl-ADP-Ribose, a Product of NAD-Dependent Histone Deacetylation. *Cell*, *121*(4), 515–527. https://doi.org/10.1016/j.cell.2005.03.035

Luo, K., Vega-Palas, M. A., & Grunstein, M. (2002). Rap1-Sir4 binding independent of other Sir, yKu, or histone interactions initiates the assembly of telomeric heterochromatin in yeast. *Genes & Development*, *16*(12), 1528–1539. https://doi.org/10.1101/gad.988802

Lynch, P. J., & Rusche, L. N. (2009). A Silencer Promotes the Assembly of Silenced Chromatin Independently of Recruitment. *Molecular and Cellular Biology*, *29*(1), 43. https://doi.org/10.1128/MCB.00983-08

Martienssen, R., & Moazed, D. (2015). RNAi and heterochromatin assembly. *Cold Spring Harbor Perspectives in Biology*, *7*(8), a019323.

Martinez, M. J., Roy, S., Archuletta, A. B., Wentzell, P. D., Anna-Arriola, S. S., Rodriguez, A. L., Werner-Washburne, M. (2004). Genomic Analysis of Stationary-Phase and Exit in Saccharomyces cerevisiae: Gene Expression and Identification of Novel Essential Genes. *Molecular Biology of the Cell*, *15*(12), 5295–5305. https://doi.org/10.1091/mbc.e03-11-0856

McKnight, J. N., Breeden, L. L., & Tsukiyama, T. (2015). A molecular off switch for transcriptional quiescence. *Cell Cycle (Georgetown, Tex.)*, *14*(23), 3667–3668. https://doi.org/10.1080/15384101.2015.1112618

Mehrotra, S., Galdieri, L., Zhang, T., Zhang, M., Pemberton, L. F., & Vancura, A. (2014). Histone hypoacetylation-activated genes are repressed by acetyl-CoA- and chromatin-mediated mechanism. *Biochimica et Biophysica Acta*, *1839*(9), 751–763. https://doi.org/10.1016/j.bbagrm.2014.05.029

Mentch, S. J., & Locasale, J. W. (2016). One-carbon metabolism and epigenetics: understanding the specificity. *Annals of the New York Academy of Sciences*, *1363*(1), 91–98. https://doi.org/10.1111/nyas.12956

Mews, P., Zee, B. M., Liu, S., Donahue, G., Garcia, B. A., & Berger, S. L. (2014). Histone methylation has dynamics distinct from those of histone acetylation in cell cycle reentry from quiescence. *Molecular and Cellular Biology*, *34*(21), 3968–3980. https://doi.org/10.1128/MCB.00763-14

Miller, A. M., & Nasmyth, K. A. (1984). Role of DNA replication in the repression of silent mating type loci in yeast. *Nature*, *312*(5991), 247–251. https://doi.org/10.1038/312247a0

Min, J., Landry, J., Sternglanz, R., & Xu, R.-M. (2001). Crystal Structure of a SIR2 Homolog–NAD Complex. *Cell*, *105*(2), 269–279. https://doi.org/10.1016/S0092-8674(01)00317-8

Minard, K. I., & McAlister-Henn, L. (2009). Redox responses in yeast to acetate as the carbon source. *Archives of Biochemistry and Biophysics*, *483*(1), 136–143. https://doi.org/10.1016/j.abb.2008.12.014

Moazed, D. (2011). Mechanisms for the Inheritance of Chromatin States. *Cell*, *146*(4), 510–518. https://doi.org/10.1016/j.cell.2011.07.013

Moretti, P., & Shore, D. (2001). Multiple Interactions in Sir Protein Recruitment by Rap1p at Silencers and Telomeres in Yeast. *Molecular and Cellular Biology*, *21*(23), 8082. https://doi.org/10.1128/MCB.21.23.8082-8094.2001

Nasmyth, K. A., & Tatchell, K. (1980). The structure of transposable yeast mating type loci. *Cell*, *19*(3), 753–764. https://doi.org/10.1016/S0092-8674(80)80051-1

Negrini, S., Ribaud, V., Bianchi, A., & Shore, D. (2007). DNA breaks are masked by multiple Rap1 binding in yeast: implications for telomere capping and telomerase regulation. *Genes & Development*, *21*(3), 292–302. https://doi.org/10.1101/gad.400907

Ngubo, M., Kemp, G., & Patterton, H. G. (2011). Nano-electrospray tandem mass spectrometric analysis of the acetylation state of histones H3 and H4 in stationary phase in Saccharomyces cerevisiae. *BMC Biochemistry*, *12*(1), 34. https://doi.org/10.1186/1471-2091-12-34

Noma, K., & Grewal, S. I. S. (2002). Histone H3 lysine 4 methylation is mediated by Set1 and promotes maintenance of active chromatin states in fission yeast. *Proceedings of the National Academy of Sciences*, *99*(suppl 4), 16438. https://doi.org/10.1073/pnas.182436399

Oki, M., & Kamakaka, R. T. (2005). Barrier Function at HMR. *Molecular Cell*, *19*(5), 707–716. https://doi.org/10.1016/j.molcel.2005.07.022

Oki, M., Valenzuela, L., Chiba, T., Ito, T., & Kamakaka, R. T. (2004). Barrier Proteins Remodel and Modify Chromatin To Restrict Silenced Domains. *Molecular and Cellular Biology*, *24*(5), 1956. https://doi.org/10.1128/MCB.24.5.1956-1967.2004

Onishi, M., Liou, G.-G., Buchberger, J. R., Walz, T., & Moazed, D. (2007). Role of the Conserved Sir3-BAH Domain in Nucleosome Binding and Silent Chromatin Assembly. *Molecular Cell*, *28*(6), 1015–1028. https://doi.org/10.1016/j.molcel.2007.12.004

Oppikofer, M., Kueng, S., Keusch, J. J., Hassler, M., Ladurner, A. G., Gut, H., & Gasser, S. M. (2013). Dimerization of Sir3 via its C-terminal winged helix domain is essential for yeast heterochromatin formation. *The EMBO Journal*, *32*(3), 437–449. https://doi.org/10.1038/emboj.2012.343

Pillus, L., & Rine, J. (1989a). Epigenetic inheritance of transcriptional states in S. cerevisiae. *Cell*, *59*(4), 637–647. https://doi.org/10.1016/0092-8674(89)90009-3

Pillus, L., & Rine, J. (1989b). Epigenetic inheritance of transcriptional states in S. cerevisiae. *Cell*, *59*(4), 637–647. https://doi.org/10.1016/0092-8674(89)90009-3

Pryde, F. E., & Louis, E. J. (1999). Limitations of silencing at native yeast telomeres. *The EMBO Journal*, *18*(9), 2538–2550. https://doi.org/10.1093/emboj/18.9.2538

Radman-Livaja, M., Ruben, G., Weiner, A., Friedman, N., Kamakaka, R., & Rando, O. J. (2011). Dynamics of Sir3 spreading in budding yeast: secondary recruitment sites and euchromatic localization. *The EMBO Journal*, *30*(6), 1012. https://doi.org/10.1038/emboj.2011.30

Radonjic, M., Andrau, J.-C., Lijnzaad, P., Kemmeren, P., Kockelkorn, T. T. J. P., van Leenen, D., … Holstege, F. C. P. (2005). Genome-Wide Analyses Reveal RNA Polymerase II Located Upstream of Genes Poised for Rapid Response upon S. cerevisiae Stationary Phase Exit. *Molecular Cell*, *18*(2), 171–183. https://doi.org/10.1016/j.molcel.2005.03.010

Raisner, R. M., Hartley, P. D., Meneghini, M. D., Bao, M. Z., Liu, C. L., Schreiber, S. L., … Madhani, H. D. (2005). Histone Variant H2A.Z Marks the 5′ Ends of Both Active and Inactive Genes in Euchromatin. *Cell*, *123*(2), 233–248. https://doi.org/10.1016/j.cell.2005.10.002

Rossmann, M. P., Luo, W., Tsaponina, O., Chabes, A., & Stillman, B. (2011). A common telomeric gene silencing assay is affected by nucleotide metabolism. *Molecular Cell*, *42*(1), 127–136. https://doi.org/10.1016/j.molcel.2011.03.007

Ruault, M., De Meyer, A., Loïodice, I., & Taddei, A. (2011). Clustering heterochromatin: Sir3 promotes telomere clustering independently of silencing in yeast. *The Journal of Cell Biology*, *192*(3), 417. https://doi.org/10.1083/jcb.201008007

Saka, K., Ide, S., Ganley, A. R. D., & Kobayashi, T. (2013). Cellular Senescence in Yeast Is Regulated by rDNA Noncoding Transcription. *Current Biology*, *23*(18), 1794–1798. https://doi.org/10.1016/j.cub.2013.07.048

Sampath, V., Yuan, P., Wang, I. X., Prugar, E., van Leeuwen, F., & Sternglanz, R. (2009). Mutational Analysis of the Sir3 BAH Domain Reveals Multiple Points of Interaction with Nucleosomes. *Molecular and Cellular Biology*, *29*(10), 2532. https://doi.org/10.1128/MCB.01682-08

Sandell, L. L., & Zakian, V. A. (1992). Telomeric position effect in yeast. *Trends in Cell Biology*, *2*(1), 10–14. https://doi.org/10.1016/0962-8924(92)90138-D

Sauve, A. A. (2010). Sirtuin chemical mechanisms. *Biochimica et Biophysica Acta*, *1804*(8), 1591–1603. https://doi.org/10.1016/j.bbapap.2010.01.021

Sauve, A. A., Moir, R. D., Schramm, V. L., & Willis, I. M. (2005). Chemical Activation of Sir2-Dependent Silencing by Relief of Nicotinamide Inhibition. *Molecular Cell*, *17*(4), 595–601. https://doi.org/10.1016/j.molcel.2004.12.032

Shia, W.-J., Li, B., & Workman, J. L. (2006). SAS-mediated acetylation of histone H4 Lys 16 is required for H2A. Z incorporation at subtelomeric regions in Saccharomyces cerevisiae. *Genes & Development*, *20*(18), 2507–2512.

Simms, T. A., Dugas, S. L., Gremillion, J. C., Ibos, M. E., Dandurand, M. N., Toliver, T. T., … Donze, D. (2008a). TFIIIC binding sites function as both heterochromatin barriers and chromatin insulators in Saccharomyces cerevisiae. *Eukaryotic Cell*, *7*(12), 2078–2086. https://doi.org/10.1128/EC.00128-08

Simms, T. A., Dugas, S. L., Gremillion, J. C., Ibos, M. E., Dandurand, M. N., Toliver, T. T., … Donze, D. (2008b). TFIIIC binding sites function as both heterochromatin barriers and chromatin insulators in Saccharomyces cerevisiae. *Eukaryotic Cell*, *7*(12), 2078–2086. https://doi.org/10.1128/EC.00128-08

Smith, J. S., & Boeke, J. D. (1997). An unusual form of transcriptional silencing in yeast ribosomal DNA. *Genes & Development*, *11*(2), 241–254.

Swygert, S. G., Senapati, S., Bolukbasi, M. F., Wolfe, S. A., Lindsay, S., & Peterson, C. L. (2018). SIR proteins create compact heterochromatin fibers. *Proceedings of the National Academy of Sciences of the United States of America*, *115*(49), 12447–12452. https://doi.org/10.1073/pnas.1810647115

Taddei, A., Hediger, F., Neumann, F. R., Bauer, C., & Gasser, S. M. (2004). Separation of silencing from perinuclear anchoring functions in yeast Ku80, Sir4 and Esc1 proteins. *The EMBO Journal*, *23*(6), 1301–1312. https://doi.org/10.1038/sj.emboj.7600144

Taddei, A., Van Houwe, G., Nagai, S., Erb, I., van Nimwegen, E., & Gasser, S. M. (2009). The functional importance of telomere clustering: global changes in gene expression result from SIR factor dispersion. *Genome Research*, *19*(4), 611–625. https://doi.org/10.1101/gr.083881.108

Takahashi, Y.-H., Schulze, J. M., Jackson, J., Hentrich, T., Seidel, C., Jaspersen, S. L., … Shilatifard, A. (2011a). Dot1 and Histone H3K79 Methylation in Natural Telomeric and HM Silencing. *Molecular Cell*, *42*(1), 118–126. https://doi.org/10.1016/j.molcel.2011.03.006

Takahashi, Y.-H., Schulze, J. M., Jackson, J., Hentrich, T., Seidel, C., Jaspersen, S. L., … Shilatifard, A. (2011b). Dot1 and histone H3K79 methylation in natural telomeric and HM silencing. *Molecular Cell*, *42*(1), 118–126. https://doi.org/10.1016/j.molcel.2011.03.006

Tanny, J. C., Dowd, G. J., Huang, J., Hilz, H., & Moazed, D. (1999). An Enzymatic Activity in the Yeast Sir2 Protein that Is Essential for Gene Silencing. *Cell*, *99*(7), 735–745. https://doi.org/10.1016/S0092-8674(00)81671-2

Tung, S.-Y., Lee, K.-W., Hong, J.-Y., Lee, S.-P., Shen, H.-H., & Liou, G.-G. (2013). CHANGES IN THE GENOME-WIDE LOCALIZATION PATTERN OF SIR3 IN SACCHAROMYCES CEREVISIAE DURING DIFFERENT GROWTH STAGES. *Computational and Structural Biotechnology Journal*, *7*(8), e201304001. https://doi.org/10.5936/csbj.201304001

van Leeuwen, F., Gafken, P. R., & Gottschling, D. E. (2002). Dot1p Modulates Silencing in Yeast by Methylation of the Nucleosome Core. *Cell*, *109*(6), 745–756. https://doi.org/10.1016/S0092-8674(02)00759-6

Wang, J., Jia, S. T., & Jia, S. (2016). New Insights into the Regulation of Heterochromatin. *Trends in Genetics : TIG*, *32*(5), 284–294. https://doi.org/10.1016/j.tig.2016.02.005

Weber, J. M., & Ehrenhofer-Murray, A. E. (2010). Design of a minimal silencer for the silent mating-type locus HML of Saccharomyces cerevisiae. *Nucleic Acids Research*, *38*(22), 7991–8000. https://doi.org/10.1093/nar/gkq689

Wellinger, R. J., & Zakian, V. A. (2012). Everything you ever wanted to know about Saccharomyces cerevisiae telomeres: beginning to end. *Genetics*, *191*(4), 1073–1105. https://doi.org/10.1534/genetics.111.137851

Wood, K., Tellier, M., & Murphy, S. (2018a). DOT1L and H3K79 Methylation in Transcription and Genomic Stability. *Biomolecules*, *8*(1), 11. https://doi.org/10.3390/biom8010011

Wood, K., Tellier, M., & Murphy, S. (2018b). DOT1L and H3K79 Methylation in Transcription and Genomic Stability. *Biomolecules*, *8*(1), 11. https://doi.org/10.3390/biom8010011

Wu, C. -t., & Morris, J. R. (2001). Genes, Genetics, and Epigenetics: A Correspondence. *Science*, *293*(5532), 1103. https://doi.org/10.1126/science.293.5532.1103

Xu, R.-M. (2003). A Pivotal Role of the Coiled Coil of Sir4. *Structure*, *11*(6), 608–609. https://doi.org/10.1016/S0969-2126(03)00102-3

Young, C. P., Hillyer, C., Hokamp, K., Fitzpatrick, D. J., Konstantinov, N. K., Welty, J. S., … Osley, M. A. (2017). Distinct histone methylation and transcription profiles are established during the development of cellular quiescence in yeast. *BMC Genomics*, *18*(1), 107–107. https://doi.org/10.1186/s12864-017-3509-9

Young, T. J., & Kirchmaier, A. L. (2012). Cell cycle regulation of silent chromatin formation. *Histone Chaperones and Chromatin Assembly*, *1819*(3), 303–312. https://doi.org/10.1016/j.bbagrm.2011.10.006

Yu, S., Smirnova, J. B., Friedberg, E. C., Stillman, B., Akiyama, M., Owen-Hughes, T., … Reed, S. H. (2009). ABF1-binding sites promote efficient global genome nucleotide excision repair. *The Journal of Biological Chemistry*, *284*(2), 966–973. https://doi.org/10.1074/jbc.M806830200